EFFECTS OF AXIAL LIGANDS ON THE REDOX PROPERTIES OF SOME METALLOPORPHYRINS: SOME PHYSICO - CHEMICAL STUDIES

SYNOPSIS

Submitted In Fulfillment
Of The Requirement
For The Degree Of
Doctor Of Philosophy

BY

AICYDALYNE SNAITANG

DEPARTMENT OF CHEMISTRY
SCHOOL OF PHYSICAL SCIENCES
NORTH EASTERN HILL UNIVERSITY
SHILLONG – 793022
APRIL 2010

Chemistry

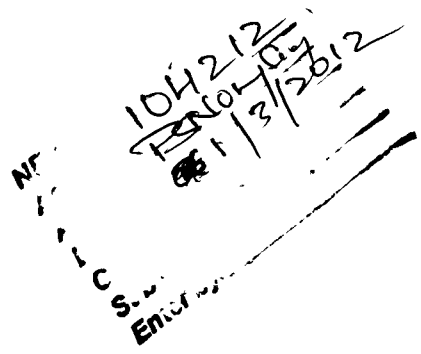

S Y N O P S I S

SYNOPSIS

This thesis entitled **"EFFECTS OF AXIAL LIGANDS ON THE REDOX PROPERTIES OF SOME METALLOPORPHYRINS"** discussed the information and results of investigations on the physico – chemical studies of some Metalloporphyrins. It consists of **six chapters**. We restrict our investigations mainly to UV – Visible absorption spectroscopy and Cyclic Voltammetric studies of some transition metal porphyrins like Manganese, Zinc and Copper porphyrins.

In the **Introduction**, natural occurrence of some metalloporphyrins and their biological functions are briefly mentioned. Also, the importance of UV – Visible spectroscopy and cyclic voltammetry in understanding the redox behaviour of metalloporphyrins is highlighted in the Introduction.

A Brief Review on the theory behind UV – Visible and Cyclic Voltammetric studies on the Effects of Axial Ligands in some Metalloporphyrins (emphasis is given to Manganese porphyrins) is presented in **Chapter 1**. This

review provides us the background information to pursue our research investigation in the right direction and to give a proper perspective for the results of the investigations presented in subsequent chapters.

Chapter 2 describes the details of the experimental procedures adopted for purification of solvents and chemicals, synthesis, purification and characterization of samples used during the course of our investigation. Besides this, brief description of physical measurements is also presented.

The Effects of Axial ligands on the UV – Visible spectra of some manganese porphyins are discussed in **Chapter 3**. In general, all three Manganese porphyins chosen to study, viz., Mn(III)[T(2-OMeP)P]OAc, Mn(III)[T(Naphthyl)P]OAc and Mn(III)[T(4-OMeP)P]OAc, exhibit similar spectral pattern. A UV – Visible absorption spectrum of a manganese porphyrin consists of one B – band or Soret band (Band V) in the range 440 – 480 nm and two Q – bands (Band III and Band IV) in the range 500 – 650 nm. Additional bands (Band Va and Band VI)

are also observed in the range 350 – 420 nm. Nitrogenous bases like Diethylamine, Triethylamine and Imidazole are used as axial ligands. It is found out that on initial addition of amine to the three Manganese porphyrins the Soret band suffers a Blue shift. This is attributed to the replacement of the axial ligand OAc^- by amine molecule which comes as a fifth ligand. On continuous addition of amine to the reaction mixture the intensity of the original Soret band diminishes and a new Soret band appears at a shorter wavelength. This could be due to two possibilities: (i) the coordination of another amine molecule as the sixth ligand, with the oxidation state of Mn remaining +3, and (ii) the second possibility is the reduction of Mn(III) to Mn(II) with amine molecules coordinating as the fifth and sixth ligands. In our studies, the first possibility is more probable. The details of this are presented in Scheme 3.1 and 3.2 in Chapter 3.

In our discussion, we also incorporate the conformations of metalloporphyrin which are affected by axial ligand – metalloporphyrin interactions. This effect brings about a change in the energy levels of the

porphyrin when the axial ligand binds with the central metal atom which appears as shift in the position of absorption bands in the UV – Visible spectrum.

Chapter 4 describes the Cyclic Voltammetric studies of the three Manganese porphyrins i.e., Mn(III)[T(2-OMeP)P] OAc, Mn(III)[T(4-OMeP)P]OAc and Mn(III)[T(naphthyl)P]OAc. All these three exhibit voltammograms of similar pattern. The positive scan voltammogram consists of three redox couples. This is attributed to the oxidation of Mn(III) to Mn(IV) and the first and second porphyrin ligand oxidations. Similarly, the negative scan gives a voltammogram which consists of three redox couples. This may be due to the reduction of Mn(III) to Mn(II) and the first and second porphyrin ligand reductions. It has been observed that out of the three Manganese porphyrins, redox potential of the first ligand oxidation is lowest in the case of Mn(III)[T(naphthyl)P]OAc. This is because non-planar porphyrins are easier to oxidize due to the interaction of d-orbitals of the metal atom with the porphyrin ligand orbitals (a_{1u}/a_{2u}) and Mn(III)[T(naphthyl)P]OAc, being

more distorted due to steric hindrance, gets oxidized at a lower potential. Thus structural effect on the redox potentials is reflected in the voltammograms which also supplements the results observed in Chapter 3.

Chapter 5 discusses the Axial Ligand Effects On The UV-Visible Spectra and the Cyclic Voltammetric studies of Zinc(II)porphyrins viz., Zn(II)[T(4-OMeP)P] and Zn(II)[T(naphthyl)P]. Zn(II) porphyrins belong to regular porphyrins which contain closed shell metal toms (d^0 or d^{10}). On axial ligation with amine the absorption bands in the UV – Visible spectrum of these Zinc porphyrins experience a Bathochromic shift (Red shift). This is due to the flow of charge from the axial ligand to the porphyin ring through the Zinc ion.

The results of the Cyclic Voltammetric studies of these Zn(II)porphyrins are also presented in this chapter. Two reversible redox couples are observed although their ΔE values are quite large. We also observed that the oxidation potentials of these Zinc porphyrins studied are lower than that of Zn(II)TPP. We attribute this to the

presence of electron donating substituents which makes oxidation easier.

Chapter 6 deals with the Axial Ligand Effects On The UV-Visible Spectra and the Redox Tuning of Copper (II) porphyrins viz., Cu(II)[T(4-OMeP)P] and Cu(II)[T(naphthyl)P]. Copper porphyrins belong to d^9 complexes. Addition of amine does not affect the UV – Visible spectra of Copper porphyrins which indicate that they do not accept axial ligands readily. In the Cyclic Voltammetric studies, the Voltammogram consists of two redox couples whose potentials are lower than that of CuTPP. This is attributed to the presence of electron donating substituents.

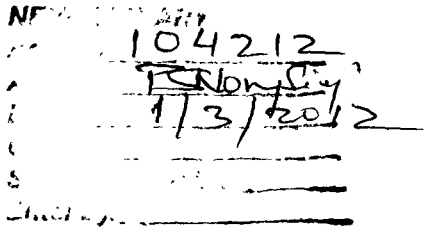

EFFECTS OF AXIAL LIGANDS ON THE REDOX PROPERTIES OF SOME METALLOPORPHYRINS:

SOME PHYSICO – CHEMICAL STUDIES

Thesis Submitted in Fulfillment
Of the Requirement
For the Degree of
Doctor of Philosophy

BY

AICYDALYNE SNAITANG

DEPARTMENT OF CHEMISTRY
SCHOOL OF PHYSICAL SCIENCES
NORTH EASTERN HILL UNIVERSITY
SHILLONG – 793022
APRIL 2010

EASTERN HILL UNIVERSITY LIBRARY

Chemistry

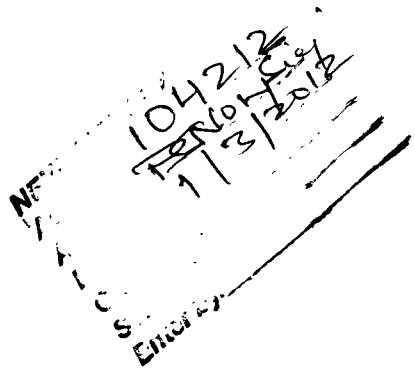

DECLARATION

NORTH EASTERN HILL UNIVERSITY
SHILLONG – 793022
APRIL 2010

I, Smt. Aicydalyne Snaitang, hereby declare that the subject matter of this thesis is the record of work done by me, that the contents of this thesis did not form basis of the award of any previous degree to me or to the best of my knowledge to any body else, and that the thesis has not been submitted by me for research degree in any other University/Institute.

This is being submitted to the North Eastern Hill University, Shillong for the Ph.D. Degree in Chemistry.

AICYDALYNE SNAITANG
(CANDIDATE)

27/04/2010

Prof. B. Myrboh
HEAD
DEPARTMENT OF CHEMISTRY
NORTH EASTERN HILL UNIVERSITY
SHILLONG – 793022

Head
Department of Chemistry
North - Eastern Hill University
Shillong - 793022

27/04/10

Dr. A. Lemtur
SUPERVISOR
Reader
Department of Chemistry
North-Eastern Hill University
Shillong- 793022

Dr. A. Lemtur
Department of Chemistry
North Eastern Hill University
Shillong - 793022

email: lemtur1@rediffmail.com
Tel. No. 0364 2722618
Fax No. 0364 2550076

CERTIFICATE

This is to certify that the thesis entitled ***"Effects of Axial Ligands on the Redox properties of some Metalloporphyrins : Some Physico Chemical studies"*** *is based on the original work done by* ***Aicydalyne Snaitang****, under my supervision in the Department of Chemistry, School of Physical Sciences, North Eastern Hill University, Shillong, Meghalaya. This work has not previously formed the basis for the award of any degree, diploma, fellowship or any other similar title and that it represents entirely an independent work on the part of the candidate.*

27/04/2010

Prof. B. Myrboh
HEAD
DEPARTMENT OF CHEMISTRY
NORTH EASTERN HILL UNIVERSITY
SHILLONG – 793022

Head
Department of Chemistry
North - Eastern Hill University
Shillong - 793022

27/04/10

Dr. A. Lemtur
SUPERVISOR
Reader
Department of Chemistry
North-Eastern Hill University
Shillong- 793022

Place : Shillong.
Date : 27th April, 2010.

ACKNOWLEDGEMENT

First of all, I would like to express my deepest and heartiest gratitude to my supervisor, ***Dr. A. Lemtur,*** *Reader, Department of Chemistry, NEHU, Shillong for his constant help and guidance, inspiration and encouragement throughout the course of this investigation.*

I would also like to express my sincere gratitude to Prof. B.Myrboh, Head, Department of Chemistry, NEHU, Shillong, for all the help rendered to me throughout the course.

I also thank all the faculty members of the Department of Chemistry, NEHU, Shillong for helping me in many ways throughout the course.

I also take this opportunity to thank all the non-teaching staff of the Department, especially to Mr. Andy Nengnong and Mrs. Florence, for their support and help in conducting different Physical measurements involving in this investigation.

My special thanks go to my husband, ***Mr. Donborlang Kharbhih*** *for all the help and moral support and for always being there for me at all times to lend a helping hand.*

I thank my senior and lab mates Dr. A. Tomba Singh, Dr. (Mrs) Cornelia Lyngdoh and Dr. A. Murugan for their constant help and assistance throughout the course.

I also acknowledge my sincere thanks to all my research colleagues for helping and encouraging me throughout the course.

I would also like to express my gratitude to all my colleagues in St. Anthony's College, Shillong, for their cooperation, support, help, inspiration and encouragement which enable me to complete my work successfully.

I also express my deep sense of gratitude to my parents, brothers and sisters for their patience, love, affection and constant encouragement throughout my academic career.

Above all I thank the Almighty God for all the blessings that He continues to shower upon me throughout my life and I am what I am now is because of Him. I also dedicate this work to Him, for without Him, none of this would have been possible.

AICYDALYNE SNAITANG

CONTENTS

		PAGE No.
List of Tables		(i)
List of Figures		(iii)
Preface		1
Introduction		4
Chapter 1:	**A Brief Review On The Axial Ligand Effects Of Some Metalloporphyrins: UV – Vis And Cyclic Voltammetric Studies**	
	1.1. UV – Vis Spectrum	6
	1.2. Manganese Porphyrins	14
	1.3. Electrochemistry and Spectroelectrochemistry	17
	References	25
Chapter 2.	**Experimental Section**	
	2.1. Introduction	31
	2.2. Purification Of Solvents And Reagents	31
	2.3. Preparation of Supporting Electrolyte	34
	2.4. Synthesis of Porphyrins	35

2.5. Synthesis of Metalloporphyrins 38

2.6. Instrumentation 42

References 46

Chapter 3. Axial Ligand Effects On The UV-Vis Spectra Of Mn(III)[T(2-OMeP)P]OAc; Mn (III)[T(4-OMeP)P]OAc And Mn(III)[T(Naphthyl)P]OAc

3.1. Introduction 47

3.2. Results 47

3.3. Discussion 51

3.4. Conclusion 57

References 71

Chapter 4. Cyclic Voltammetric Study Of Mn(III)[T(2-OMeP)P]OAc Mn(III)[T(4-OMeP)P]OAc And Mn(III)[T(Naphthyl)P]OAc

4.1. Introduction 75

4.2. Results 76

4.3. Discussion 78

4.4. Conclusion 80

References 89

Chapter 5. Axial Ligand Effects on the UV – Vis Spectra and The Cyclic Voltammetric Studies of Zn(II)[T(4-OMeP)P] and Zn(II)[T(naphthyl)P]

5.1. Introduction 91

5.2. UV – Visible Studies 92

5.3. Discussion 93

5.4. Cyclic Voltammetric Studies 94

5.5. Conclusion 96

References 105

Chapter 6. Axial Ligand Effects on the UV – Vis Spectra and Redox Tuning of Cu(II)[T(4-OMeP)P] and Cu(II)[T(naphthyl)P]

6.1. Introduction 107

6.2. Results 108

6.3. Discussion 109

6.4. Conclusion 110

References 116

Summary 117

LIST OF TABLES

		Page No.
TABLE : 3.A.	UV-Vis Absorption Spectral Data Of Mn(III)[T(2-OMeP)P]OAc at Room Temperature	58
TABLE : 3.B.	UV-Vis Absorption Spectral Data Of Mn(III)[T(4-OMeP)P]OAc at Room Temperature	59
TABLE : 3.C.	UV-Vis Absorption Spectral Data Of Mn(III)[TNP]OAc at Room Temperature	60
TABLE: 4.A.	Redox potentials of Mn(III)[T(2-OMeP)P]OAc at Room temperature	81
TABLE: 4.B.	Redox potentials of Mn(III)[T(4-OMeP)P]OAc at Room temperature	82

TABLE: 4.C.	**Redox potentials of Mn(III)[TNP]OAc at Room temperature**	**83**
TABLE: 5.A.	**UV-Vis Absorption Spectral Data Of Zn(II)Porphyrins at Room Temperature.**	**97**
TABLE: 5.B.	**Cyclic Voltammetric Data of Zn(II)Porphyrins at Room Temperature.**	**98**
TABLE 6.A :	**UV-Vis Absorption Spectral Data Of Copper Porphyrins at Room Temperature.**	**111**
TABLE: 6.B.	**Cyclic Voltammetric Data of Copper Porphyrins at Room Temperature.**	**112**

LIST OF FIGURES

		PAGE No.
Figure: 1.1.	Structure of Free Base Porphyrin (FBP)	20
Figure: 1.2.	HOMO (a_u), Next HOMO (b_{1u}), LUMO (b_{2g}) And Next LUMO (b_{3g}) Orbitals of FBP and Naphthacene.	21
Figure: 1.3.	HOMOs and LUMOs and Possible Electronic Transitions	22
Figure: 1.4.	UV-Visible absorption spectrum of a Porphyrin.	23
Figure: 1.5.	UV-Visible absorption spectrum of Manganese Porphyrin.	24

Figure: 2.1.	**Scheme showing the synthesis Of Manganese Porphyrin.**	**44**
Figure: 2.2.	**Scheme showing the synthesis Of Zinc and Copper Porphyrins.**	**45**
Figure: 3.2.1.a.	**UV-Visible absorption spectrum of Mn(III)[T(2-OMeP)P]OAc in CH_2Cl_2 at Room Temperature on addition of 0.1mL of Diethylamine.**	**61**
Figure: 3.2.1.b.	**UV-Visible absorption spectrum of Mn(III)[T(2-OMeP)P]OAc in CH_2Cl_2 at Room Temperature on addition of 0.3 mL of Diethylamine.**	**62**

Figure: 3.2.1.c. **UV-Visible Overlay spectra of Mn(III)[T(2-OMeP)P]OAc in CH_2Cl_2 at Room Temperature on continuous addition of Diethylamine.** **63**

Figure: 3.2.1.d. **UV-Visible Overlay spectra of Mn(III)[T(2-OMeP)P]OAc in CH_2Cl_2 at Room Temperature on continuous addition of Triethylamine.** **64**

Figure: 3.2.2.a. **UV-Visible absorption spectrum of Mn(III)[T(4-OMeP)P]OAc in CH_2Cl_2 at Room Temperature on addition of 0.1mL of Diethylamine.** **65**

Figure: 3.2.2.b. **UV-Visible absorption spectrum of Mn(III)[T(4-OMeP)P]OAc in CH_2Cl_2 at Room Temperature on continuous addition of Diethylamine.** **66**

Figure: 3.2.2.c. **UV-Visible Overlay spectra of Mn(III)[T(4-OMeP)P]OAc in CH_2Cl_2 at Room Temperature on continuous addition of Triethylamine.** **67**

Figure: 3.2.3.a. **UV-Visible absorption spectrum of Mn(III)[TNP]OAc in CH_2Cl_2 at Room Temperature on addition of 0.2mL of Diethylamine.** **68**

Figure: 3.2.3.b. UV-Visible overlay spectra of Mn(III)[TNP]OAc in CH_2Cl_2 at Room Temperature on continuous addition of Diethylamine. 69

Figure: 3.2.3.c. UV-Visible Overlay spectra of Mn(III)[TNP]OAc in CH_2Cl_2 at Room Temperature on continuous addition of Triethylamine. 70

Figure: 4.2.1.a. Cyclic Voltammogram of Mn(III)[T(2-OMeP)P]OAc in CH_2Cl_2 containing 0.1M TBAP at Room Temperature. 84

Figure: 4.2.2.a. Cyclic Voltammogram of Mn(III)[T(4-OMeP)P]OAc in CH_2Cl_2 containing 0.1M TBAP at Room Temperature. 85

Figure: 4.2.2.b. Cyclic Voltammogram of Mn(III)[T(4-OMeP)P]OAc in CH_2Cl_2 containing 0.1M TBAP at Room Temperature. 86

Figure: 4.2.3.a. Cyclic Voltammogram of Mn(III)[TNP]OAc in CH_2Cl_2 containing 0.1M TBAP at Room Temperature. 87

Figure: 4.2.3.b. Cyclic Voltammogram of Mn(III)[TNP]OAc in CH_2Cl_2 containing 0.1M TBAP at Room Temperature. 88

Figure: 5.2.1.(i).a. UV-Visible absorption spectrum of Zn(II)[T(4-OMeP)P] in CH_2Cl_2 at Room Temperature on addition of 0.1mL of Diethylamine. 99

Figure: 5.2.1.(i).b. UV-Visible overlay spectra of Zn(II)[T(4-OMeP)P] in CH_2Cl_2 at Room Temperature on continuous addition of Triethylamine. 100

Figure: 5.2.1.(ii).a. UV-Visible overlay spectra of Zn(II)[T(naphthyl)P] in CH_2Cl_2 at Room Temperature on continuous addition of Diethylamine. 101

Figure: 5.2.1.(ii).b. UV-Visible overlay spectra of Zn(II)[T(naphthyl)P] in CH_2Cl_2 at Room Temperature on continuous addition of Triethylamine. 102

Figure: 5.4.1.i. Cyclic Voltammogram of Zn(II)[T(4-OMeP)P] in CH_2Cl_2 containing 0.1M TBAP at Room Temperature. 103

Figure: 5.4.1.ii. **Cyclic Voltammogram of Zn(II)[T(naphthyl)P] in CH_2Cl_2 containing 0.1M TBAP at Room Temperature.** **104**

Figure: 6.2.1.a. ***UV-Visible overlay spectra of Cu(II)[T(naphthyl)P] in CH_2Cl_2 at Room Temperature on continuous addition of Diethylamine.*** **113**

Figure: 6.2.2.i. **Cyclic Voltammogram of Cu(II)[T(4-OMeP)P] in CH_2Cl_2 containing 0.1M TBAP at Room Temperature.** **114**

Figure: 6.2.2.ii. **Cyclic Voltammogram of Cu(II)[T(naphthyl)P] in CH_2Cl_2 containing 0.1M TBAP at Room Temperature.** **115**

PREFACE

Porphyrin Chemistry is an extensively studied and researched field. This is because porphyrins are involved in many fundamental biological functions and they also find their way in the field of material sciences and medicines. Many new porphyrin ligands are synthesized and more information and results emerge in the literature every day. Thus it opens up an opportunity to study their physico – chemical properties. This prompted us to carry out more physico – chemical studies in metalloporphyrins which will provide us more understanding of their roles in biological systems, application in medicine and their possible uses in material sciences. Thus, this thesis embodies the new results and information on the physico – chemical studies of some Manganese porphyrins, Zinc porphyrins and Copper porphyrins, which are not reported so far in the literature.

This thesis consists of six chapters. The significance of metalloporphyrins in the biological system is highlighted in the **Introduction.**

Chapter 1 presents a Brief Review on the UV – Visible and Cyclic Voltammetric studies on the Effects of Axial Ligands in some Metalloporphyrins.

Chapter 2 presents all the experimental techniques and measurements employed in the course of this investigation.

Chapter 3 describes the Effects of Axial Ligands on the UV - Visible spectra of some Manganese porphyrins.

Chapter 4 embodies the Cyclic Voltammetric Study of some Manganese porphyrins.

Chapter 5 deals with Axial Ligand Effects On The UV – Visible Spectra And Cyclic Voltammetric studies of some Zinc porphyrins.

Chapter 6 deals with Axial Ligand Effects On The UV – Visible Spectra And Redox Tuning of some Copper pophyrins.

INTRODUCTION

Porphyrins are group compounds which are extensively studied and researched. In fact, porphyrin chemistry is an old chemistry. Inspite of the widely studied area, porphyrin chemistry appears to grow day by day. This is evident from the number of papers published every year. This is because porphyrins occupy a significant place among the biological occurring molecules. Iron porphyrins occur as heme in hemoglobins (transporting O_2) and in myoglobins (as storage); Mg porphyrins as chlorophyll (in photosynthesis); in cytochromes (electron transfer) and in many other enzymatic reactions such as peroxidase and catalases etc. In a very broad sense there are two classes of porphyrins viz. naturally occurring porphyrins and synthetically modified porphyrins. Apart from the naturally occurring porphyrins, at present a large number of synthetically modified porphyrins are available in the literature. Thus, it provides us an opportunity to investigate and understand their properties both experimentally and

theoretically. UV – Visible spectroscopy coupled with cyclic voltammetry can provide quite a good amount of information about its redox behaviour.

With this broad view in our mind we undertook this research work with the following objectives:-

(i) Metalloporphyrins serve as biological model systems.

(ii) To explore and to understand the physico – chemical properties of some synthetic metalloporphyrins (which is an open field) which in turn may throw some light on the possible uses of such metalloporphyrins.

CHAPTER – 1

A BRIEF REVIEW ON THE EFFECTS OF AXIAL LIGANDS IN SOME METALLOPORPHYRINS: UV - VISIBLE AND CYCLIC VOLTAMMETRIC STUDIES

CHAPTER – 1

1.1. UV – VISIBLE SPECTRUM:

To understand and to appreciate this research work, a very brief review of the theory behind the UV – Visible absorption spectra of porphyrins is presented here. We avoid the complex theoretical treatment (mathematical)/ discussion and present only the non-mathematical results. Both synthetically modified porphyrins as well as naturally occurring porphyrins exhibit similar optical and electro-chemical properties. This is because all these molecules contain four pyrroles linked by four methine bridges and are rich in π – electrons. In 1960s Martin Gouterman[1 - 3] laid the theoretical foundation of the absorption spectra of porphyrins which is known as the Four Orbital Model, i.e. two HOMOS (Highest occupied molecular orbitals, a_{1u} and a_{2u}) and two LUMOS (lowest unoccupied molecular orbital, e_g). The main part of a porphyrin molecule is the inner 16 – membered ring containing four nitrogen atoms with 18 delocalized π - electrons. Transitions between HOMOs and

LUMOs give rise to the absorption bands in the optical spectrum (π – π* transitions). The basic unsubstituted porphyrin is termed as porphine (P) or a free base porphyrin (FBP) (Figure: 1.1).

FBP with 18 π – electrons is similar to naphthacene which is also a conjugated system (alternant hydrocarbon) with 18 π – electrons (Figure:1.2).

Gouterman's four orbitals corresponds to two HOMOs and two LUMOs of naphthacene[4 - 6] (pairing properties are also satisfied). The two HOMOs are very close and nearly degenerate. The difference in energy is about 0.5 eV and is quite sensitive to substitutions. The two LUMOs are degenerate (Figure : 1.3)

Mixing between them splits the energy levels giving rise to higher energy $1e_u$ state with larger oscillator strength

which gives rise to Soret band or B band around 380nm to 420nm and a lower energy state $1e_u$ with smaller oscillator strength giving rise to Q bands around 500nm – 650nm (Figure: 1.4)

In Figure:1.3. (1, 1′) and (2, 2′) are pair of orbitals. The configuration energy due to excitation of an electron from the orbital i to the orbital $j'$is equal to the energy obtained by excitation from j orbital to j'orbital (due to pairing property).

Thus, for one electron transition moment vectors

$$i \longrightarrow j'$$

$$j \longrightarrow i' \text{ (Where } i \neq j \text{)}$$

are similar in magnitude and parallel in their orientation in the alternant hydrocarbons.

Further, the linear combination of the two degenerate configurations generate (–) and (+) states. The minus (–)

state is a covalent state while plus (+) state is ionic state. Thus, the excitation:

HOMO $\longrightarrow$ LUMO (1 $\longrightarrow$ 1′) gives rise to the lowest $^1B_{2u}^+$ state with ionic character while the excitations 1 $\longrightarrow$ 2′ and 2 $\longrightarrow$ 1′ give rise to covalent $^1B_{3u}^-$ and ionic $^1B_{3u}^+$ states.

For transition of the type $i \longrightarrow i'$, the dipole moment vector of 1 $\longrightarrow$ 1′ is anti-parallel to 2 $\longrightarrow$ 2′ dipole moment vector. Thus the transition to $^1B_{3u}^-$ is pseudo parity forbidden where as transitions to $^1B_{2u}^+$ and $^1B_{3u}^+$ are dipole allowed.

In the case of FBP, the ground state is 1^1A_g state and the transition to the Q – band is dipole allowed.

The lower components of the Q bands ($^1B_{3u}$) are due to transitions

$a_u \longrightarrow b_{3g}$ (1 $\longrightarrow$ 2/) and $b_{1u} \longrightarrow b_{2g}$ (2 $\longrightarrow$ 1/) and mixing occurs (mix with different sign).

The upper components of the Q bands ($^1B_{2u}$) are due to transitions

$a_u \longrightarrow b_{2g}$ (1 $\longrightarrow$ 1/) and $b_{1u} \longrightarrow b_{3g}$ (2 $\longrightarrow$ 2/).

Their transition dipole moment vectors are parallel in their orientations and almost same in magnitude leading to the cancellation in their intensities. The weakness of the Q - band is due to symmetry which is alternant resulting in pseudoparity forbidden transitions and not due to orbital degeneracy. This pseudoparity can be broken by:

(i) modification of the porphyrin ligand with substitution,

(ii) modification of the conjugation pathway, and

(iii) with central metallation.

Thus, the Q - band intensities can be enhanced. It is also to be noted that FBP with D_2h symmetry exhibit four banded visible absorption spectrum while a metalloporphyrin with a D_4h symmetry exhibits two banded visible absorption spectrum. This is clearly a reflection of the molecular symmetry. It also means that in a metalloporphyrin, the b_{2g} and the b_{3g} orbitals are degenerate because of four – fold axis.

Basing on UV – Visible and Fluorescence properties metalloporphyrins can be broadly divided into two groups viz., regular and irregular. Regular metalloporphyrins are those whose metal d – orbitals (valence shell) have closed shell configuration (i.e, d^o or d^{10}) while irregular are those in which the metal d – orbitals are partly filled or having open shell configuration (d^m, m = 6-9). In regular metalloporphyrins, the central metal atom has very little effect on the optical absorption spectrum (only a small perturbation on the π electrons of the porphyrin ligand). On the other hand irregular porphyrins do exhibits stronger

effects on the visible absorption spectrum. These metalloporphyrins are also called hypsoporphyrins. In hypsoporphyrins, there is considerable interactions between the d_π orbitals of the metal and the π^* orbitals of the porphyrin ligand (metal to ligand π back bonding)[7,8]. As a result energy level between π and π^* of the porphyrin ligand increases giving rise to hypsochromic shift i.e. the blue shift.

In addition to the regular and hypso types there is another type known as hyper type[9 - 15]. Manganese porphyrins exhibit this hyper type (d – hyper type) electronic absorption spectra.

In addition to the above general description, UV-Visible spectrum of a metalloporphyrin is affected by its structural conformations, axial ligands and the nature of the solvents[16]. A metalloporphyrin with a planar conformation possesses a D_4h symmetry where metal d_π orbitals and ligand orbitals (a_{1u}, a_{2u}) are orthogonal. But

the scenario is different in the case of non planar metalloporphyrins. A considerable interaction between metal $d_{x^2-y^2}$ orbital and porphyrin ligand orbital a_{2u} exists in a saddled conformation while metal d_{xy} orbital interact with porphyrin a_{2u} orbital in a ruffled conformation. Evidently, the UV-Visible spectrum of a metalloporphyrin will be affected by:-

(i) Coordination of the axial ligand.

(ii) Peripherial substitution on the porphyrin ligand, and

(iii) The conformation of the metalloporphyrin.

1.2. MANGANESE PORPHYRINS:

The literature is so exhaustive and voluminous to give a comprehensive review on the subject (axial ligand binding), so we restrict the review to manganese porphyrins.

Normally the UV-Visible spectrum of a manganese Porphyrin exhibits two visible bands, viz., Q bands between 500nm - 650nm and an intense Soret band (B band) between 440nm – 480nm (Figure: 1.5). Additional bands are also observed between 400 nm – 500nm which are attributed to charge transfer (CT) transitions i.e. due to a_{1u} (π) a_{2u} $\pi \longrightarrow e_g(d\pi)$. Also, some bands (bands V_a and VI) appear in between 350nm – 420nm. Boucher[10 - 14] has shown that intensity ratio of band V and VI varies with the fifth ligand and with substituents on the porphyrin ligand. The visible bands I & II (Q bands) which are normally observed in FBP are shifted to Infra red and are not observable in a metalloporphyrin spectrum[6]. The axial ligand and the peripherial substituents on the porphyrin ligand do exhibit a profound effect on the Soret band (band V).

Manganese atom in a manganese porphyrin show variable oxidation states. Thus it can accommodate fifth and the sixth ligand.

1.2.1. Mn(IV) PORPHYRINS:

Synthesis, isolation and structural elucidation have been reported for Mn(IV)(porphyrin)X_2 and Mn(IV)(porphyrin X)$_2$ O [17 - 19] . Oxidation of Mn(III)TPPX in alkaline methanolic solutions by iodosyl benzene or sodium hypochlorite leads to formation of Mn(IV)TPPX_2, where X = OCH_3^-, N_3^-, or NCO^-. (Porphyrin)Mn(IV) – O – Mn(IV) (porphyrin) system is also reported. The complexes [$(N_3$Mn(IV)TPP$]_2$O and [(OCN)Mn(IV)TPP$]_2$O are thermally unstable and decomposes[20]. Formation of O=Mn(IV)(TPP) in manganese porphyrin nitrates and O=Mn(IV)$(TPP)^+$ in the perchlorates and periodates on photolysis are also reported[21,22]. Oxo manganese(IV) porphyrin complexes viz., Mn(IV)TMP(O) and Mn(IV)TMP(O)(OH) (where TMP = tetra mesityl porphyrin) were produced from a mixture of Mn(III) TMP(Cl) and

NORTH EASTERN HILL UNIVERSITY LIBRARY
104212
DATE 15

TBA(OH) (tetra – n – butyl ammonium hydroxide), isolated and characterized[23]. However, Oxo manganese(IV) porphyrin is not stable and rapidly converts to Oxo manganese(II) porphyrin.

1.2.2. Mn(V) PORPHYRINS:

Synthesis of Mn(V)nitrido porphyrin is also reported[24,25]. Treatment of Mn(III)P with sodium hypochlorite or iodosyl benzene in presence of excess of ammonia leads to the formation of PMn(V)≡N. UV-Visible spectrum exhibits soret band at 428nm and Q bands at 538nm and 626nm. Synthesis of Oxo-like mono(iodosyl benzene)(TPP)Mn(V) from Mn(III)TPP(3-$NH_2C_6H_4CO_2$)with iodosyl benzene is reported[26]. The UV-Visible spectrum shows the soret band at 407nm and broad absorption bands at 379 nm, 478 nm, 582 nm and 618 nm. Oxo manganese (V) porphyrin Viz., O=Mn(V)TMPyP(H_2O), (where, TMPyP = meso tetrakis (N – methyl – 4 – pyridyl)porphyrinato dianion) was produced by oxidation of Mn(III)TMPyP and characterized by stop-flow spectrophotometry[27]. Characterization was also proven by NMR[28].

1.3. ELECTROCHEMISTRY AND SPECTRO-ELECTRO CHEMISTRY:

Solvent effect and axial ligand dissociation on the electrode reactions of Mn(III)TPP(ClO_4) is reported[29]. The effect of electrolyte concentration on axial anionic ligand in manganese (III)TPPCl is also reported[30]. The axial ligand binding is weak[29] and is removed on addition of Ag^+ with increasing electrolyte concentration[30]. Mn(III/II) couple is observed with shift in potential. Furhop and co-workers[31] have reported multivalent manganese porphyrin hetero dimers and - trimers in aqueous solutions and observed that multivalent manganese porphyrinates like Mn(III) – Mn(IV) – Mn(III) are not accessible to axial ligand. Spectro electro chemical study of (meso-tetrakis (3-carboxyphenyl) porphyrinato)Mn(III)chloride have shown the formation of Mn(II) and Mn(IV). Blue shifts of the soret band by 34 nm and Q band by 4 – 8 nm are also observed. Reaction of (Cl_8TPP)Mn(III)Cl with OH(H_2O) in MeCN solution is also reported[32]. Initial Soret band at 476 nm is shifted to 444 nm

in the final product. This is attributed to reduction of Mn (III) to Mn(II) i.e, (Cl_8TPP)Mn(II)(OH). The same is observed for the reaction of (Cl_8TPP)Mn(III)Cl with excess of OH(H_2O) in ligating solvent pyridine which gives the product (Cl_8TPP)Mn(II)(py) (Soret band at 444 nm). However, the favoured product is attributed to five coordinated Mn(II) rather than six coordinated Mn(II). The redox behaviour of Mn(III)porphyrins viz., Mn(III)TPP(X) (where, X = Cl^-, ClO_4^- and OH^-) are also reported[33]. The redox potential of Mn(III/II) are found to be in the range – 0.03 V to – 0.70 V while Mn(IV/III) potential for Mn(III)TPP$(OH)_2$ is at + 0.43V (in acetonitrile). Spectro electrochemical measurement at +0.53V, Mn(III)P$(OH)_2$ have shown the spectrum corresponding to that of Mn(IV)TPP(OH). The $E_{½}$ value for Mn(IV/III) is found to be + 0.43V. However, Oxo manganese(IV) porphyrin is unstable at room temperature and decomposes. Another interesting observation is that on bulk electrolysis of Mn(III)TPP(OAc) at + 1.05V replacement of the axial ligand OAc^- by $ClO4^-$ is observed.

Electrochemical oxidation of water soluble Mn(III) (2-TMPyP) generates Mn(IV) and Mn(V)porphyrins[34]. These species were generated and characterized by spectro electrochemical method. One – electron oxidation of Mn(III)(2-TMPyP) exhibits different forms of Oxo manganese (IV) porphyrin at different pH. The redox couple for Mn(III/II) at – 0.03V shifts to – 0.14V at pH 11.6. Another metal centered redox couple appears at + 0.53 V which shifts to + 0.28 V as pH increases to 11.6. Spectro electrochemical oxidation of Mn(III)(2-TMPyP) in pH 12 at + 0.92 V exhibits a new band at 432 nm which is attributed to Oxo manganese(V)porphyrin species O_2Mn(V)(2-TMPyP). Deprotonation of the axial H_2O molecule or hydroxide ion generates the dioxo species.

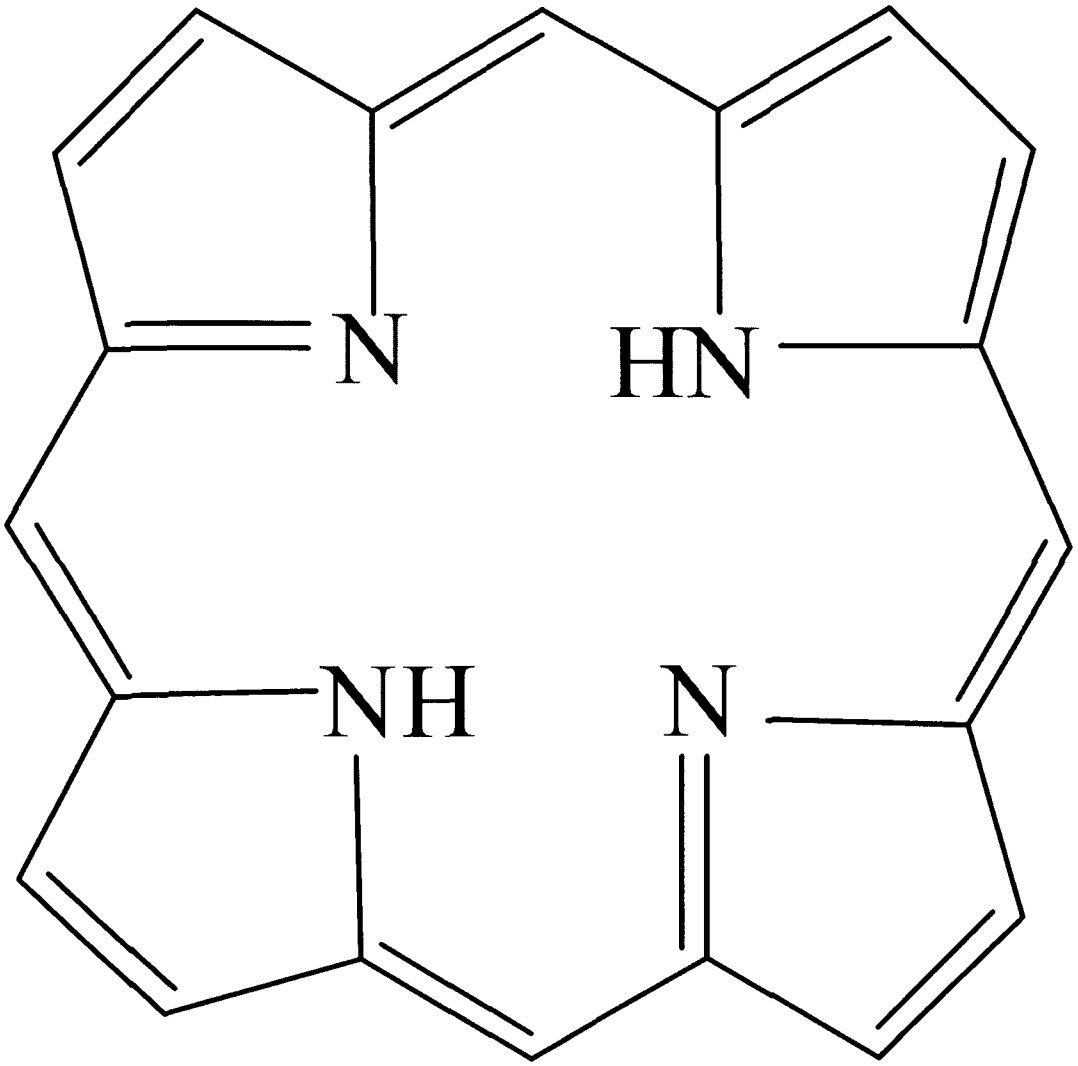

Figure: 1.1. Structure of Free Base Porphyrin (FBP)

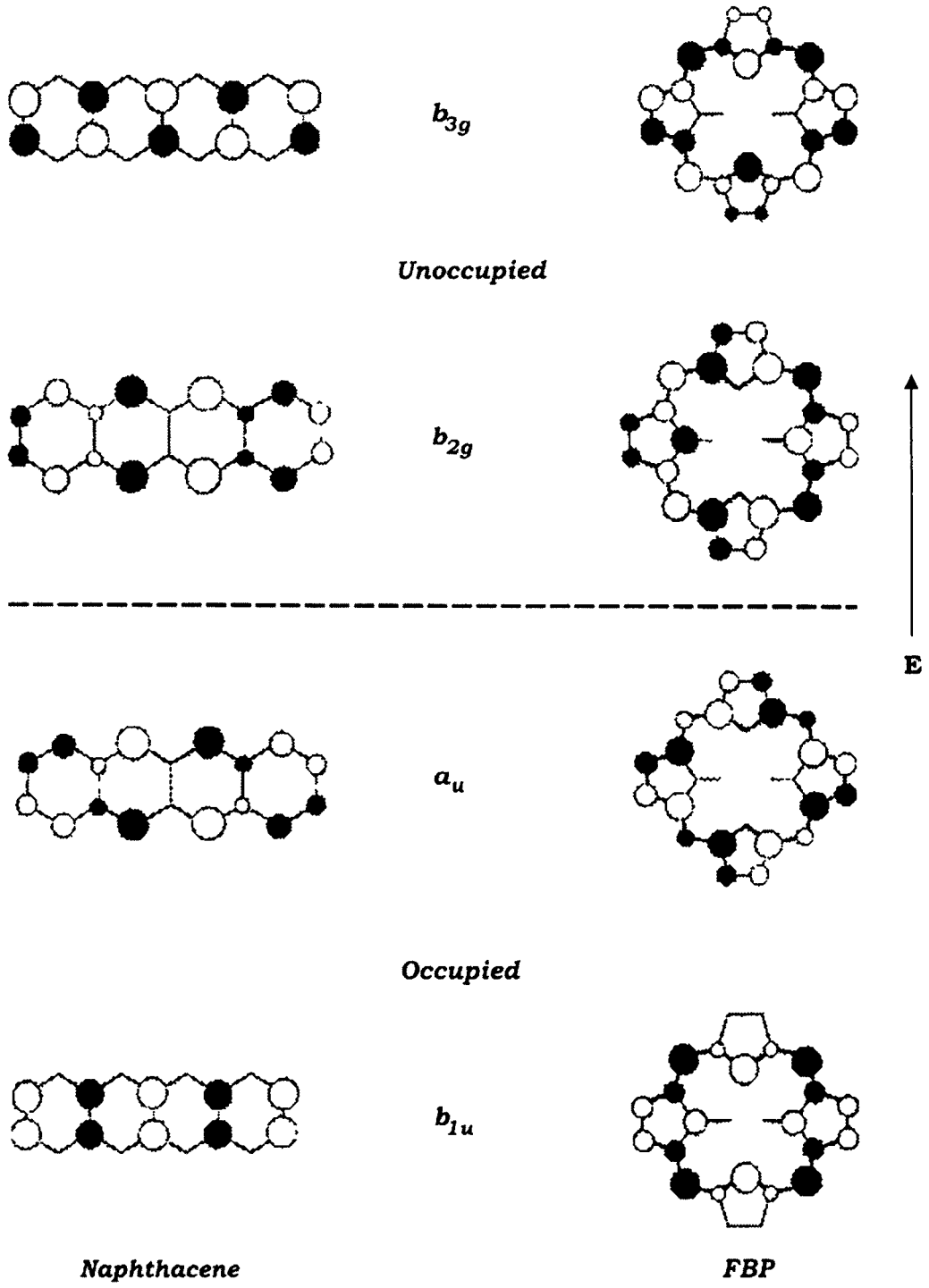

Figure : 1.2. HOMO (a_u), Next HOMO (b_{1u}), LUMO (b_{2g}) and Next LUMO (b_{3g}) Orbitals of FBP and Naphthacene.

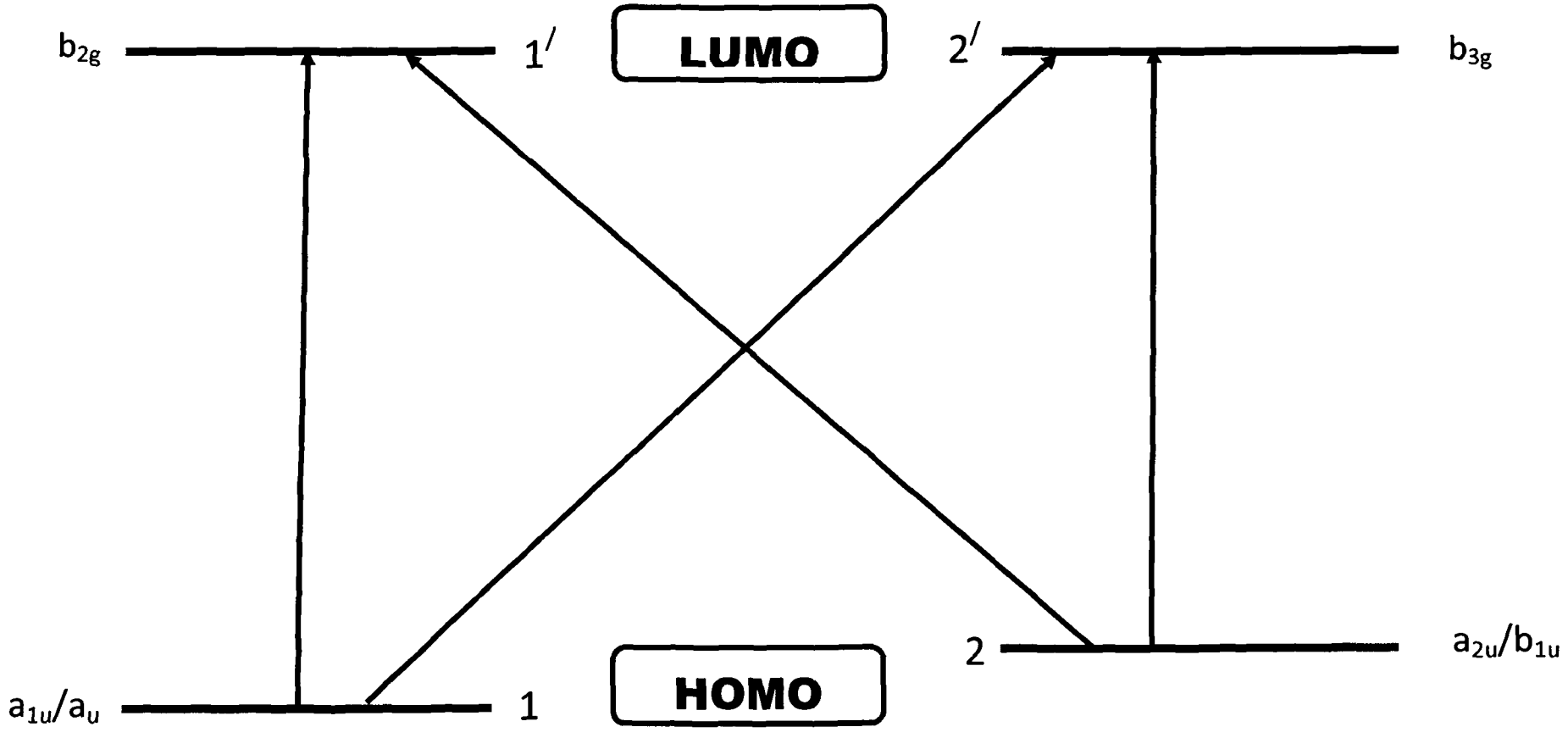

Figure: 1.3. HOMOs and LUMOs and Possible Electronic Transitions.

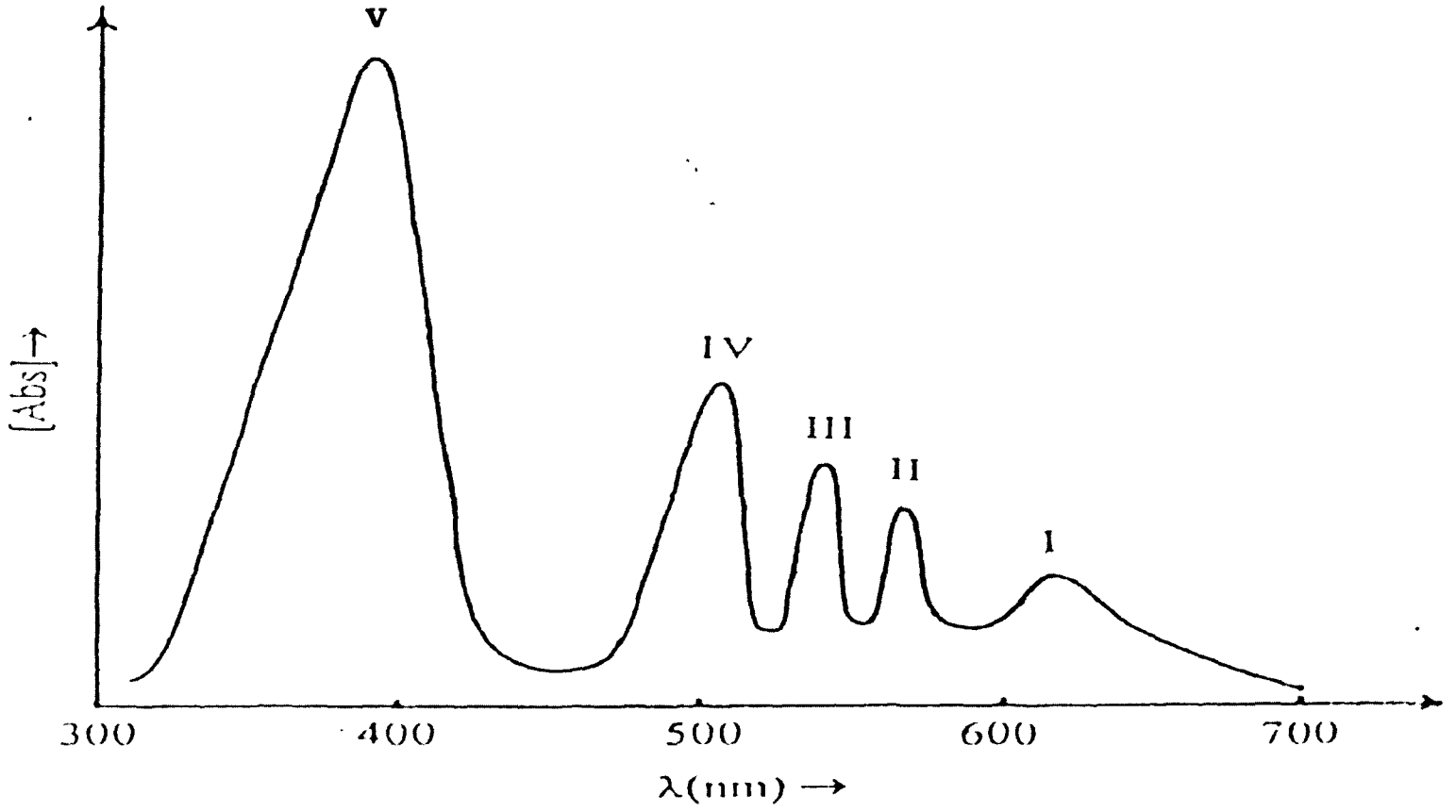

Figure: 1.4. UV-Visible Absorption Spectrum Of A Porphyrin.

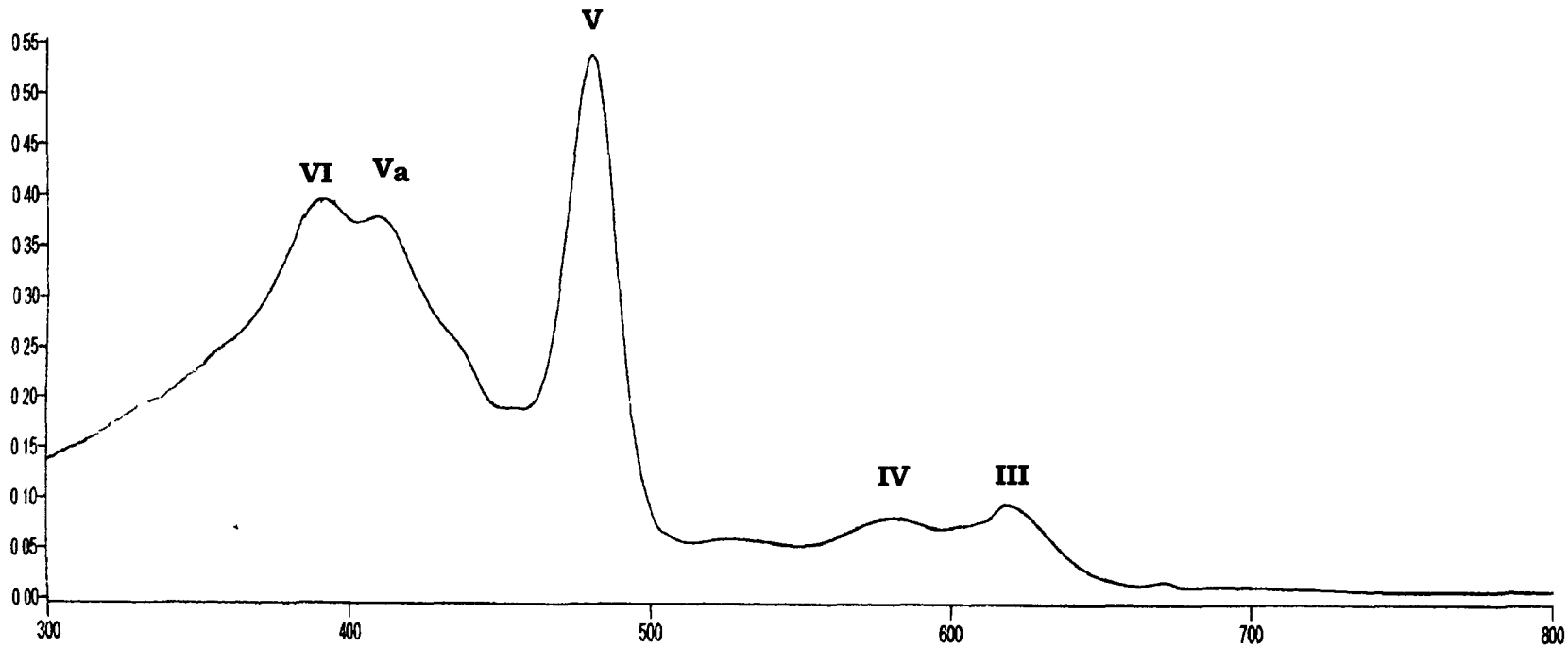

Figure : 1.5. UV-Visible absorption spectrum of Manganese Porphyrin

REFERENCES:

1. M. Gouterman, *J.Chem.Phys.*, **30**, 1139 (1959).

2. M. Gouterman, *J. Mol. Spectroscopy,* **6**,138 (1961).

3. M. Gouterman in *The Porphyrins* **Vol. III**, Part A, Edited by D. Dolphin, Academic Press, INC, Newyork, 1979.

4. T. Hashimoto, N. Nakano and K. Hirao, *J.Chem.Phys.* **104**, 6244 (1996).

5. B.D. Berezin, *Coordination compounds of porphyrins and phthalocyanines*, Wiley – Inter science, Chichester, 1981.

6. T. Hashimoto, Y.K. Choe, H. Nakano and K. Hirao, *J. Phys Chem. A*, **103**, 1894 (1999).

7. G. Simoneaux, V. Schunemann, C. Morice, L. Carel, L. Toupet, H. Winkler, A.X. Trantwein and F.A. Walker, *J. Am. Chem. Soc.*, **122**, 4366 (2000).

8. A. Ghosh, I. Halvorsen, H.J. Nilsen, E. Steene, T. Wondimagegn, R. Lie, E.V. Caemelbecke, N. Gou, Z. Ou and K.M. Kadish, *J. Phys. Chem. B,* **105**, 8120 – 8124 (2001).

9. A.D. Adler, F.R. Longo, J.D. Finarelli, J. Goldmacher, J. Assour and L. Korsakoff, *J.Org. Chem.*, **32**, 476 – 480 (1967).

10. L.J. Boucher, *Coord. Chem. Rev.*, **7**, 289 (1972).

11. L.J. Boucher, *J. Am. Chem. Soc.*, **90**, 6640 (1968).

12. L.J. Boucher, *J. Am. Chem. Soc.*, **92**, 2725 (1970).

13. L.J. Boucher and H.K. Garber, *Inorg. Chem.*, **9**, 2644 (1970).

14. L.J. Boucher, *Ann. N.Y. Acad. Sci.*, **206**, 409 (1973).

15. E.F. – Cosma, M.C. Mirica, I. Balcu, C. Buco Vicean, C. Cretu, I. Armeanu and G.F. – Cosma, *Molecules*, **14**, 1370 – 1388 (2009).

16. J.A. Shelnutt, X. – Z. Song, J. – G. Ma, S. – L. Jia, W. Jenzen and C.J. Medforth, *Chem. Soc. Rev.*, **27**, 31 (1998).

17. M.J. Camenzind, F. J. Hollander, C.L. Hill, *Inorg. Chem.*, **22**, 3777 (1983).

18. M.J. Camenzind, F. J. Hollander, C.L. Hill, *Inorg. Chem.*, **21**, 4301 (1982).

19. J.A. Smegal, B.C. Shardt and C.L. Hill, *J. Am. Chem. Soc.*, **105**, 3510 (1983).

20. C.L. Hill, *Inorg. Chem.*, **23**, 1984 (1984).

21. K.S. Suslick and R.A. Watson, *Inorg. Chem.*, **30**, 912 (1991).

22. K.S. Suslick, R.A. Watson and S.R. Wilson, *Inorg. Chem.*, **30**, 2311 – 2317 (1991).

23. J.T. Groves and M.K. Stern, *J. Am. Chem. Soc.*, **110**, 8628 (1988).

24. C.L. Hill and F.J. Hollander, *J. Am. Chem. Soc.*, **104**, 7318 (1982).

25. J.W. Buchler, C. Dreher, K.L. Lay, Y.J. Lee and W.R. Scheidt, *Inorg. Chem.*, **22**, 888.

26. R. Jim, C.S. Cho, S.B. Park and S.C. Shim, *Bull. Korean Chem. Soc.*, **18** (1), 106 (1997).

27. J.T. Groves, J. Lee and S.S. Marla, *J.Am. Chem. Soc.*, **119**, 6269 (1997).

28. J.T. Groves, N. Jim, *J. Am. Chem. Soc.*, **121**, 2923 (1999).

29. S.L. Kelly and K.M. Kadish, *Inorg. Chem.*, **21**, 3631 (1982).

30. G.J. Furan, R.S. Armstrong, M.J. Crossley and P.A. Lay, *Inorg. Chem.*, **31**, 1463 – 1470 (1992).

31. L.R. Ruhlmann, A. Nakamura, J.G. Vos and J. – H. Furhop, *Inorg. Chem.*, **37**, 6052 – 6059 (1998).

32. S. Jeon, H.K. Lee and Y. – K. Choi, *Bull. Korean Chem. Soc.*, **17** (10), 929 (1996).

33. C.– H. Chang, S.– H. Cheng and Y.O. Su, *J. Chinese Chem. Soc.*, **46**, 221 – 227 (1999).

34. F. – C. Chen, S. – H. Cheng, C. – H. Yu, M. – H. Liu and Y.O. Su, *J. Electro anal. Chem.*, **474**, 52 – 59 (1999).

CHAPTER – 2

EXPERIMENTAL SECTION

CHAPTER – 2

2.1. INTRODUCTION:

This chapter describes the general experimental techniques involving purification of solvents and reagents, preparation of supporting electrolytes, synthesis of porphyrins and metalloporphyrins. Brief descriptions of the UV – Visible spectrophotometric measurements and Cyclic Voltammetric instrumentation are also presented.

2.2. PURIFICATION OF SOLVENTS AND REAGENTS:

Common solvents and reagents used throughout this work have been purified according to the standard procedures described[1].

2.2.1. Dichloromethane : Drum sample of Dichloromethane was refluxed with anhydrous

potassium carbonate for about 2 hours and allowed to stand overnight. It was distilled and stored over molecular sieves (Linde-4A). For UV-Visible spectroscopy and Cyclic Voltammetric measurements, Dichloromethane of spectroscopic grade was used.

2.2.2. **Chloroform** :

Drum sample of Chloroform was purified by passing through a column of basic alumina and then the eluate was distilled twice before using. For recrystallization and other physical measurements, Chloroform of spectroscopic grade was used.

2.2.3. **Methanol** :

Drum samples of Methanol were refluxed over anhydrous CaO for about 2 hours and distilled twice before using. For recrystallization and other physical measurements, spectroscopic grade samples were used.

2.2.4. **Pyrrole** :

Pyrrole was purified by distillation under reduced pressure from KOH pellets and stored in a dark sealed vessel.

2.2.5. **2-Methoxybenzaldehyde**:

2-Methoxybenzaldehyde was distilled and used.

2.2.5. **4-Methoxybenzaldehyde**:

4-Methoxybenzaldehyde was distilled and used.

2.2.6. **1-Naphthaldehyde**:

1-Naphthaldehyde was distilled and used.

2.2.7. **Diethylamine, Triethylamine:**

Diethylamine and Triethylamine were distilled before using.

2.2.8. Reagent grade Imidazole, Manganese acetate, Zinc acetate, Copper acetate, Sodium acetate, BF_3-etherate, p-Chloranil, DDQ, Sodium carbonate, Perchloric acid, Tetrabutylammonium bromide, etc. were used as received.

2.3. PREPARATION OF SUPPORTING ELECTROLYTE [2,3]:

Preparation of supporting electrolyte, Tetrabutylammonium perchlorate (TBAP) involves two steps as follows:

i) Preparation of Sodium perchlorate:

Sodium perchlorate was prepared by neutralization of Sodium carbonate with Perchloric acid. The volume of the reaction mixture was reduced by concentrating it in a water bath and then allowed to cool when crystals of sodium perchlorate separate out. The crystals were filtered out and recrystallized several times from distilled water.

ii) Preparation of Tetra-n-butylammonium perchlorate (TBAP):

A saturated solution of tetrabutylammonium bromide was prepared in distilled water. To this solution, sodium perchlorate crystals were added when crystals of TBAP separates out instantly. Constant stirring is done till precipitation of TBAP is completed. The crystals of TBAP were filtered out, washed several times with distilled water and then recrystallized twice from methanol. Glassy crystals of TBAP were formed and the purity of the product was check by running a Cyclic Voltammogram.

2.4. SYNTHESIS OF PORPHYRINS:

2.4.1. meso-5,10,15,20 – Tetrakis(2-methoxyphenyl) porphyrin:

meso-5,10,15,20 – Tetrakis(2-methoxyphenyl) porphyrin, [T(2-OMeP)P] was prepared by the method of Wagner and Lindsey[4]. In a 500mL round bottom flask fitted with a reflux condenser and a nitrogen

bubbler,2-Methoxybenzaldehyde (0.485mL, 2.98mmol) and pyrrole (210μL, 2.98 mmol) were dissolved in 300mL of distilled chloroform. After purging the solution with nitrogen gas for 5 minutes, the reaction was initiated by adding catalytic amount of BF_3-etherate (120 μL of 2.5M stock solution). The reaction mixture was then stirred at room temperature for 1 hour. The progress of the reaction was monitored by taking aliquots of the reaction mixture at regular intervals, oxidizing with *p*-chloranil, followed by absorption spectrophotometry[5]. At the end of 1 hour, *p*-Chloranil (0.7327g, 2.98mmol) was added in powder form and the reaction mixture was gently refluxed (61°C) for 1 hour. The completion of the reaction was monitored by UV –Vis spectroscopy and ^1H NMR spectroscopy. The mixture was evaporated to dryness and the crude product was washed with methanol until the filtrate was clear. It was then purified by silica gel column chromatography using

dichloromethane as the eluent. The purity of the product was checked by TLC and UV – Visible absorption spectra.

λ_{max} (nm) (in chloroform): 414, 513, 546, 588, 642.

2.4.2. meso-5,10,15,20–Tetrakis(4-methoxyphenyl) porphyrin:

meso - 5, 10, 15, 20 – Tetrakis (4 - methoxy phenyl) porphyrin, [T(4-OMeP)P] was prepared by the method of Wagner and Lindsey[4] by taking 4-Methoxybenzaldehyde and pyrrole as described above.

λ_{max} (nm) (in chloroform): 421, 518, 556, 593, 649.

2.4.3. meso-5,10,15,20–Tetrakis(1-naphthyl) porphyrin, (TNP):

(TNP) was prepared by the method of Wagner and Lindsey[4] as described above by taking 1-Naphthaldehyde and pyrrole.

λ_{max} (nm) (in chloroform): 423, 515, 548, 589, 644.

2.5. SYNTHESIS OF METALLOPORPHYRINS:

2.5.1. MANGANESE PORPHYRINS:

(Figure – 2.1)

2.5.1.1 $Mn^{(III)}$[T(2-OMeP)P] OAc:

Mn[T(2-OMeP)P] OAc was prepared as described in the literature[6,7]. The reaction was carried out by taking a mixture of Manganese (II) acetate (335mg, 1.37mmol) in methanol and [T(2-OMeP)P] (358.2mg, 0.42mmol) in chloroform and then refluxed in a 100mL round bottom flask for about 5 hours. The completion of the reaction was monitored by UV – Visible absorption spectroscopy. The crude product was washed with water several times and then purified by silica gel column chromatography using dichloromethane as an eluent. The purity of the product was checked by TLC and UV-visible spectra.

λ_{max} (nm) (in chloroform): 391, 406, 480, 581, 616.

2.5.1.2. $Mn^{(III)}$[T(4-OMeP)P]OAc:

Mn[T(4-OMeP)P]OAc was prepared according to the above procedure as described in the literature[6,7]

λ_{max} (nm) (in chloroform): 391, 406, 480, 581, 619.

2.5.1.3. $Mn^{(III)}$[TNP]OAc:

Mn [TNP]OAc was prepared according to the above procedure as described in the literature[6,7]

λ_{max} (nm) (in chloroform): 391, 406, 480, 581, 619.

2.5.2. COPPER PORPHYRINS: (Figure – 2.2)

2.5.2.1. Cu[T(4-OMeP)P] :

Cu[T(4-OMeP)P] was prepared as described in the literature[6,7]. The reaction was carried out by taking a mixture of Cupric (II) acetate (335mg, 1.37mmol) in methanol and [T(4-OMeP)P] (358.2mg, 0.42mmol) in chloroform and then refluxed in a 100mL round bottom flask for about 5 hours. The completion of the reaction was monitored by UV –Vis absorption

spectroscopy. The crude product was washed with water several times and then purified by silica gel column chromatography using dichloromethane as an eluent. The purity of the product was checked by TLC and UV-visible spectra.

λ_{max} (nm) (in chloroform): 419, 541.

2.5.2.2. Cu [TNP]:

Cu[TNP] was described according to the above procedure as described in the literature[6,7].

λ_{max} (nm) (in chloroform): 420, 540.

2.5.3. ZINC PORPHYRINS: (Figure – 2.2)

2.5.3.1. Zn[T(4-OMeP)P] :

Zn[T(4-OMeP)P] was prepared as described in the literature[6,7]. The reaction was carried out by taking a mixture of Zinc acetate (335mg, 1.37mmol) in methanol and [T(4-OMeP)P] (358.2mg, 0.42mmol) in chloroform and then refluxed in a 100mL round

bottom flask for about 3 hours. The completion of the reaction was monitored by UV –Vis absorption spectroscopy. The crude product was washed with water several times and then purified by silica gel column chromatography using dichloromethane as an eluent. The purity of the product was checked by TLC and UV-visible spectra.

λ_{max} (nm) (in chloroform): 423, 473, 549, 590.

2.5.3.2. Zn [TNP]:

Zn[TNP] was described according to the above procedure as described in the literature[6,7].

λ_{max} (nm) (in chloroform): 424, 548, 601.

2.6 INSTRUMENTATION :

2.6.1. UV-VIS SPECTROPHOTOMETRIC MEASUREMENTS:

UV - Visible absorption spectroscopy was measured at room temperature by BECKMAN DU@ 650 SPECTROPHOTOMETER and PERKIN ELMER LAMBDA 25 UV/VIS SPECTROPHOTOMETER. The reactions between the metalloporphyrins and different amines were done in the spectrophotometric quartz cuvette. UV - Visible absorption spectra were recorded in between the range 350 – 750 nm. The amine was added to the solution in the cell, shaken thoroughly and allowed to stand for some time and then recorded. The process was continued for each addition of amine till saturation was attained.

2.6.2. CYCLIC VOLTAMMETRIC MEASUREMENTS:

Redox potentials were measured by using CHI 620B ELECTROCHEMICAL ANALYZER. The electrolytic cell consists of a platinum electrode used as the working electrode, an Ag/AgCl electrode employed as the reference electrode and a platinum wire which served as the auxiliary electrode. Dichloromethane was used as the solvent and Tetrabutylammonium perchlorate (TBAP) as the supporting electrolyte. 10^{-3}M metalloporphyrin solution was taken in the cell and deaeration was accomplished by bubbling nitrogen gas through the solution before every measurement. Nitrogen blanketed the solution during the recordings.

Calibration of $E_{1/2}$ values and diffusion current were done by using a known concentration of pure ZnTPP in dichloromethane /TBAP medium.

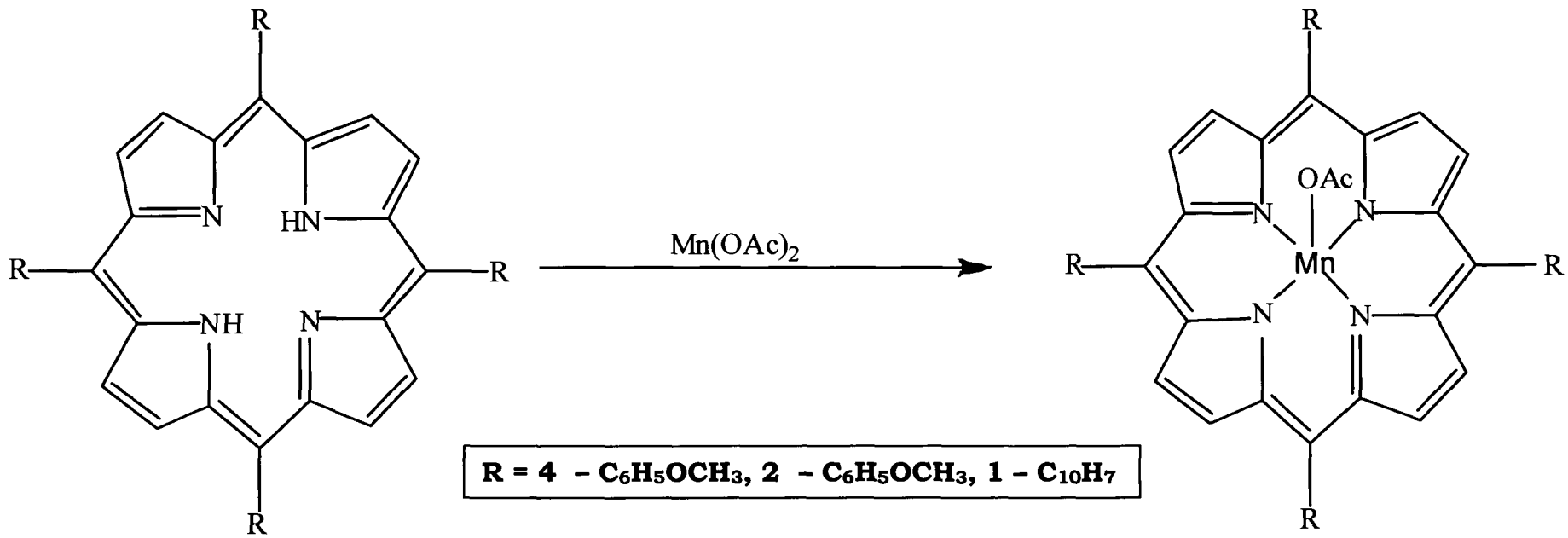

Figure: 2.1: ***Scheme Showing The Synthesis Of Manganese Porphyrin.***

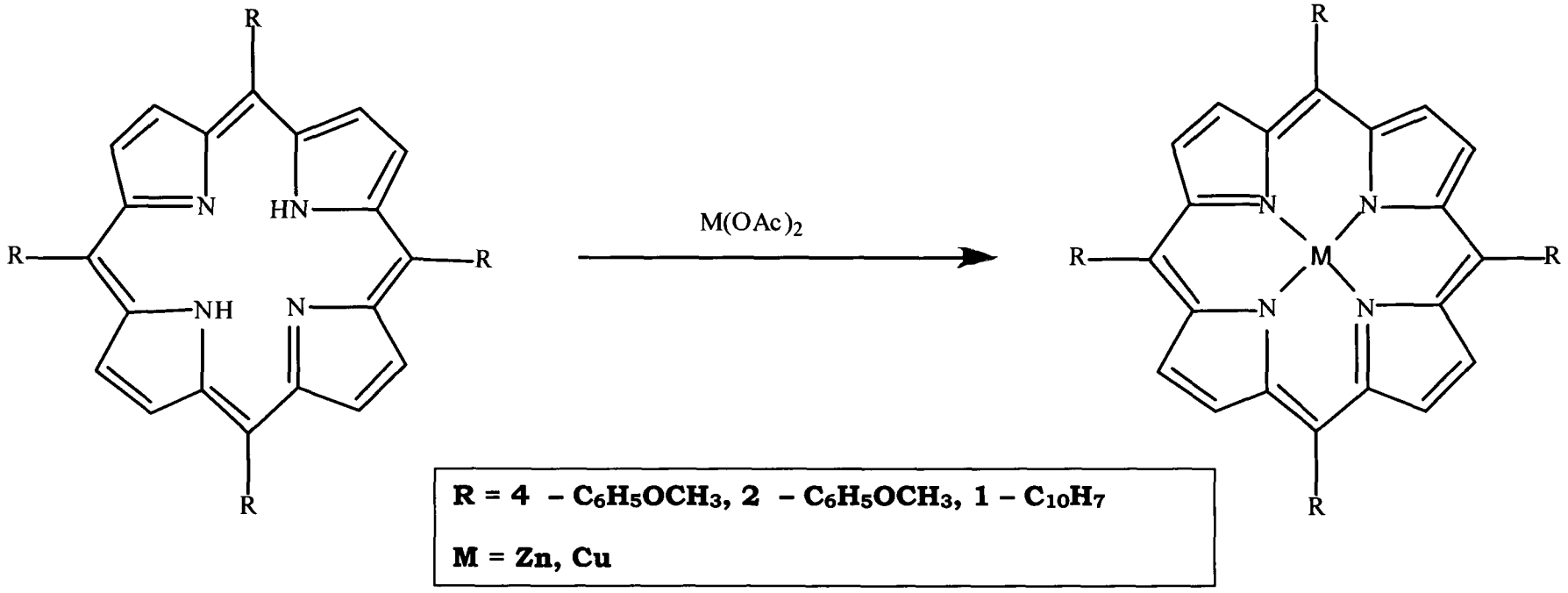

Figure: 2.2: ***Scheme Showing The Synthesis Of Zinc And Copper Porphyrin.***

REFERENCES:

1. A.I. Vogel, *A text book of practical organic Chemistry*, Fourth Edition (ELBS) Longman, London, 1978.

2. *Hand book of Preparative Inorganic Chemistry*, Edited by G.Brauer (Academic Press, New York, 1965) **Vol. II.** pp 1185.

3. *Inorganic Synthesis*, Editor-in-Chief: Therald Moellur (McGraw Hill, 1975), **Vol.5**, pp154.

4. Richard W. Wagner, David S. Lawrence, and J. S. Lindsey., *Tetrahedron Letters*, **28**, 3069 (1987).

5. J.S. Lindsey, H.C. Hsu, I.C. Schreiman, *Tetrahedron Lett.*, **27**, 4969 (1986).

6. J.G. Erdman, V.G. Ramsay, N.W. Kalenda, and W.E. Hanson, *J.Am.Chem.Soc.*, **78**, 5844 (1956).

7. A.D. Adler, F.R. Longo, F. Kampus, and J.Kim, *J. Inorg. Nucl. Chem.* **32**, 2443 (1970).

CHAPTER -3

EFFECTS OF AXIAL LIGANDS ON THE UV-VISIBLE SPECTRA OF Mn(III)[T(2-OMeP)P]OAc; Mn (III)[T(4-OMeP)P]OAc AND Mn(III) [T(naphthyl)P]OAc

CHAPTER – 3

3.1. INTRODUCTION:

This chapter deals with the effect of axial ligands such as diethylamine, triethylamine and imidazole on the UV-Visible spectra of Mn(III) porphyrins. The changes in the spectral pattern of the three metalloporphyrins are presented and discussed in this chapter.

3.2. RESULTS:

All three metalloporphyins exhibit similar spectral pattern. Results are summarized in Tables 3.A, 3.B and 3.C.

3.2.1. Mn(III)[T(2-OMeP)P] OAc:

The absorption band positions (wavelength) of 10^{-5}M solution of Mn(III)[T(2-OMeP)P])]OAc in CH_2Cl_2 are presented in the Table: 3.A. Addition of 0.1 mL of diethylamine show some shifts in the absorption

bands. The B band (Soret band) shifts from 480 nm to 471 nm with slightly increased intensity. Band III shifts from 616 nm to 609 nm while band IV shifts from 581 nm to 575 nm (Figure: 3.2.1.a). On adding 0.3 mL of diethylamine a new band (Soret band) appears at 441nm (Figure:3.2.1.b). Further additions of diethylamine exhibits decrease in the intensity of the Soret band at 471nm and it subsequently disappears while the intensity of the new Soret band at 441 nm increases (Figure: 3.2.1.c). The intensities of the band at 609 nm and the band at 575 nm diminishes (due to dilution). All three bands i.e. band III, band IV and band V are found to be blue shifted. The pattern of spectra with triethylamine remains same except with an additional feature, the occurrence of an isosbestic point at 458 nm (Figure: 3.2.1.d).

3.2.2. Mn (III)[T(4-OMeP)P]OAc:

The absorption band positions (wavelength) of 10^{-5}M solution of Mn(III)[T(4-OMeP)P] in CH_2Cl_2 are

given in the Table: 3.B. Initial addition of diethylamine (0.1 mL) exhibits shifts of the Soret band from 480 nm to 473 nm (decreased intensity), band III from 619 nm to 617 nm and the band IV from 581nm to 579 nm (Fig:3.2.2.a). Further addition of diethyl amine gives the product which exhibits a spectrum with Soret band at 441nm, band III at 617 nm and band IV at 579 nm. An additional new band at 676 nm is observed the intensity of which goes on increasing with the addition of diethylamine (Fig: 3.2.2.b).

The changes in the spectral pattern remains more or less the same with triethylamine except the additional band at 676nm is absent (Fig: 3.2.2.c) .

With imidazole the band V (Soret band) shows a blue shift from 480 nm to 473 nm and the band IV is also blue shifted from 581nm to 576 nm. On the other hand band III shows a red shift from 619nm to

622nm. It is to be noted that the Soret band do not show any further shift to 441nm on subsequent addition of imidazole.

3.2.3 Mn(III)[TNP]OAc:

The UV-Visible absorption spectrum of 10^{-5}M solution of Mn(III)[TNP]OAc exhibits Soret band at 481nm, band IV at 577 nm and band III at 607 nm (Table: 3.C). Addition of 0.1ml diethylamine shows a blue shift of the Soret band from 481nm to 475 nm with slightly increase in the intensity. Band III and IV show slight red shifts. On adding 0.2 mL (further addition of 0.1 mL) of diethylamine the Soret band splits into two, one at 445 nm (ε=0.39) and the other at 475 nm (ε=1.28) (Fig: 3.2.3.a). On subsequent addition of diethylamine the intensity of the new Soret band at 445 nm increases while that of the Soret band at 475 nm decreases and disappears (Fig: 3.2.3.b).

With triethylamine, the new soret band occurs at 443 nm while the band III at 607 nm is red shifted to 610 nm and band IV at 577 nm is slightly blue shifted to 573 nm (Fig: 3.2.3.c).

3.3. DISCUSSION:

On initial Addition of amine to all the three manganese porphyrins, viz. Mn(III)[T(2-OMeP)P]OAc, Mn(III)[TNP]OAc and Mn(III)[T(4-OMeP)P]OAc, the UV-Visible spectra exhibit blue shifted Soret band within the range 472nm - 475 nm. This is due to the replacement of the axial ligand OAc^- with amine. On subsequent addition of amine the intensity of this Soret band diminishes and a new Soret band appears at around 441nm - 445nm. This could be due to the coordination of amine as the sixth ligand as presented in the Scheme: 3.1. Another possibility is the reduction of Mn(III) to Mn(II)[1, 2] by amine coordinating as the fifth and sixth ligands as represented in the

Scheme:3.2. These schemes are proposed because the added amine in the cuvette could be in excess and may act as ligating solvent although the solvent used is CH_2Cl_2. Initial addition of 0.1 ml amine does not show Soret band around 441 – 445nm.

$$[Mn(III)P\ OAc] + Amine = [Mn(III)P\{Amine)]^+ + OAc^-$$

$$[Mn(III)P\ (Amine)]^+ + Amine = [Mn(III)\ P\ (Amine)_2]^+$$

(Where P=T(2-OMeP)P, T(4-OMeP)P and TNP).

Scheme: 3.1

$$[Mn(III)P\ OAc] + Amine = [Mn(III)\ P\ (Amine)]^+ + OAc^-$$

$$[Mn(III)\ P(Amine)]^+ + Amine = [Mn(II)\ P\ (Amine)_2]$$

Scheme: 3.2.

Scheme: 3.1 is most preferred because in a ligating solvent or when potential ligands are present, the six – coordinated Mn(III) prophyrins are obtained.

Scheme: 3.2 is possible only when there is electron transfer from axial ligand to Mn(III) ion. Lanskey et.al[3] have reported the spectro - electrochemical reduction of Mn(V) - Oxo corrolazine in Pyridine and obtained the corresponding Mn(III) product with Soret band at λ_{max} = 447 nm. Y.O. Su and co-workers [6] have reported the spectrophotometric pH titration of Mn(III) (2-TMPyP) in the range of pH = 7.0 to 11.4, and have shown the formation of Mn(III) (2-TMPyP) $(OH)_2$ with Soret band at λ_{max} = 442 nm. The possibility of reduction of Mn(III) to Mn(II) is also proposed for $(Cl_8TPP)Mn(IIII)OH(Sol)$ to manganese (II) porphyrin in a ligating solvent[4]. S. Jeon and co-workers [5] have reported the possible mechanism for the reaction of $(Cl_8TPP)Mn(III)Cl$ with hydroxide ion in a ligating medium MeCN. Three intermediates were observed viz. $(Cl_8TPP)Mn(III)OH(Sol)$ with Soret band at λ_{max} = 476 nm, $(Cl_8TPP)Mn(II)(sol)$ with Soret band at λ_{max} = 436 nm and $[(Cl_8TPP)Mn(II)(OH)]^-$ with Soret band at λ_{max} = 444 nm. They have also reported that

in excess of $OH(H_2O)$ a stable species $[(Cl_8TPP)Mn(II)(OH)]^-$ is formed. Reaction of $(Cl_8TPP)Mn(III)Cl$ with excess OH (H_2O) in pyridine as a ligating solvent also produces the species $(Cl_8TPP)Mn(II)Py$ or $[(Cl_8TPP)\ Mn(II)(OH)]$.

Another important aspect to incorporate in our discussion is the conformations of porphyrin ligand[7-15]. Porphyrin ligands exhibit different conformations such as planar, ruffled and saddled forms. In a non planar metalloporphyrin some interactions exist between d-orbitals of the metal atom and the porphyrin ligand orbitals (symmetry - allowed) enabling charge flow between metal atom and the porphyrin ligand. In a ruffled metallo-porphyrin an interaction of metal d_{xy} – porphyrin (a_{2u}) exists. Such an interaction has been characterized by NMR of a low - spin six -coordinated iron (III) porphyrins. This type of interaction is also indicated theoretically. On the other hand in a saddled porphyrin metal $(d_{x^2-y^2})$ –

porphyrin (a_{2u}) orbital interaction occurs. Such interactions were observed in (Cu(II) (OETPP)·)]$^+$ cation.

Axial ligand – metalloporphyrin interactions also affect the conformation of the metalloporphyrin. As a result orientation of the axial ligand may affect the spectroscopic and redox properties of the metalloporphyrin. In addition to it, the flow of charge (electrons) from the axial ligand via the metal atom to the porphyrin ligand may cause red shift in the visible spectrum[16 - 21] . Red shifts are generally observed for non planar porphyrins. These red shifts are due to decrease in energy gap between the HOMO (a_1u/a_2u) and the LUMO (e_g) orbitals of the porphyrin ligand. In the present case with the addition of amine, B bands (Soret bands) are observed to be blue shifted. One reason we attribute is due to change in conformations from more distorted i.e. ruffled/saddled form to less distorted form on coordinating with the axial ligands. In a planar metalloporphyrin the metal d - orbitals and

the porphyrin ligand orbitals (a_1u/a_2u) are orthogonal. On the other hand [Mn(III)POAc] is in ruffled/saddled form. Thus, we observed blue shifted B band in $[Mn(III)P(Amine)_2]^+$. By the same token, [Mn(III)[TNP] $(Amine)_2]^+$exhibit lesser blue shift (λ_{max} = 445 nm).

Another interesting observation is the reproduction of the original [Mn(III)POAc] spectra after the removal of amine (by warming). It is obvious that $[Mn(III)P(Amine)_2]^+$ is formed in excess of amine. However, similar blue shift of B - band (λ_{max} = 441 nm - 445 nm) could not be observed with imidazole.

3.4 CONCLUSION:

From the UV - Visible studies of Managanese (III) porphyrins following observations are made:

(i) Initial addition of amine replaces the acetate ion as axial ligand.

(ii) Further addition of amine generates six – coordinated Mn(III) porphyrin.

(iii) The possibility of reduction of Mn(III) to Mn (II) is also not ruled out.

(iv) Change of metalloporphyrin conformation from ruffled/saddled form towards planar form on coordinating with the amine as the sixth ligand. Thus the B bands are blue shifted.

We conclude here with a note that the above observations will be further supplemented by Cyclic Voltammetry in the next chapter.

TABLE: 3.A. UV-Visible Absorption Spectral Data Of Mn(III)[T(2-OMeP)P])]OAc At Room Temperature

SOLVENT : Dichloromethane

CONCENTRATION : 10^{-5} M

Compounds	Amine Used	Vol. Of Amine Added (mL)	Absorption Bands (nm)					Isobestic Point (nm)
			III	IV	V	Va	VI	
$Mn^{III}[T(2\text{-}OMeP)P]OAc$		0	616 (0.12)	581 (0.16)	480 (1.4)	406 (1.2)	391 (1.2)	-
$Mn^{III}[\{T\ (2\text{-}OMeP)P\}(Et_2NH)]^+$	Diethylamine	0.1	609 (0.1)	575 (0.15)	471 (1.42)	405 (1.2)	378 (1.2)	-
$Mn^{III}[\{T(2\text{-}OMeP)P\}(Et_2NH)]^+ + Mn^{III}[\{T(2\text{-}OMeP)P\}(Et_2NH)_2]^+$	Diethylamine	0.3	609 (0.1)	575 (0.15)	441 (0.66) 471 (1.19)	405	378 (1.2)	-
$Mn^{III}[\{T(2\text{-}OMeP)P\}(Et_2NH)_2]^+$	Diethylamine	0.9	609 (0.09)	575 (0.14)	441 (1.72)	-	-	-
$Mn^{III}[\{T\ (2\text{-}OMeP)P\}(Et_3N)]^+$	Triethylamine	0.1	608 (0.1)	575 (0.15)	471 (1.50)	406 (1.2)	391 (1.2)	-
$Mn^{III}[\{T(2\text{-}OMeP)P\}(Et_3N)]^+ + Mn^{III}[\{T(2\text{-}OMeP)P\}(Et_3N)_2]^+$	Triethylamine	0.3	608 (0.1)	575 (0.15)	441 (0.34) 471 (1.46)	406 (1.2)	380 (1.2)	-
$Mn^{III}[\{T(2\text{-}OMeP)P\}(Et_3N)_2]^+$	Triethylamine	1.5	608 (0.05)	574 (0.08)	441 (1.46)	-	-	458

TABLE: 3.B. UV-Vis Absorption Spectral Data Of Mn(III)[T(4-OMeP)P])]OAc At Room Temperature

SOLVENT : Dichloromethane

CONCENTRATION : 10^{-5} M

Compounds	Amine Used	Vol. Of Amine Added (mL)	Absorption Bands (nm)				
			III	IV	V	Va	VI
$Mn^{III}[T(4\text{-}OMeP)P]OAc$		0	619 (0.13)	581 (0.11)	480 (1.4)	406 (1.2)	391 (1.2)
$Mn^{III}[\{T\ (4\text{-}OMeP)P\}(Et_2NH)]^+$	Diethylamine	0.1	617 (0.12)	579 (0.1)	473 (1.3)	405 (1.2)	380 (1.2)
$Mn^{III}[\{T(4\text{-}OMeP)P\}(Et_2NH)]^+ + Mn^{III}[\{T(4\text{-}OMeP)P\}(Et_2NH)_2]^+$	Diethylamine	0.3	617 (0.1) 676 (0.05)	579 (0.09)	441 (0.3) 473 (1.19)	-	-
$Mn^{III}[\{T(4\text{-}OMeP)P\}(Et_2NH)_2]^+$	Diethylamine	0.9	617 (0.09) 676 (0.21)	579 (0.08)	441 (1.42)	-	-
$Mn^{III}[\{T\ (4\text{-}OMeP)P\}(Et_3N)]^+$	Triethylamine	0.1	616 (0.12)	576 (0.10)	472 (1.50)	406 (1.2)	378 (1.2)
$Mn^{III}[\{T(4\text{-}OMeP)P\}(Et_3N)]^+ + Mn^{III}[\{T(4\text{-}OMeP)P\}(Et_3N)_2]^+$	Triethylamine	0.4	616 (0.1)	576 (0.09)	441 (0.8) 472 (1.34)	406 (1.2)	380 (1.2)
$Mn^{III}[\{T(4\text{-}OMeP)P\}(Et_3N)_2]^+$	Triethylamine	1.5	616 (0.05)	576 (0.03)	441 (1.48)	-	-
$Mn^{III}[\{T\ (4\text{-}OMeP)P\}(IM)]^+$	Imidazole (IM)	0.1	622 (0.1)	576 (0.1)	473 (1.38)	-	-

TABLE: 3.C. UV-Vis Absorption Spectral Data Of Mn(III)[TNP]]]OAc At Room Temperature

SOLVENT : Dichloromethane

CONCENTRATION : 10^{-5} M

Compound	Amine Used	Vol. Of Amine Added (mL)	Absorption Bands (nm)				
			III	IV	V	Va	VI
$Mn^{III}[TNP]OAc$		0	607 (0.06)	577 (0.11)	481(1.14)	406 (1.2)	391 (1.2)
$Mn^{III}[\{TNP\}(Et_2NH)]^+$	Diethylamine	0.1	612 (0.04)	579 (0.09)	475 (1.19)	405 (1.1)	380 (1.1)
$Mn^{III}[\{TNP\}(Et_2NH)]^+ + Mn^{III}[\{TNP\}(Et_2NH)_2]^+$	Diethylamine	0.2	617 (0.03)	579 (0.07)	445 (0.39) 475 (1.28)	-	-
$Mn^{III}[\{TNP\}(Et_2NH)_2]^+$	Diethylamine	1.5	609 (0.03)	575 (0.06)	445 (1.93)	-	-
$Mn^{III}[\{TNP\}(Et_3N)]^+$	Triethylamine	0.1	610 (0.04)	573 (0.1)	475 (1.22)	406 (1.1)	378 (1.1)
$Mn^{III}[\{TNP\}(Et_3N)]^+ + Mn^{III}[\{TNP\}(Et_3N)_2]^+$	Triethylamine	0.6	610 (0.03)	573 (0.09)	443 (0.33) 475 (1.33)	-	-
$Mn^{III}[\{TNP\}(Et_3N)_2]^+$	Triethylamine	1.5	610 (0.03)	573 (0.08)	443 (0.63)	-	-

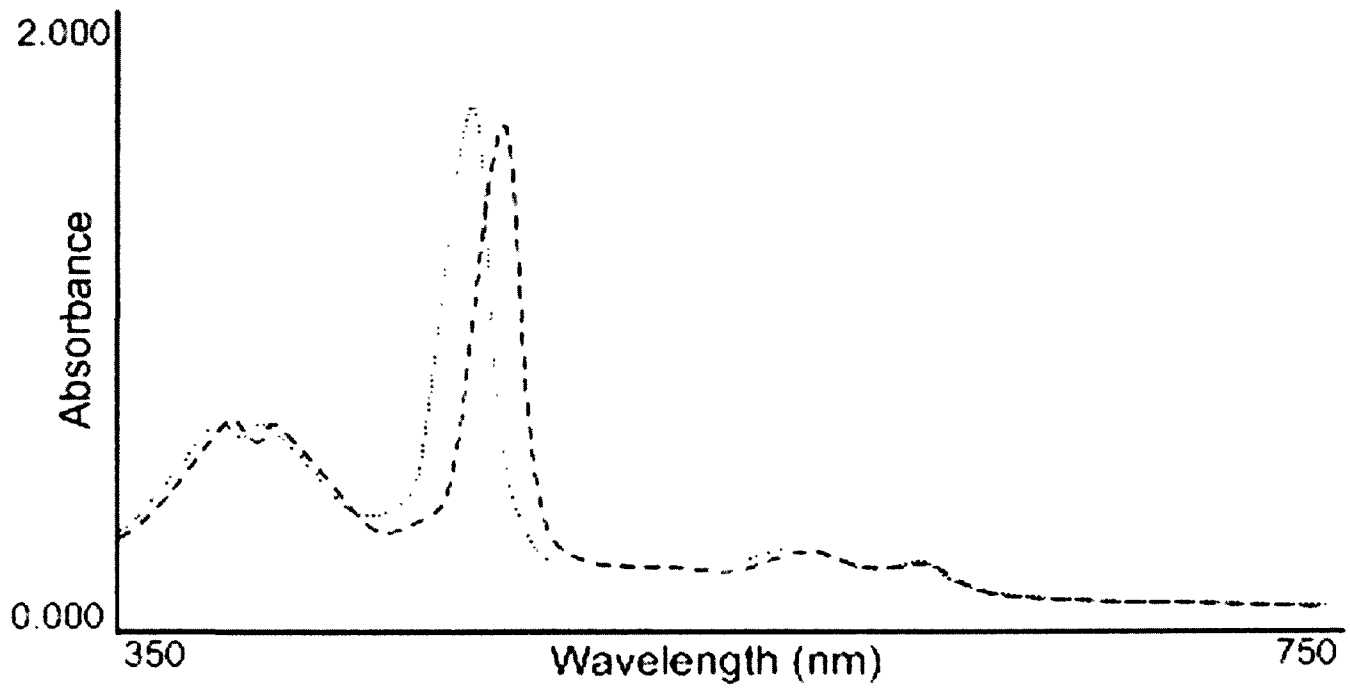

Figure 3.2.1.a. **UV-Visible Absorption Spectrum of Mn(III)[T(2-OMeP)P]OAc in CH_2Cl_2 at room temperature (------); on addition of 0.1ml of Diethylamine (.....).**

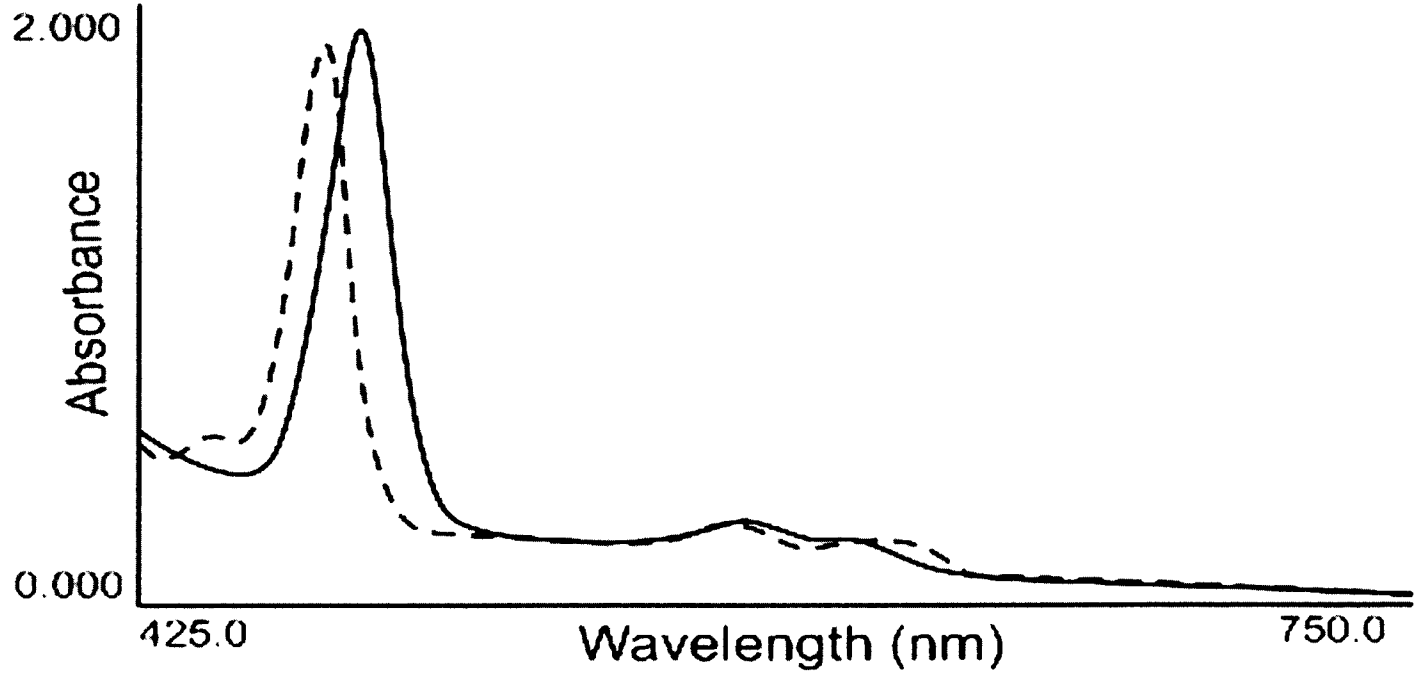

Figure 3.2.1.b. **UV-Visible Absorption Spectrum of Mn(III)[T(2-OMeP)P]OAc in CH_2Cl_2 at room temperature (————); on addition of 0.3 ml of Diethylamine (— — —).**

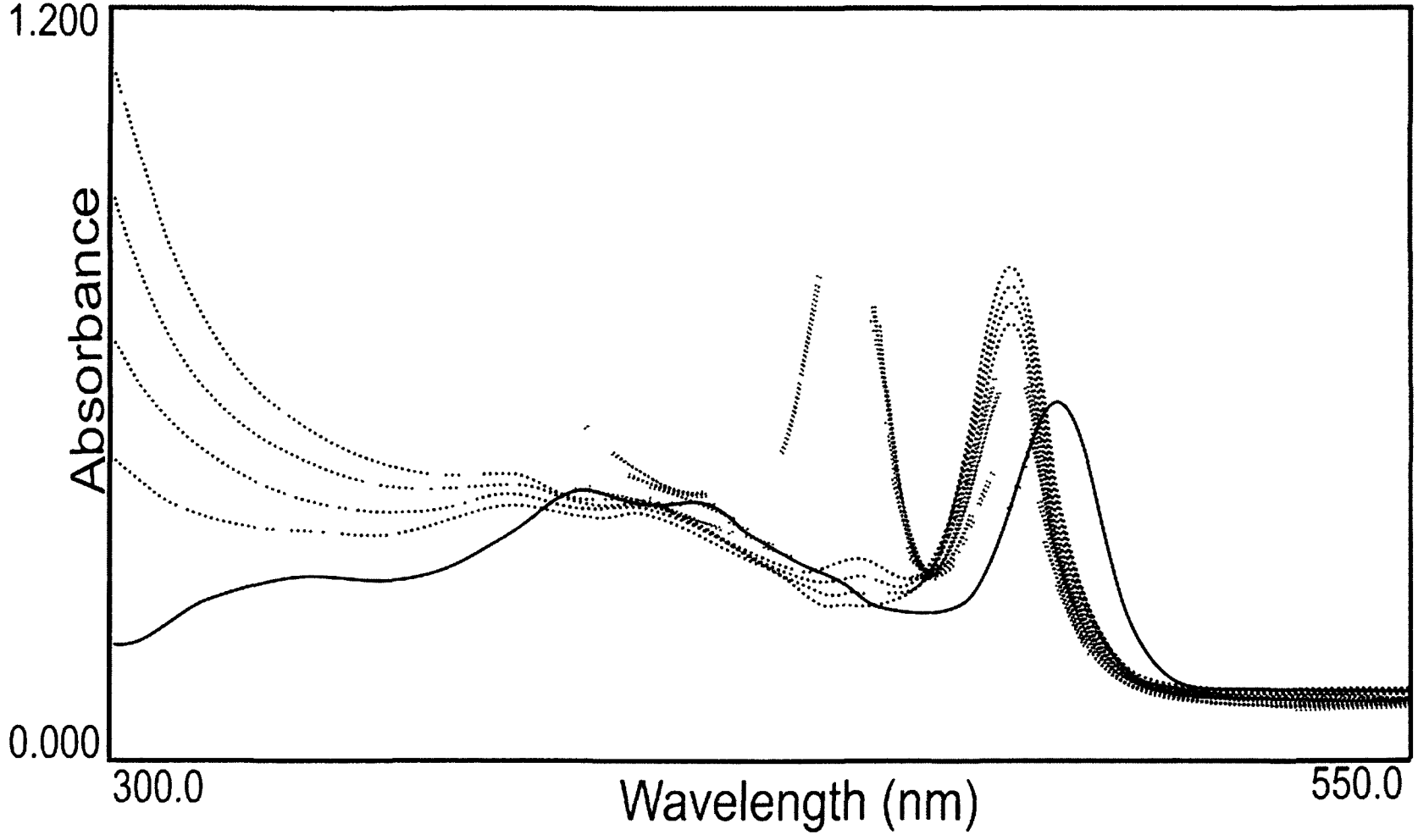

Figure 3.2.1.c. **UV-Visible Overlay Spectra of Mn(III)[T(2-OMeP)P]OAc in CH_2Cl_2 at room temperature (————); on continuous addition of Diethylamine (— — —).**

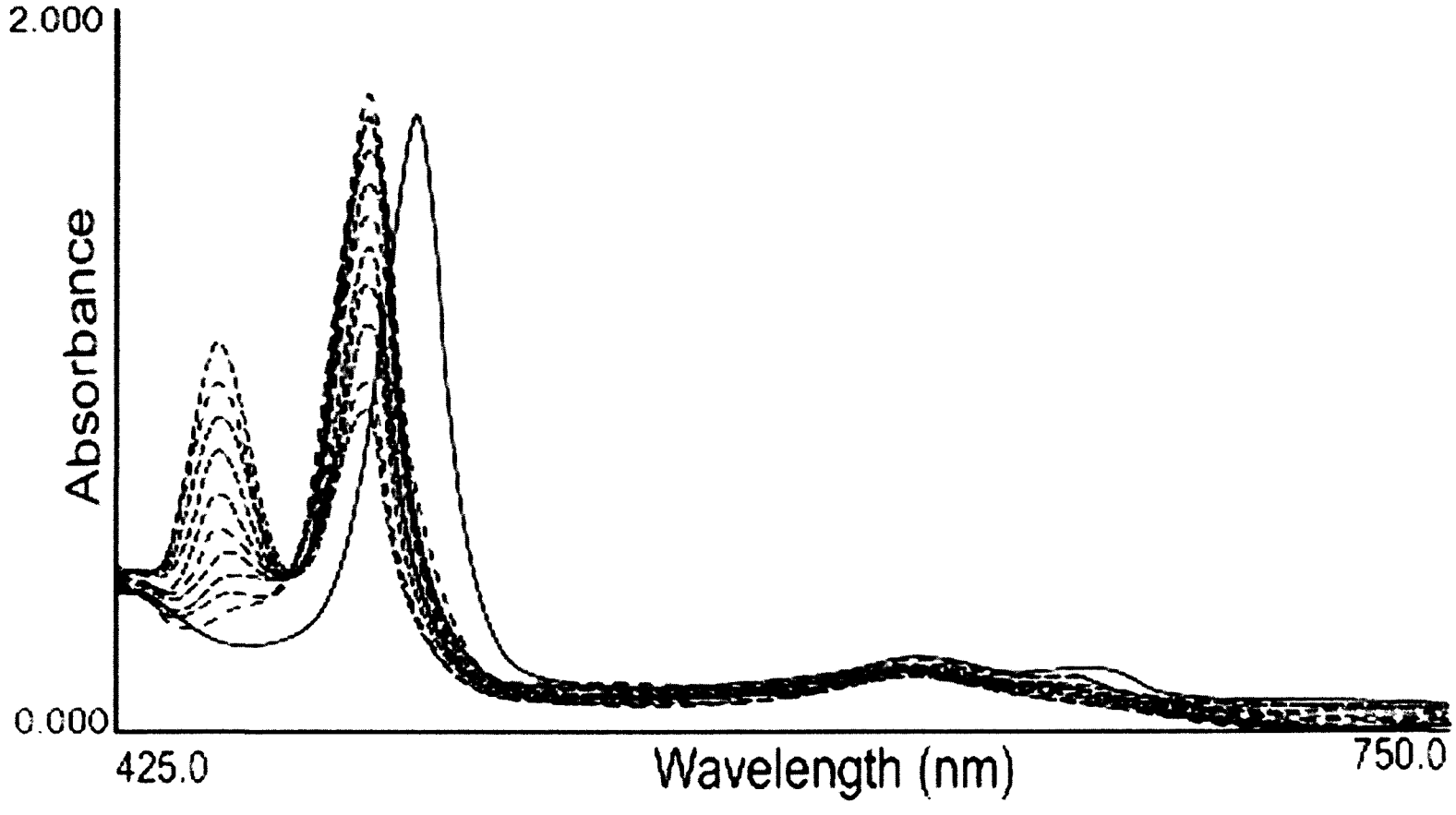

Figure 3.2.1.d. **UV-Visible Overlay Spectra of Mn(III)[T(2-OMeP)P]OAc in CH_2Cl_2 at room temperature (————); on addition of Triethylamine (— — —).**

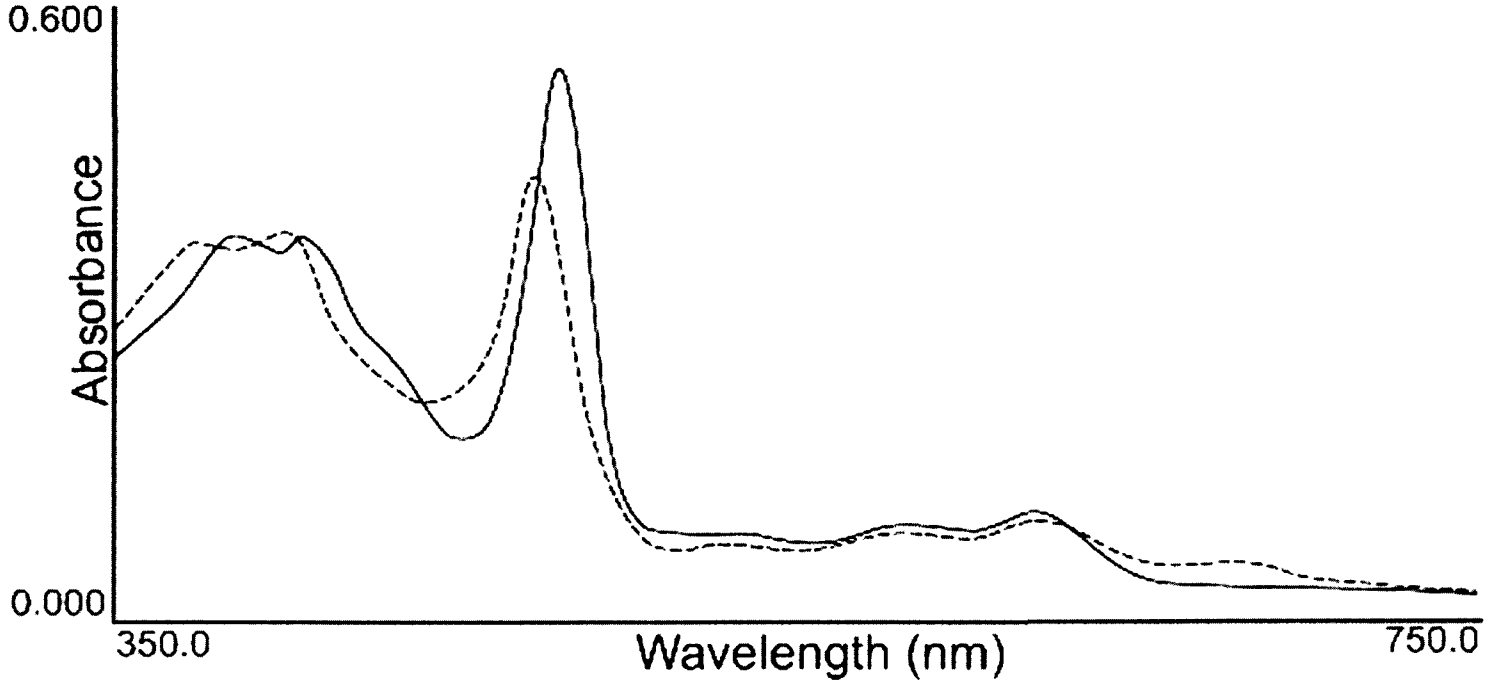

Figure 3.2.2.a. UV-Visible Absorption Spectrum of Mn(III)[T(4-OMeP)P]OAc in CH_2Cl_2 at room temperature (————); on addition of 0.1ml of Diethylamine (— — —).

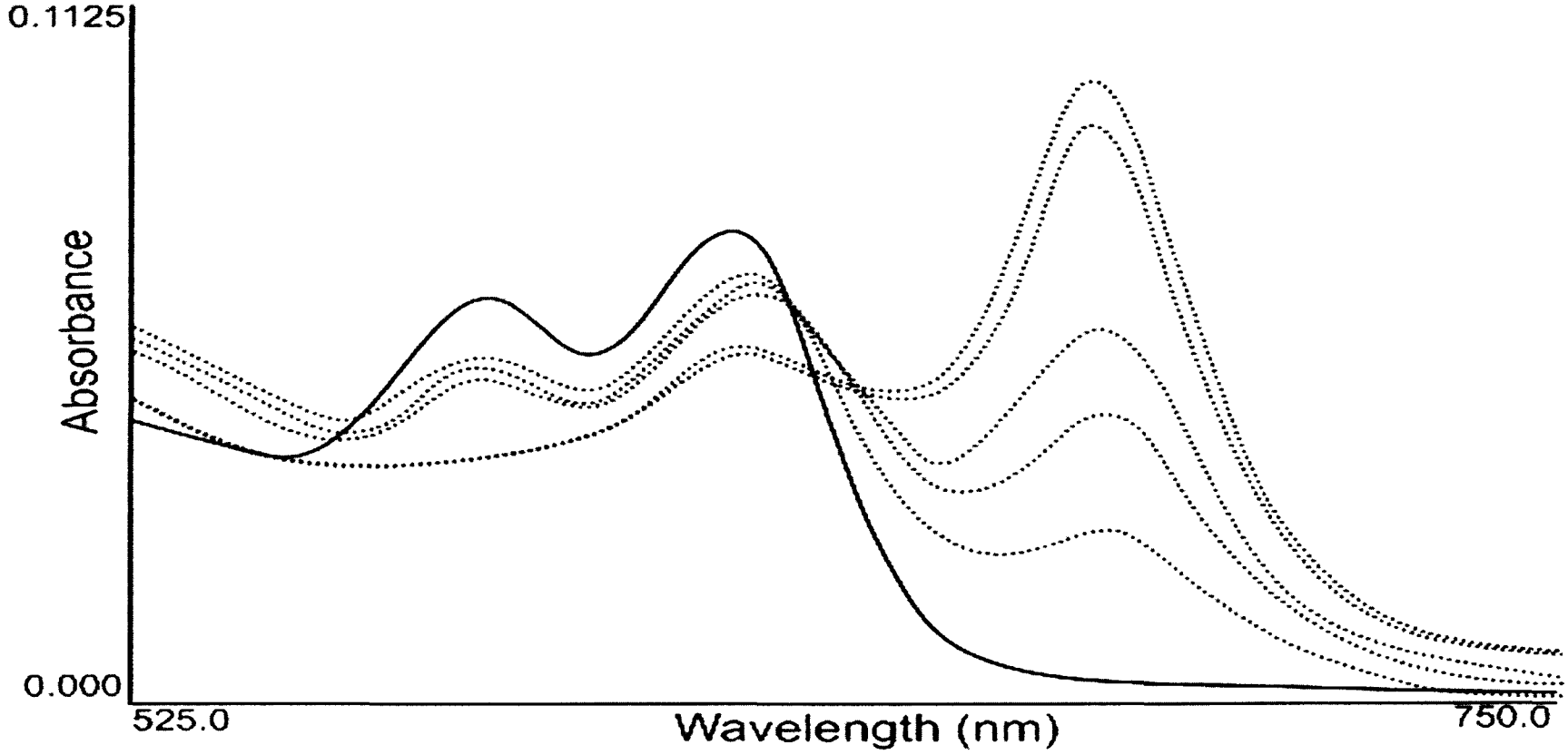

Figure 3.2.2.b. UV-Visible Absorption Spectrum of Mn(III)[T(4-OMeP)P]OAc in CH_2Cl_2 at room temperature (————); on continuous addition of Diethylamine (— — — -).

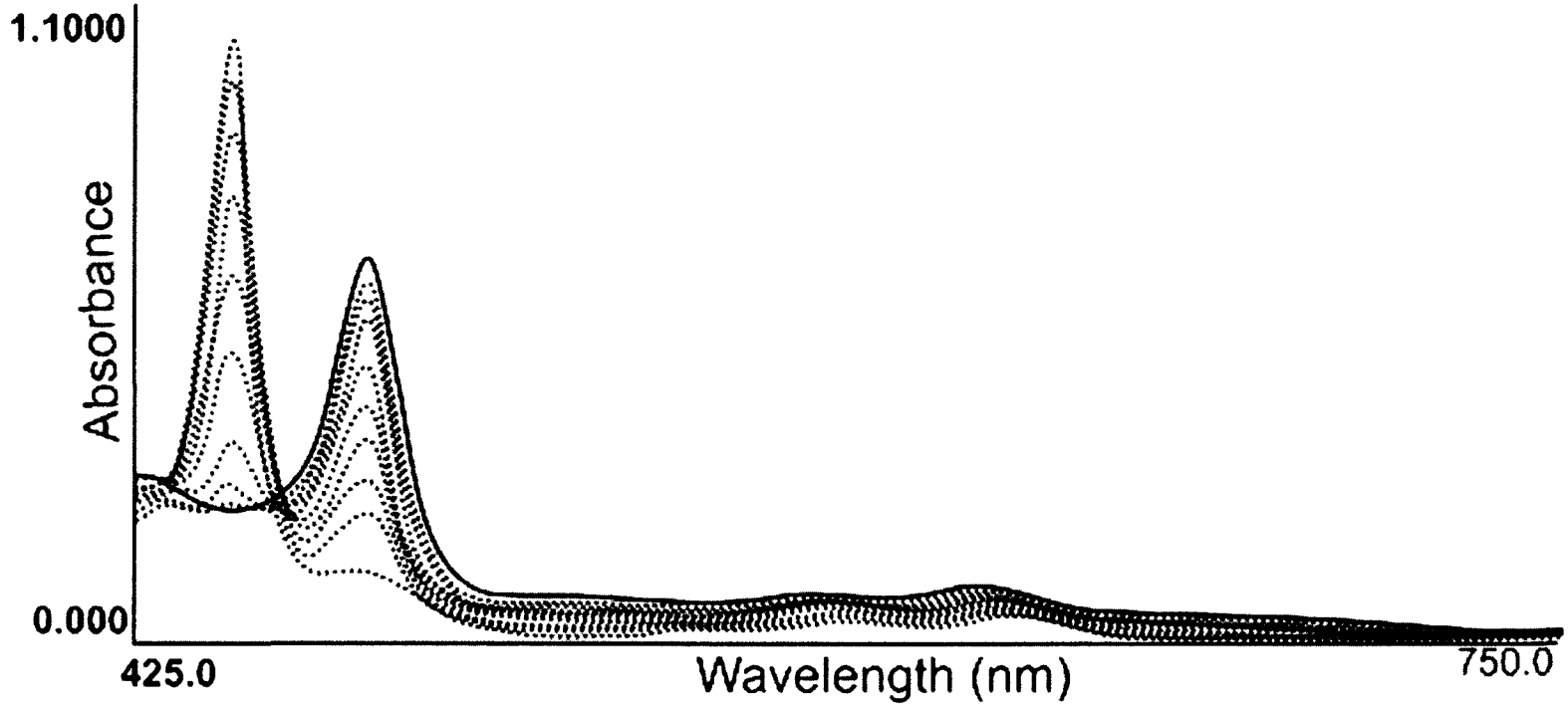

Figure 3.2.2.c. **UV-Visible Overlay Spectra of Mn(III)[T(4-OMeP)P]OAc in CH_2Cl_2 at room temperature (————); on addition of Triethylamine (— — — -).**

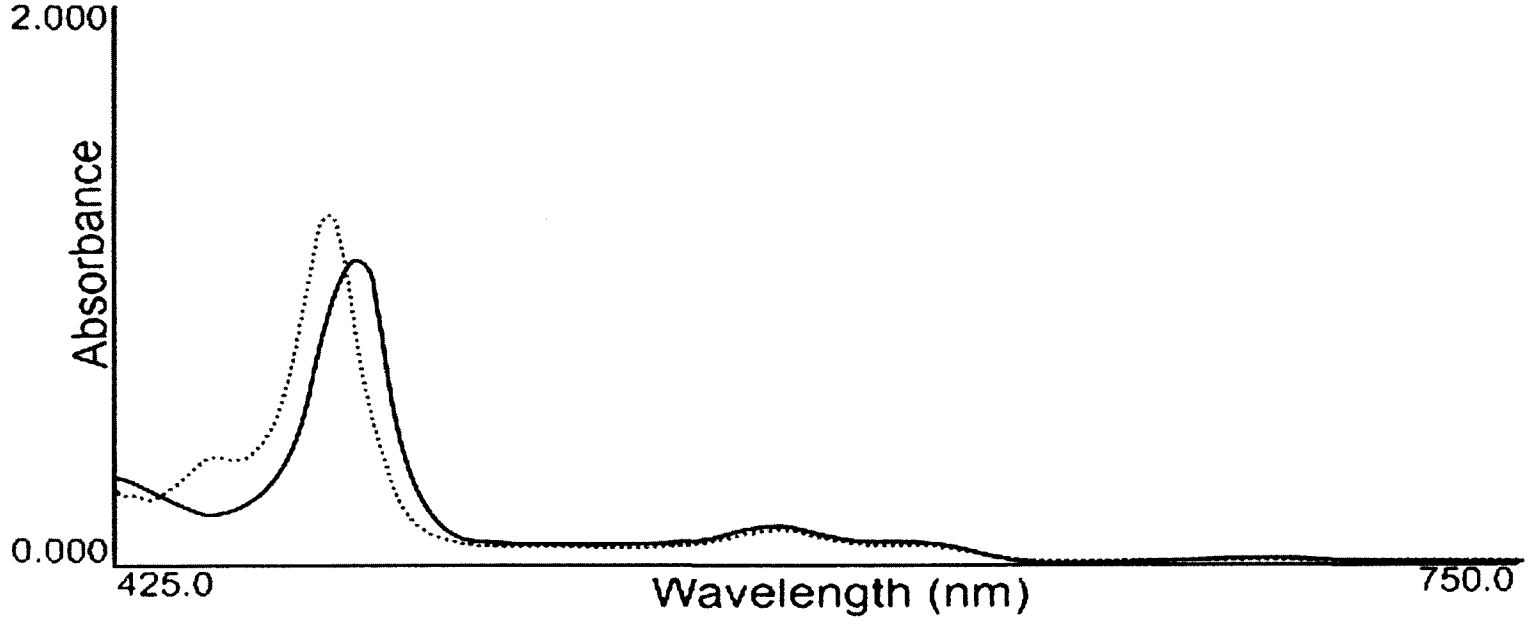

Figure 3.2.3.a **UV-Visible Absorption Spectrum of Mn(III)[TNP]OAc in CH_2Cl_2 at room temperature (————); on addition of 0.2mL of Diethylamine (— — —).**

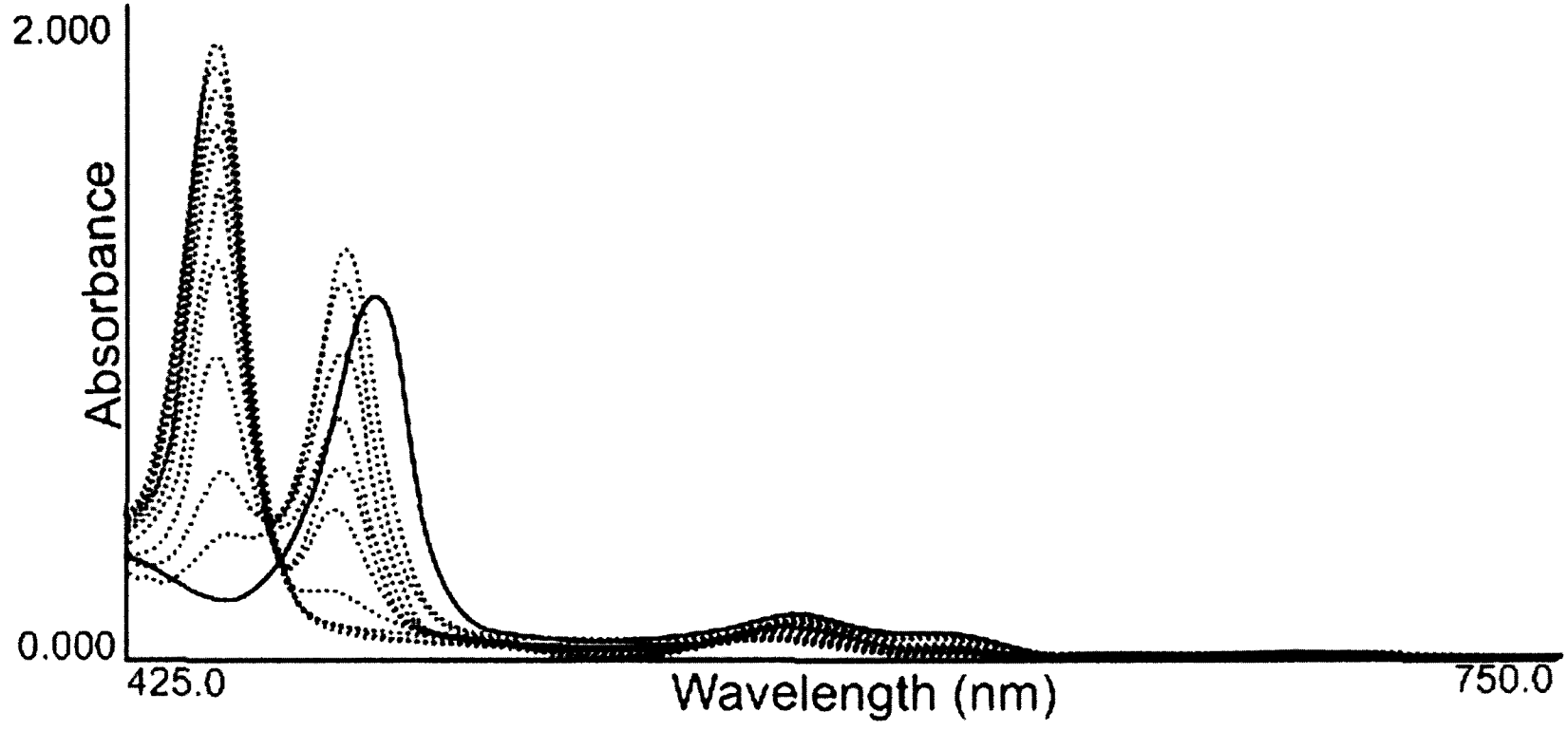

Figure 3.2.3.b. UV-Visible Overlay Spectra of Mn(III)[TNP]OAc in CH_2Cl_2 at room temperature (_____); on Continuous addition of Diethylamine (— — —).

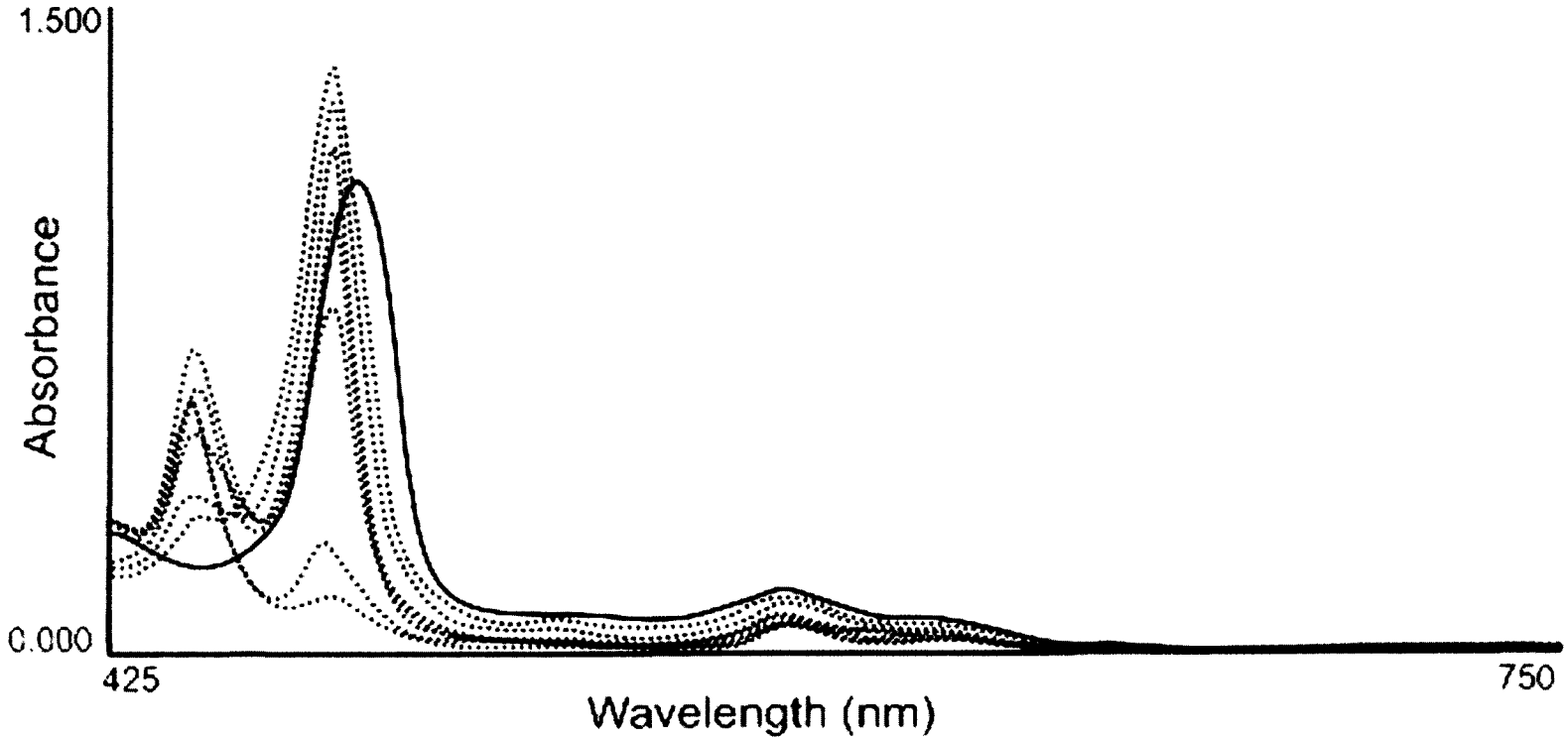

Figure 3.2.3.c. **UV-Visible Overlay Spectra of Mn(III)[TNP]OAc in CH_2Cl_2 at room temperature (————); on continuous addition of Triethylamine (— — — -).**

REFERENCES:

1. R.D. Arasingham, T.C. Bruice, *Inorg. Chem.*, **29**, 1422(1990).

2. P.C. Nakagaki, T.S. Calderwood and T.C. Bruice, *Proc. Natl. Acad. Sci. USA,* **85,** 5424 (1988).

3. D.E. Lansky, B. Mandimutsira, B. Randha, M. Clausen, J. Penner ~ Halon, S.A. Zvyagin, J. Telsev, J. Krzystek, R. Zhan, Z. Ou, K.M. Kadish, L. Zakharov, A.L. Rheingold and D.P. Goldberg, *Inorg. Chem.* **44**, B, 4485 (2005).

4. G.S. Srivatsa and D.T. Sawyer, *Inorg. Chem.*, **24**,1732(1985).

5. S. Jeon, H.K. Lee and Y. – K. Choi, *Bull. Korean. Chem. Soc.* **17** (10), 929 (1996).

6. F.– C. Chen, S.– H. Cheng, C.– H. Yu, M.– H. Liu and Y.O.Su, *J. Electroanal. Chem.* **474,** 52 – 59 (1999).

7. J.A. Shelnutt, X.– Z. Song, J. – G. Ma, S. – L. Jia, W. Jentzen and C.J. Medforth, *Chem. Soc. Rev.*, **27**, 31 (1998).

8. A. Gosh, I. Halvorsen, H.J. Nilsen, E. Steene, T. Wondimagegn, R. Lie, E.V. Camelbecke, N. Gou, Z. Ou and K.M. Kadish, *J. Phys. Chem. B*, **105**, 8120 – 8124 (2001).

9. G. Simoneaux, V. Shenemann, C. Morice, L. Carel, L. Toupet, H. Winkler, A.X. Trantwein and F.A. Walker, *J. Am. Chem. Soc.*, **122**, 4366 (2000).

10. M.K. Safo, M.J.M. Nesset, F.A. Walker, P.G. De Brunner, W.R. Scheidt, *J. Am. Chem. Soc.*, **119**, 9438 (1997).

11. F.A. Walker, H. Nasri, I. Turowskatyrk, K. Mohanrao, C.T. Watson, N.V. Shokhirev, P.G. De Brunner, W.R. Scheidt, *J. Am. Chem. Soc.*, **118**, 12109 (1996).

12. M.R. Cheesman, F.A. Walker, *J. Am. Chem. Soc.*, **118**, 8, 7373 (1996).

13. M.K. Safo, F.A. Walker, A.M. Raitsimring, W.P. Walters, D.P. Dolata, P.G. De Brunner, W.R. Scheidt, *J. Am. Chem. Soc.*, **116**, 7760 (1994).

14. M.K. Safo, G.P. Gupta, C.T. Watson, U. Simonis, F.A. Walker and W.R. Scheidt, *J. Am. Chem. Soc.*, **114,** 7066 (1992).

15. A. Gosh, E. Gonzalez, T. Vanberg, *J. Phys. Chem. B,* **103**, 1363 (1999).

16. W. Jentzen, M.C. Simpson, J.D. Hobbs, X. – Z. Song, R. Ramasseul, J.C. March on, T. Takenchi, W.A. Goddard III and J.A. Shelnutt, *J. Am. Chem. Soc.*, **117,** 11085 (1995).

17. X. – Z. Song, W. Jentzen, S.– L. Jia, L. Jaquinod, D.J. Nurco, C.J. Medforth, K.M. Smith and J.A. Shelnutt, *J. Am. Chem. Soc.*, **118**, 12975 (1996).

18. P. Bhyrappa, V. Krishnan and M. Nethaji, *J. Chem. Soc. Dalton trans.*, 1901 (1993).

19. J.A. Shelnutt, *J. Phys. Chem.*, **88** (21), 4988 – 4992 (1984).

20. C. – L. Lin, M. – Y. Fang and S. – H. Cheng, *J. Electroanal. Chem.*, **531**, 155 – 162 (2002).

21. F. Juan, Z. Huijuan, X. Junfang, A. Xi Cheng, Z. Xingkang, X. Guangzhi and Z. Jianping, *Science in China (Series B)*, **46** (2), 137 – 143 (2003).

CHAPTER -4

CYCLIC VOLTAMMETRIC STUDY OF Mn(III)[T(2-OMeP)P]OAc Mn(III)[T(4-OMeP)P]OAc and Mn(III)[T(naphthyl)P]OAc

CHAPTER – 4

4.1. INTRODUCTION:

In a metalloporphyrin with D_4h symmetry the two HOMOS a_{1u} and a_{2u} orbitals are very close lying. The energy gap between these two orbitals is of the order of 0.5 eV or less. As a result, the relative ordering of these two levels is quite sensitive to the central metal ion, substitution in the periphery, axial ligation and on the structural conformations of the metalloporphyrin. Axial ligand orientation may also have some effect on the spectroscopic and redox properties of a metalloporphyrin[1]. Such subtle changes in the energy levels are usually reflected in their redox potentials.

Manganese porphyrins respond to electrochemical processes such that the redox processes may occur both in the metal centre as well as in the porphyrin ligand. Thus the redox behaviour

will give some information regarding electron transfer reaction and to a certain extent structural conformations.

4.2. RESULTS:

4.2.1 Mn(III) [T(2-OMeP)P] OAc:

The voltammogram (Figure: 4.2.1.a) consist of three redox couples having half wave potentials ($E_{½}$) 0.734 V, 1.1225 V and 1.3915 V. Although ΔE values are large they all look to be reversible. The negative scan also show three redox couples with $E_{½}$ values – 0.265 V, – 0.543 V and – 1.050 V (Fig.4.2.1.a). Redox Potentials are summarized in the Table: 4.A.

4.2.2. Mn(III)[T(4-OMeP)P] OAc:

On scanning from 0 to 1.8 V the voltammogram exhibits three reduction peaks while the oxidation side exhibits only two peaks (Figure

4.2.2.a). The two redox couples are at $E_{½}$ values of 1.1955V and 1.453 V respectively. The only reduction peak occurs at a potential 0.420 V. When the scan is from +1.8V to –1.8V, the oxidation peak corresponding to the reduction peak at 0.420 V occurs around 0.5 V with $E_{½}$ value 0.46V (Fig .4.2.2.b). The negative scan shows three couples with $E_{½}$ values –0.334 V, – 0.6055 V and –1.172 V (Table: 4.B.)

4.2.3. Mn(III)[T(naphthyl)P]OAc:

The positive scan from 0.0V to 1.8V exhibits a voltammogram consisting of three redox couples with $E_{½}$ values 0.527 V, 0.961V and 1.408 V (Fig. 4.2.3.a). The corresponding negative scan also exhibits three redox couples with $E_{½}$ values – 0.35 V, – 0.588 V and – 1.115 V (Fig.4.2.3.b) (Table: 4.C.). All these redox couples appear to be reversible inspite of their high ΔE values.

4.3. DISCUSSION:

The three manganese porphyrins viz. Mn(III)[T(2-OMeP)P]OAc, Mn(III)[T(4-OMeP)P]OAc and Mn(III)[T(naphthyl)P]OAc exhibit voltammograms of similar pattern. The positive scan voltammogram consists of three redox couples. Similarly, the negative scan gives a voltammogram which consists of three redox couples. Oxidation of Mn(III) to Mn(IV) is observed around 0.46 V to 0.734 V [2,3]. The first porphyrin ligand oxidations are observed around 0.961V to 1.225V while the second porphyrin ligand oxidations occurs around 1.3915V to 1.4536V. Mn(III)to Mn(II) reduction occur at around –0.265 V to – 0.35 V [4 - 6] . The first porphyrin ligand reductions occur at around – 0.543 V to – 0.588 V and the second reductions occur at around – 0.055 V to – 1.173 V. Out of the three manganese porphyrins, the redox potential of the first ligand oxidation of Mn(III)[T(naphthyl)P] OAc, is the lowest while that of the Mn(III)[T(4-OMeP)P]OAc is the highest. Non planar

porphyrins are easier to oxidize than planar porphyrins [7,8]. Out of the three manganese porphyrins Mn(III)[T(napthyl)P]OAc is expected to be more distorted due to steric factors while Mn(III)[T(4-OMeP)P]OAc is expected to be more closer to the planar form. Thus, the structural effect on the redox potential is reflected on the voltammogram. The effect is also observed in the UV – Visible spectrum. The B band (Soret band) of Mn(III)[T{(napthyl)P}$(Et_3N)_2$] shows a lesser blue shift.

4.4. CONCLUSION:

From the cyclic Voltammetric study, following observations are made:

(i) Higher oxidation state of manganese i.e. Mn(III) to Mn(IV) is observed.

(ii) Reduction of Mn(III) to Mn(II) is also observed.

(iii) Oxidation potentials are lower for more distorted metalloporphyrins. This may be due to the interaction of d-orbitals of the metal atom with the porphyrin ligand orbitals (a_1u/a_2u). Obviously, less distorted metalloporphyrins exhibit higher oxidation potentials.

Table: 4.A. **Cyclic Voltammetric Data of Mn(III)[T(2-OMeP)P]OAc at Room temperature**

Solvent : **Dichloromethane**

Concentration : **10^{-3}M**

Supporting electrolyte : **TBAP**

Reference Electrode : **Ag/AgCl**

Scan Rate : **0.1 (V/S)**

COMPOUND	Switching Potential (V)	$E_{pa}(1)$ (V)	$E_{pa}(2)$ (V)	$E_{pa}(3)$ (V)	$E_{pc}(1)$ (V)	$E_{pc}(2)$ (V)	$E_{pc}(3)$ (V)	$E_{1/2}(1)$ (V)	$E_{1/2}(2)$ (V)	$E_{1/2}(3)$ (V)	ΔE_1 (V)	ΔE_2 (V)	ΔE_3 (V)
Mn^{III} [T(2-OMeP)P] OAc	0 to 1.8	0.879	1.20	1.49	0.589	1.045	1.293	0.734	1.1225	1.3915	0.290	0.155	0.197
Mn^{III} [T(2-OMeP)P] OAc	0 to -1.8	-0.195	-0.446	-0.87	-0.335	-0.64	-1.23	-0.265	- 0.543	- 1.05	-0.14	-0.194	- 0.3(

Table: 4.B. **Cyclic Voltammetric Data of Mn(III)[T(4-OMeP)P]OAc at Room temperature**

Solvent : Dichloromethane

Concentration : 10^{-3}M

Supporting electrolyte : TBAP

Reference Electrode : Ag/AgCl

Scan Rate : 0.1 (V/S)

COMPOUND	Switching Potential (V)	$E_{pa}(1)$ (V)	$E_{pa}(2)$ (V)	$E_{pa}(3)$ (V)	$E_{pc}(1)$ (V)	$E_{pc}(2)$ (V)	$E_{pc}(3)$ (V)	$E_{1/2}(1)$ (V)	$E_{1/2}(2)$ (V)	$E_{1/2}(3)$ (V)	ΔE_1 (V)	ΔE_2 (V)	ΔE_3 (V)
Mn^{III} [T(4-OMe)PP] OAc	0 to 1.8	-	1.299	1.615	0.420	1.092	1.291	-	1.1955	1.453	-	0.207	0.324
Mn^{III} [T(4-OMe)PP] OAc	0 to -1.8	-0.171	-0.463	-1.017	-0.497	-0.748	-1.327	-0.334	-0.6055	-1.172	-0.326	-0.285	-0.31

Table: 4.C. **Cyclic Voltammetric Data of Mn(III)[TNP]OAc at Room temperature**

Solvent : Dichloromethane

Concentration : 10^{-3}M

Supporting electrolyte : TBAP

Reference Electrode : Ag/AgCl

Scan Rate : 0.1 (V/S)

COMPOUND	Switching Potential (V)	$E_{pa}(1)$ (V)	$E_{pa}(2)$ (V)	$E_{pa}(3)$ (V)	$E_{pc}(1)$ (V)	$E_{pc}(2)$ (V)	$E_{pc}(3)$ (V)	$E_{1/2}(1)$ (V)	$E_{1/2}(2)$ (V)	$E_{1/2}(3)$ (V)	ΔE_1 (V)	ΔE_2 (V)	ΔE_3 (V)
Mn^{III} [TNP] OAc	0 to 1.8	0.585	1.010	1.525	0.469	0.912	1.291	0.527	0.961	1.408	0.116	0.098	0.234
Mn^{III} [TNP] OAc	0 to -1.8	-0.245	-0.535	-0.942	-0.455	-0.641	-1.288	-0.35	-0.588	-1.115	-0.21	-0.105	-0.346

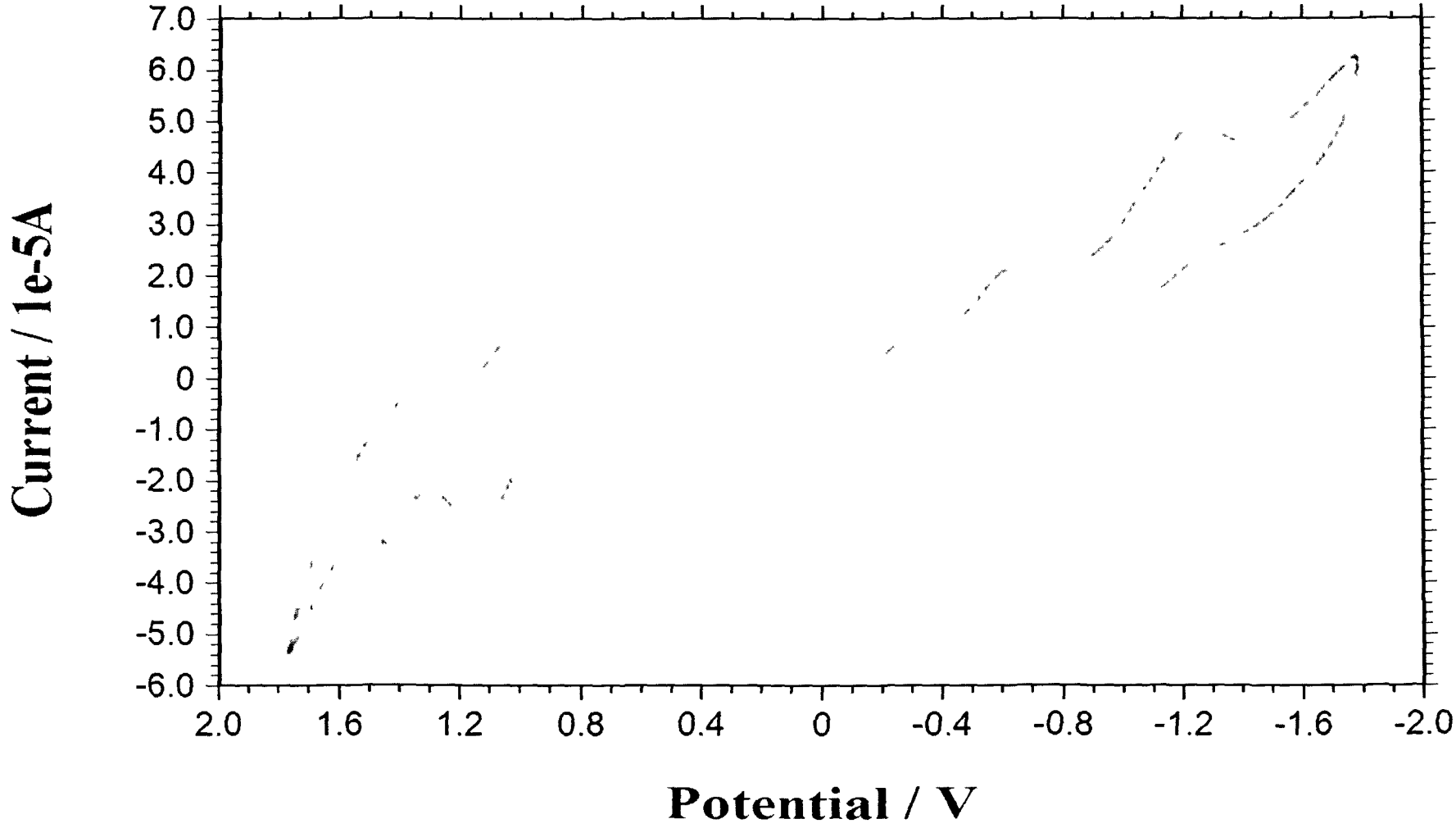

Figure: 4.2.1.a. Cyclic Voltammogram of Mn(III)[T(2-OMeP)P]OAc in CH_2Cl_2 containing 0.1M TBAP at Room Temperature.

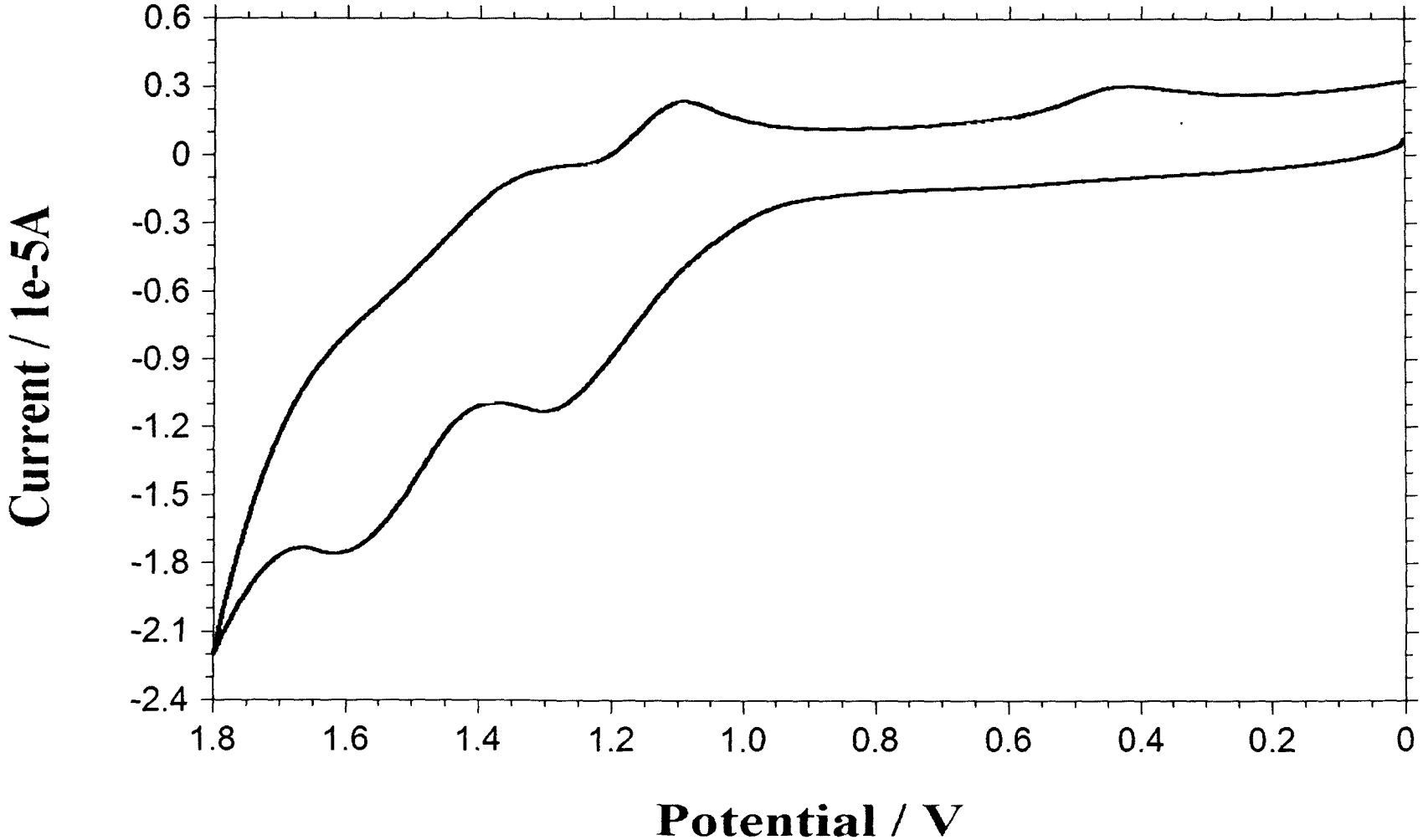

Figure: 4.2.2.a. Cyclic Voltammogram of Mn(III)[T(4-OMeP)P]OAc in CH_2Cl_2 containing 0.1M TBAP at Room Temperature.

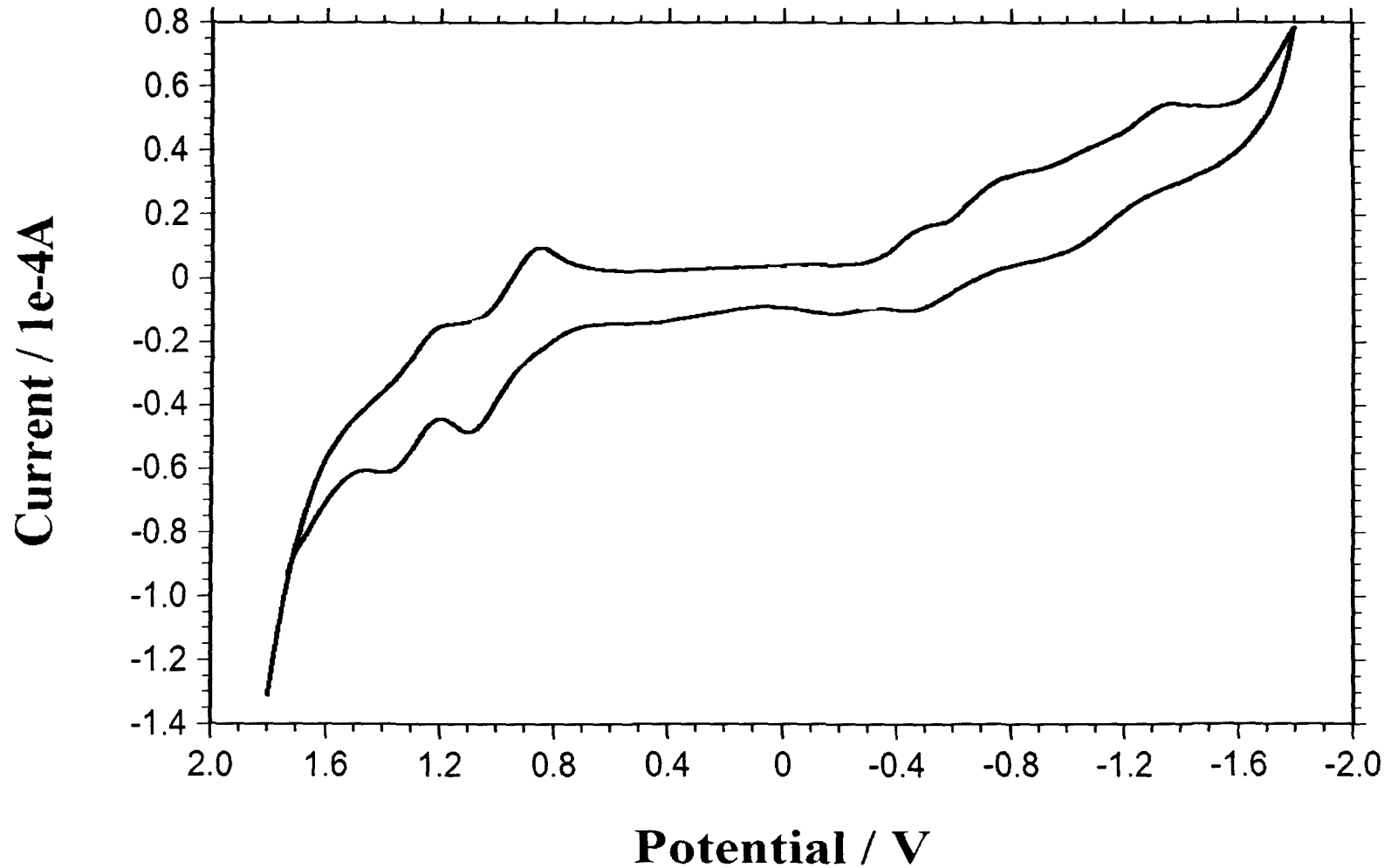

Figure: 4.2.2.b. Cyclic Voltammogram of Mn(III)[T(4-OMeP)P]OAc in CH_2Cl_2 containing 0.1M TBAP at Room Temperature.

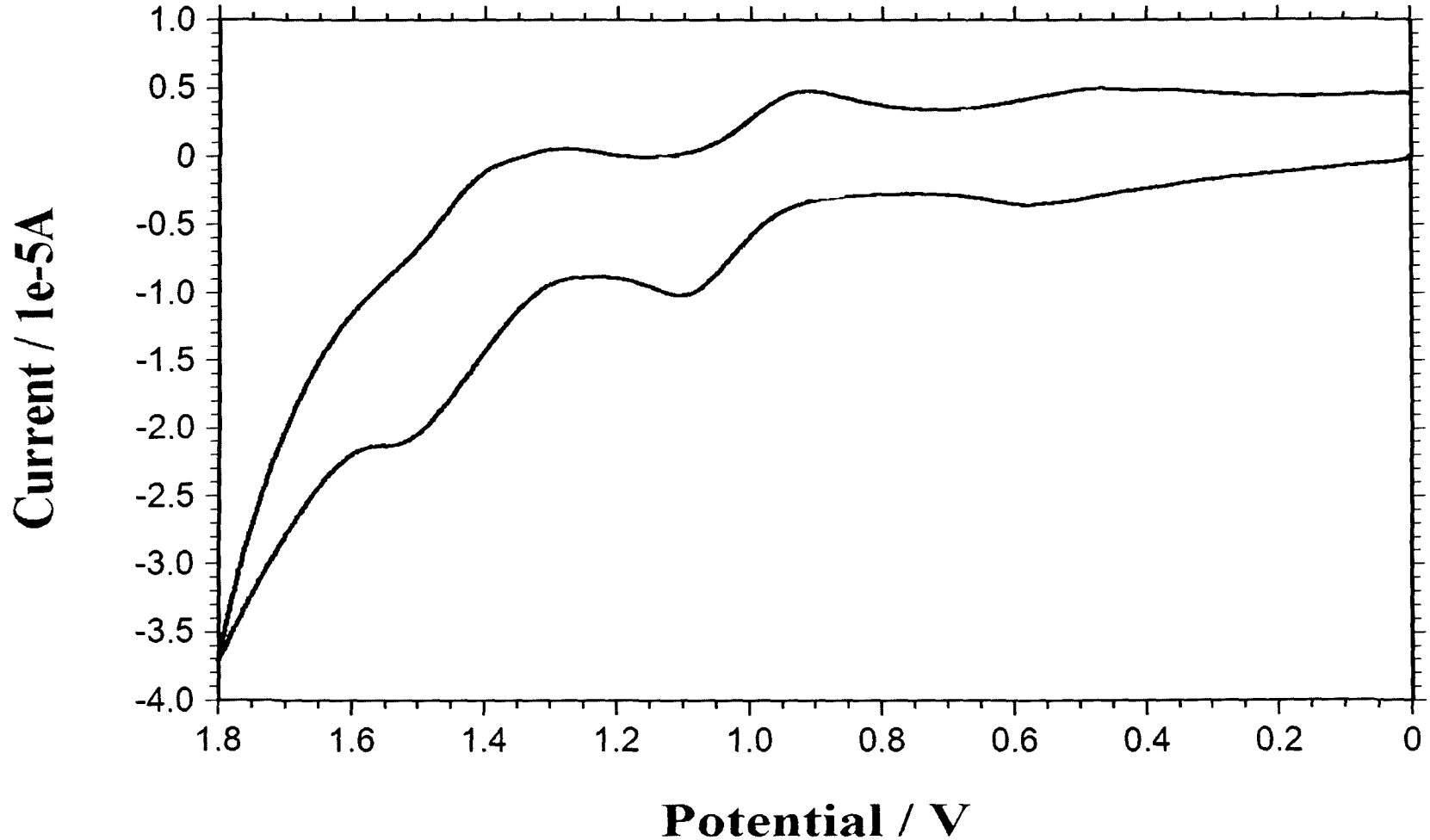

Figure: 4.2.3.a. Cyclic Voltammogram of Mn(III)[TNP]OAc in CH_2Cl_2 containing 0.1M TBAP at Room Temperature.

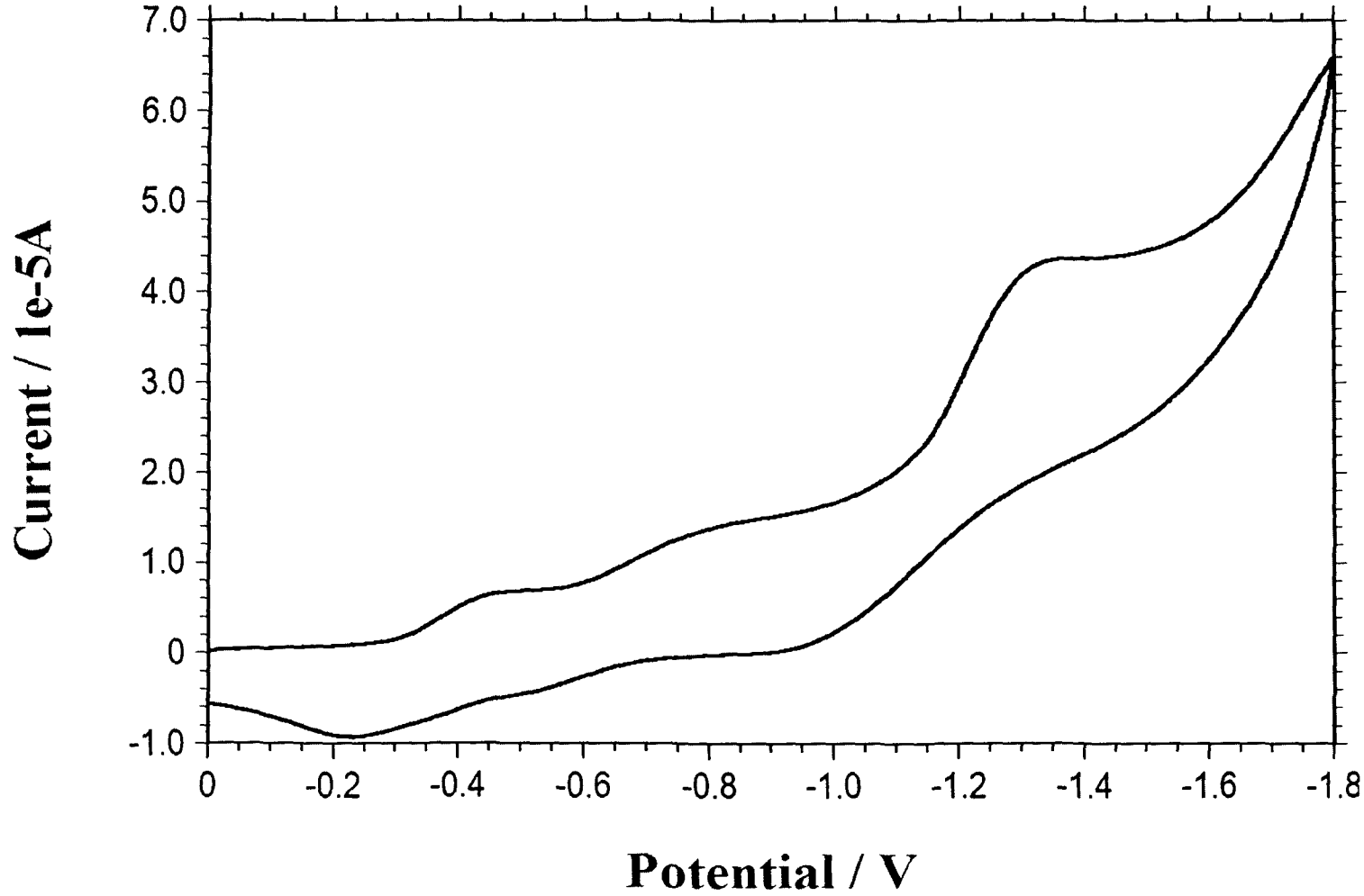

Figure: 4.2.3.b. Cyclic Voltammogram of Mn(III)[TNP]OAc in CH_2Cl_2 containing 0.1M TBAP At Room Temperature

REFERENCES:

1. J. A. Shelnutt, X. – Z. Song, J. – G. Ma, S, – L. Jia, W. Jentzen and C.J. Medforth, *Chem. Soc. Rev.* **27**, 31(1998).

2. N. Carmieri, A. Harriman and G. Porter, *J. Chem. Soc. Dalton, trans,* 931 (1982).

3. G.F. – Suetta, D. Vitturi, I.B. – Haberle, I. Fridovich, S. Goldstein, G. Czapski and R. Radi, *J. Biol. Chem.*, **278**, 30, 27432 – 27438 (2003).

4. C.– H.Chang, S,– H. Cheng and Y.O. Su, *J. Chin. Chem. Soc.* **46**, 221– 227(1999).

5. F.– C. Chen, S.– H. Cheng, C.–H. Yu, M.– H. Liu and Y.O. Su, *J. Electroanal. Chem.*, **474**, 52 – 59(1999).

6. C.- H. Yu, Y,O. Su, *J. Electroanal. Chem.*, **368**, 323 (1994).

7. K.M. Bhargigia, L. Chantranupong, K.M. Smith and J. Fajer, *J. Am. Chem. Soc.*, **110**, 7566 (1988).

8. M. Ravikanth and T.K. Chandrashekar, *Structure and bonding*, **82**,105 (1995).

CHAPTER -5

AXIAL LIGAND EFFECTS ON THE UV-VISIBLE SPECTRA AND CYCLIC VOLTAMMETRIC STUDIES OF Zn(II)[T(4-OMeP)P] and Zn(II)[T(naphthyl)P]

CHAPTER – 5

5.1. INTRODUCTION:

Zn(II)porphyrins are most extensively studied porphyrins. Zn(II) porphyrins belong to regular porphyrins which contains closed shell metal atoms (d^0 or d^{10})[1]. The $d_\pi(d_{xz},d_{yz})$ orbitals of Zn(II) are relatively low in energy. These orbitals do not have significant effect on the energy levels of the porphyrin ligand orbitals (i.e., π, π^*)[2]. Early studies of Mg, Cu, Zn, Cd and Hg complexes of TPP with pyridine (axial ligand) have shown red shifted visible spectra [3-7]. Such studies are still open for theoretical and structural studies[2]. It is well established that the out of plane Zn(II) ion can coordinate with only one axial ligand. Solvent and axial ligand effect on the visible spectra and redox potentials of Zinc porphyrins are well documented in the literature[8 - 10]. For comparative studies we have undertaken Zn(II)[T(4-OMeP)P] and Zn(II)[T(naphthyl)P]. Besides, their interactions with

Diethylamine and Triethylamine and their UV-Visible spectra in neutral solvent, CH_2Cl_2 are not well documented.

Not much Cyclic Voltammetric data are available for Zn(II)[T(naphthyl)P]. Therefore, its cyclic voltammetric study is done for comparative study.

5.2. UV – VISIBLE STUDIES:

5.2.1. RESULT:

Results are summarised in the Table: 5. A.

5.2.1 (i) Zn(II)[T(4-OMeP)P]:

Addition of 0.1 ml of diethyl amine exhibit red shifts (Figure: 5.2.1.(i).a). The B - band (Soret band) shifts from 423 nm to 432 nm and the Q - bands at 549 nm shifts to 580 nm while the band at 590 nm shifts to 608 nm. A shoulder at 473 nm disappears

while a new band develops at 632 nm. The intensity of the new band at 632 nm increases while the intensity of the band at 608 nm decreases and disappears on further additions of diethylamine. Similar patterns are observed with triethylamine (Figure: 5.2.1.(i).b).

5.2.1. (ii). Zn(II)[T(naphthyl)P]:

Addition of 0.1 ml diethylamine shifts the Soret band from 424 nm to 434 nm, and Q - bands from 548nm to 563 nm and 601 nm to 602 nm respectively. A new band develops at 638nm (Figure: 5.2.1.(ii).a). The intensity of the new band at 638nm increases with subsequent addition of amine. Similar pattern is observed with triethylamine (Figure: 5.2.1.(ii).b).

5.3. DISCUSSION:

The spectra of Zinc porphyrins exhibit a considerable red shifts in the absorption bands on axial ligation with amines. This is due to flow of charge from the axial ligand to the porphyrin ring through the

Zinc ion [11-15]. This essentially destabilizes the HOMOs (a_{1u} & a_{2u}) of the porphyin. Since a_{1u} orbital has nodes at nitrogen atoms, the perturbation is felt mainly by the a_{2u} orbital raising its energy level, thereby decreases the energy gap. This causes the red shifts.

5.4. CYCLIC VOLTAMMETRIC STUDIES:

5.4.1. RESULTS:

Results are summarized in the Table: 5.B.

5.4.1 (i) Zn(II)[T(4-OMeP)P]:

The voltammogram consists of two redox couples with $E_{1/2}$ values 0.624 V and 0.995 V (Figure: 5.4.1.i). The redox couples disappear on addition of amines and the voltammogram could not be resolved.

5.4.1. (ii). Zn(II)[T(naphthyl)P]:

The voltammogram exhibits two clear redox couples with their E ½ values 0.6975 V and 0.951 V (Figure: 5.4.1.ii). The voltammogram could not be resolved in the presence of amine.

5.4.2. DISCUSSION:

For both Zinc porphyrins two reversible redox couples are observed (although their ΔE values are large). The oxidation potentials are lower than that of Zn(II)TPP (Table: 5.B).This is due to substituents which are electron rich and electron donating in nature. In addition to this the conformations of the two Zinc porphyrins are expected to be more distorted than ZnTPP. As a result the distorted porphyrins are easier to oxidize. Thus the oxidation potentials are lower than that of Zn(II)TPP[16].

5.5. CONCLUSION:

From the UV- Visible studies and cyclic voltammetric studies the following observations are put forward:

(i) Charge flows from the axial ligand through the Zinc ion to the porphyrin ligand[11-15]. This perturbs the a_{2u} orbital raises its energy level resulting in the red shifts of absorption bands in the spectrum.

(ii) Axial ligand exert some effects on the Conformational changes such as ruffled or saddled form. This in turn makes the oxidation of the porphyrin easier, thus lowering the oxidation potentials.

TABLE: 5.A. **UV-Vis Absorption Spectral Data Of Zn(II)Porphyrins At Room Temperature**
Solvent : Dichloromethane
Concentration : 10^{-5} M

COMPOUNDS	AMINE USED	VOL. OF AMINE ADDED (mL)	ABSORPTION BANDS (nm)				
			B	Q			
Zn^{II}[T(4-OMeP)P]		0	423	473	549	590	-
	Diethylamine	0.1	432	-	580	608	632
	Triethylamine	0.1	430	-	562	604	632
Zn^{II}[T(naphthyl)P]		0	424	-	548	601	-
	Diethylamine	0.1	434	-	563	602	638
	Triethylamine	0.1	434	-	563	602	638

TABLE: 5.B. **Cyclic Voltammetric Data of Zn(II)Porphyrins at Room Temperature.**

Solvent : Dichloromethane

Concentration : 10^{-3} M

Supporting Electrolyte : TBAP

Reference Electrode : Ag/AgCl

Scan Rate : 0.1 (V/S)

COMPOUND	$E_{pa}(1)$ (V)	$E_{pa}(2)$ (V)	$E_{pc}(1)$ (V)	$E_{pc}(2)$ (V)	$E_{1/2}(1)$ (V)	$E_{1/2}(2)$ (V)	ΔE_1 (V)	ΔE_2 (V)	REFERENCE
$Zn^{II}TPP$					0.71	1.03			16
Zn^{II} [T(4-OMeP)P]	0.785	1.150	0.463	0.840	0.624	0.995	0.322	0.310	
Zn^{II} [T(naphthyl)P]	0.745	0.998	0.650	0.904	0.6975	0.951	0.095	0.094	

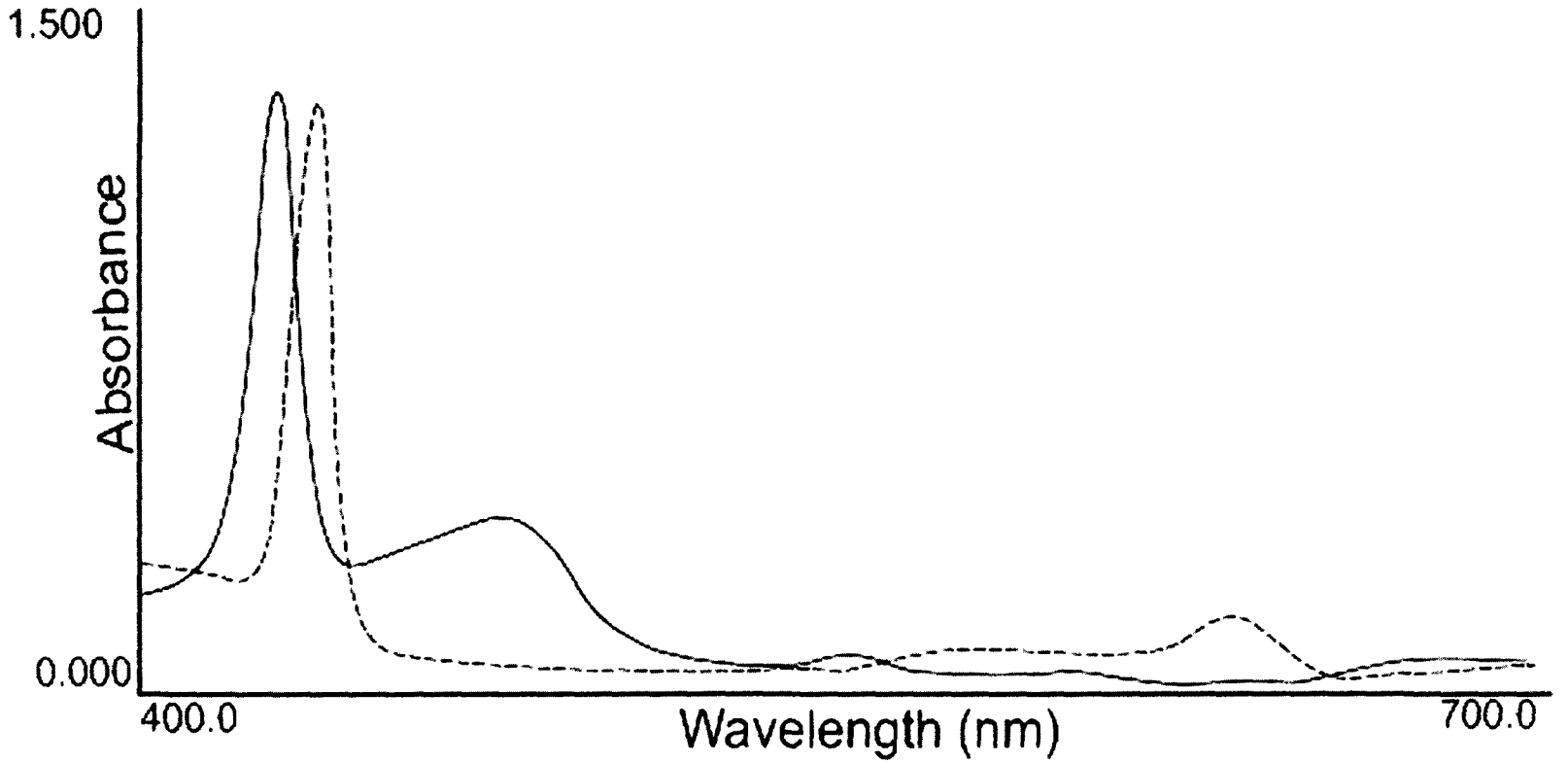

Figure 5.2.1.(i).a. UV-Visible absorption spectrum of Zn(II)[T(4-OMeP)P] in CH_2Cl_2 at room temperature (————); on addition of 0.1 mL of Diethylamine (---------).

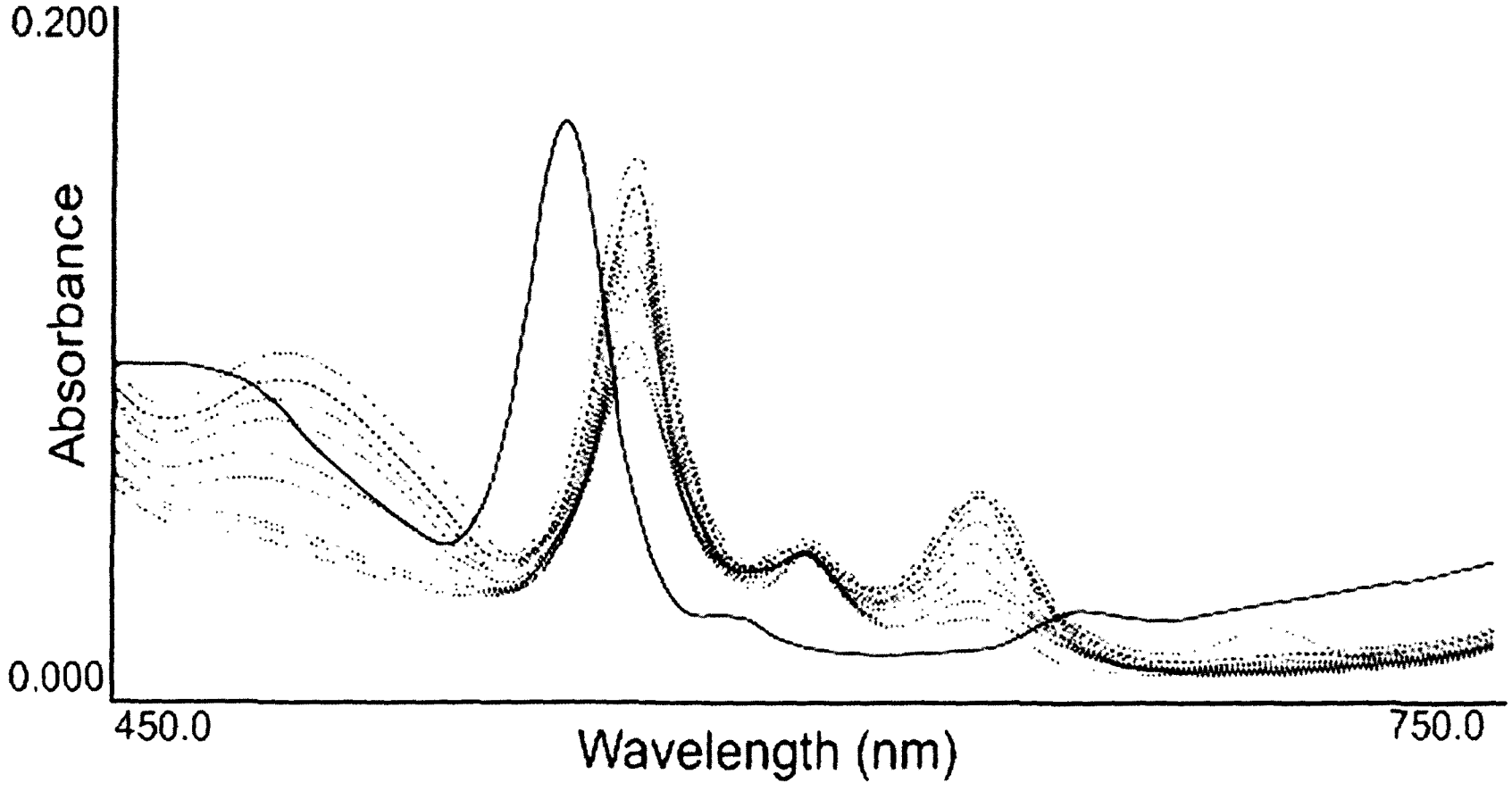

Figure 5.2.1.(i).b . **UV-Visible Overlay Spectra of Zn(II)[T(4-OMeP)P] in CH_2Cl_2 at room temperature (———);on continuous addition of Triethylamine (– – – – ·).**

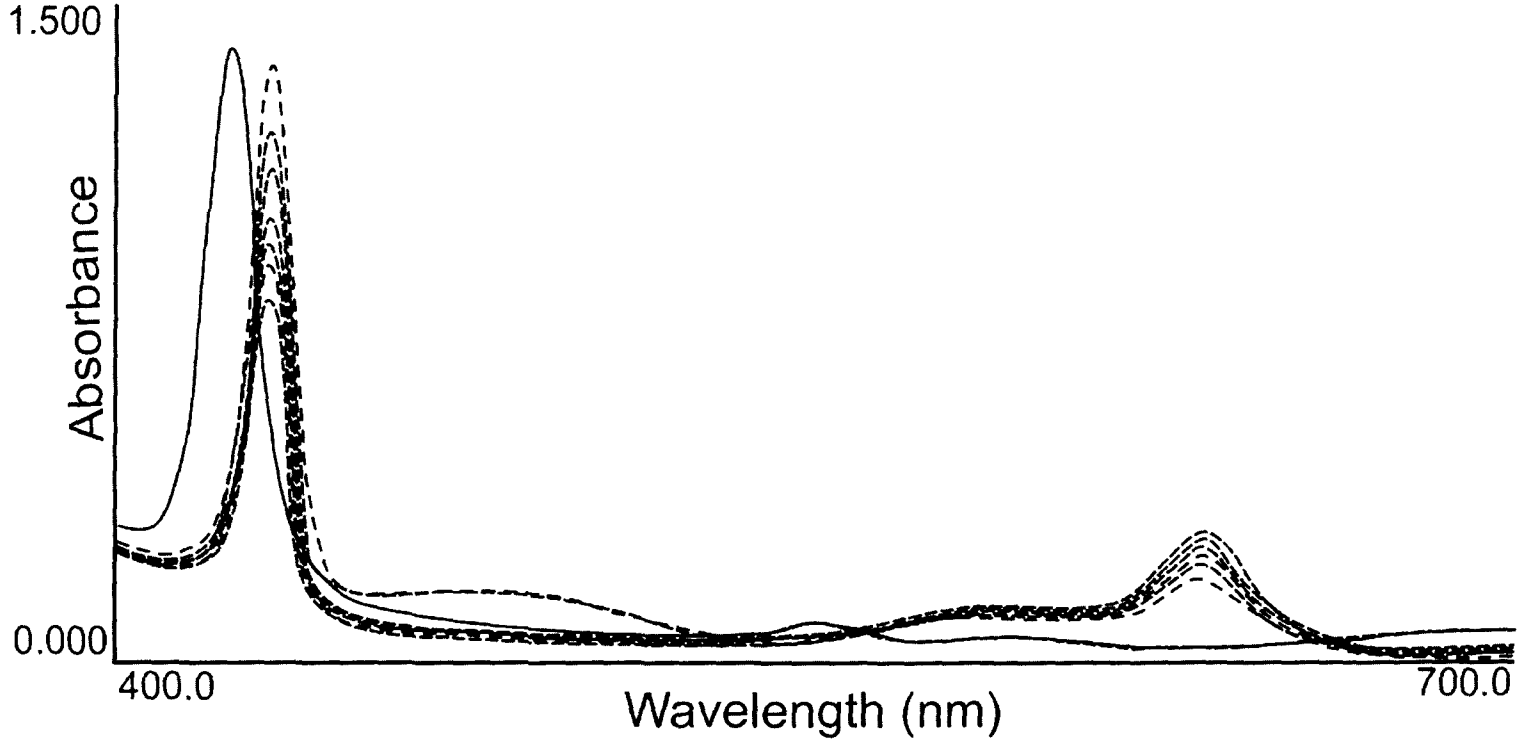

NORTH EASTERN HILL UNIV
DATE 10/4/12

Figure 5.2.1.(ii).a. **UV-Visible Overlay Spectra of Zn(II)[T(naphthyl)P] in CH_2Cl_2 at room temperature (———); on continuous addition of *Diethylamine* (- - - - -).**

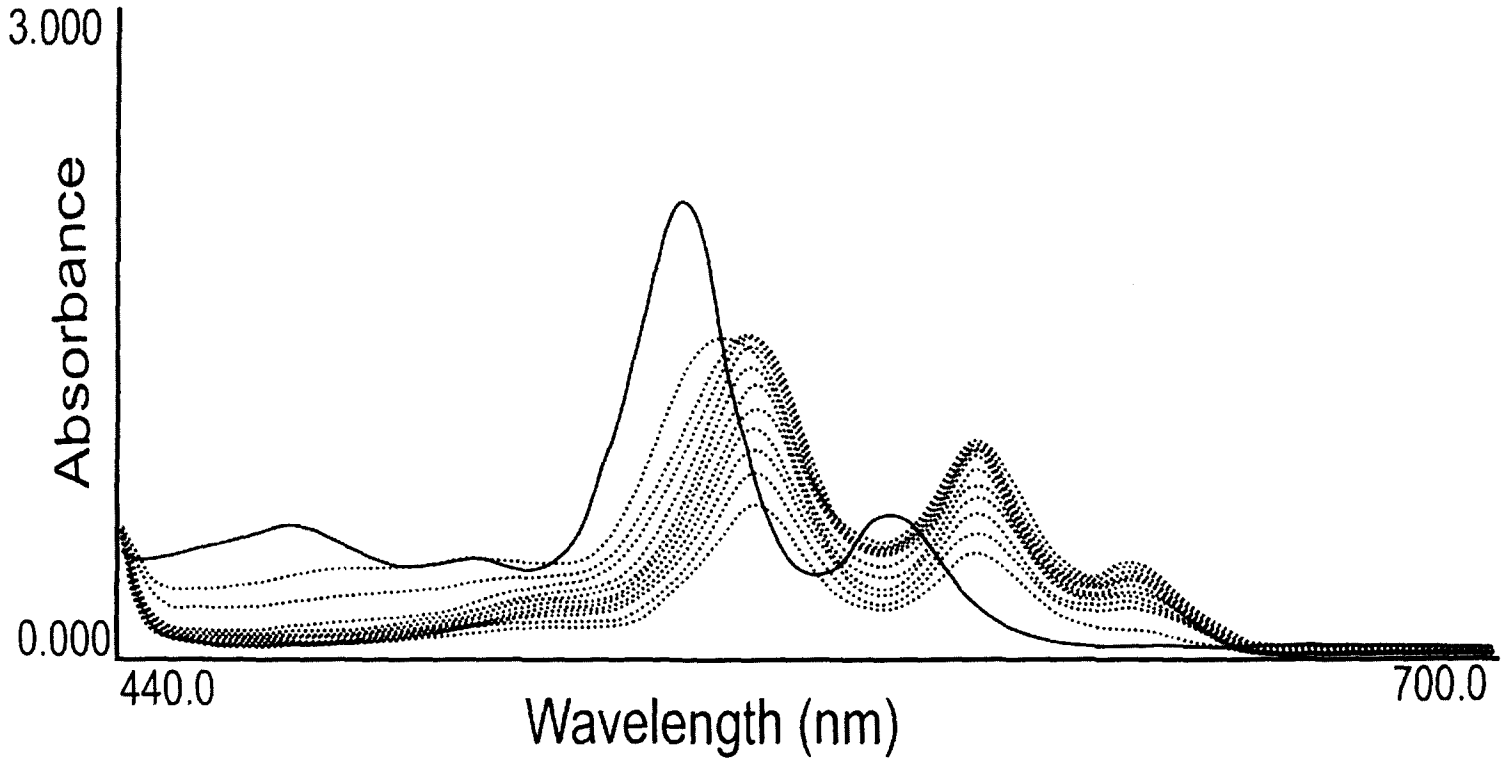

Figure 5.2.1.ii(b) . **UV-Visible Overlay Spectra of Zn(II)[T(naphthyl)P in CH_2Cl_2 at room temperature (————); on continuous addition of Triethylamine (------).**

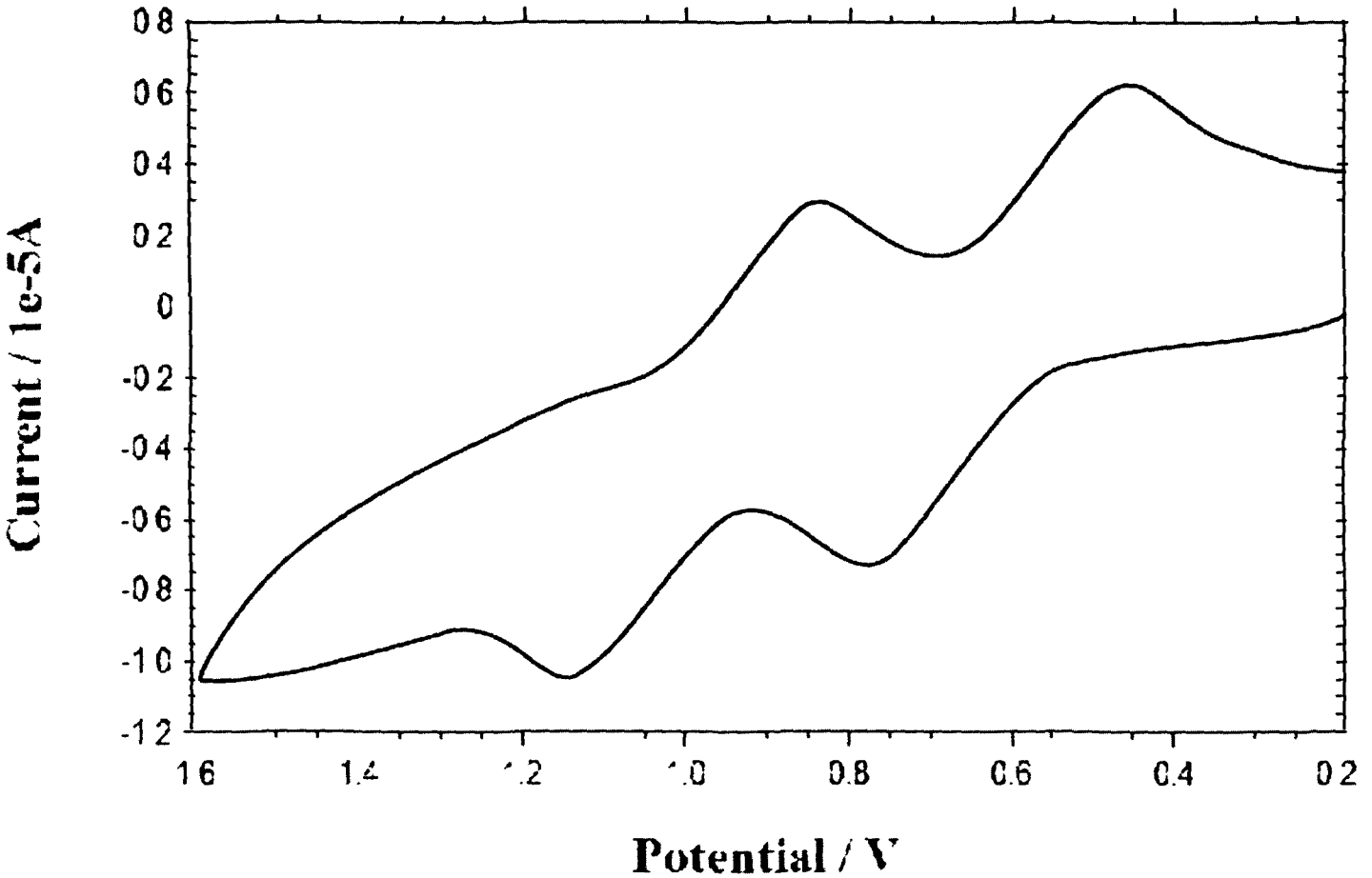

Figure: 5.4.1.i. Cyclic Voltammogram of Zn(II)[T(4-OMeP)P] in CH_2Cl_2 containing 0.1M TBAP at Room Temperature.

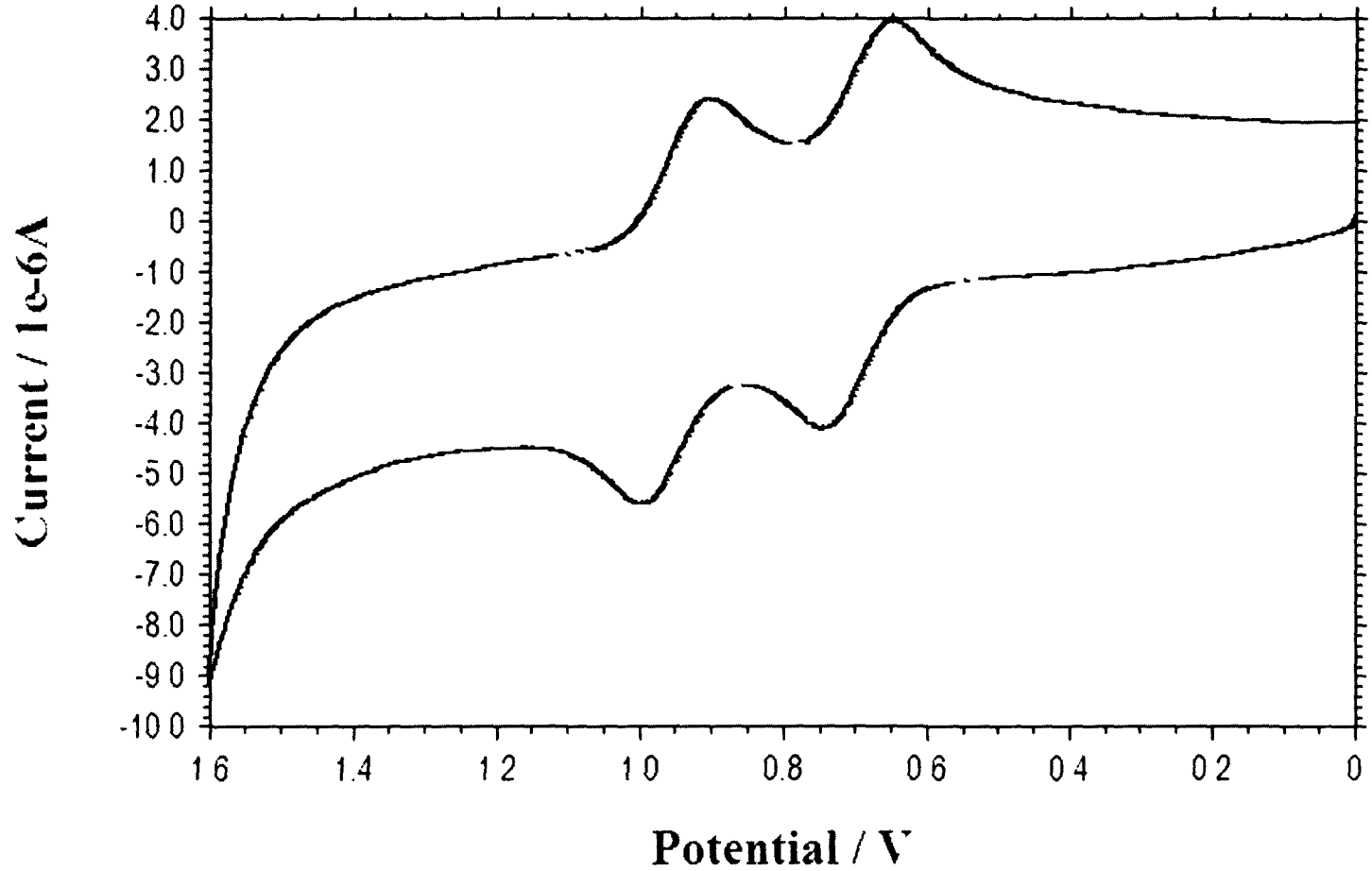

Figure: 5.4.1.ii. Cyclic Voltammogram of Zn(II)[T(naphthyl)P] in CH_2Cl_2 containing 0.1M TBAP at Room Temperature.

REFERENCES:

1. M. Gouterman in *The Porphyrins* **Vol.III**, part A, Edited by D. Dolphin, Academic Press, INC, Newyork, 1979.

2. T. Hashimoto, Y. – K. Choe, H. Nakano and K. Hirao, *J. Phys. Chem. A*, **103**, 1894 – 1904 (1999).

3. J.R. Miller and G.D. Dorough, *J. Am. Chem. Soc.* **74**, 3977 (1952).

4. W.R. Scheidt in *The Porphyrins* **Vol. III**, part A, Edited by D. Dolphin, Academic Press, INC, Newyork, 1979.

5. C.H. Kirsley, P. Hambright and C.B. Storm, *Inorg. Chem.* **8,** 2141 (1969).

6. G.C. Vogel and B.A. Beckmann, *Inorg.Chem.,* **15,** 483 (1976).

7. M. Nappa and J.S. Valentine, *J. Am. Chem. Soc.,* **100**, 5075 (1978).

8. O.W. Kooling, *Anal. Chem.*, **54**, 260 (1982).

9. R.M. Wang and B.M. Hoffman, *J. Am. Chem. Soc.*, **106,** 4235 (1984).

10. K.M. Kadish, L.R. Shiue, R.K. Rhodes and L.A. Bottomley, *Inorg.Chem.*, **20**, 1274 – 1277 (1981).

11. P. Bhyrappa and B. Purushottam, *J. Chem.Soc. Perkin trans.*, **2**, 238 – 242 (2001).

12. P. Bhyrappa, V. Krishnan and M. Nethaji, *J. Chem. Soc. Dalton trans.*, 1901 (1993).

13. J.A. Shelnutt, *J. Phys. Chem.*, **88** (21), 4988 – 4992 (1984).

14. C. – L. Lin, M. – Y. Fang and S. – H. Cheng, *J. Elect. anal. Chem.*, **531**, 155 – 162 (2002).

15. F. Juan, Z. Huijuan, X. Junfeng, A. Xicheng, Z. Xingkang, X. Guangzhi and Z. Jianping, *Science in China (Series B),* **46 (2)**, 137 – 143 (2003).

16. A. Wolberg and J. Manassen, *J. Am. Chem. Soc.*, **92,** 2982 (1970)

CHAPTER -6

AXIAL LIGAND EFFECTS ON THE UV-VISIBLE SPECTRA AND REDOX TUNING OF Cu(II)[T(4-OMeP)P] and Cu(II)[T(naphthyl)P]

CHAPTER – 6

6.1. INTRODUCTION:

Copper porphyrins belong to d^9 complexes[1]. They are four coordinated system and prefer a planar geometry. They have very poor tendency to accept axial ligand[2]. Copper porphyrins are also extensively studied compounds. However, we carried out these works for comparative studies and the necessity of obtaining the electrochemical data (redox potentials) of Cu(II)[T(naphthyl)P]. Interestingly, Chmielewski et.al [5] have observed Cu^{III}/Cu^{II} and also Cu^{II}/Cu^{I} couples in Copper (II) complexes of inverted porphyrins.

6.2. RESULTS:

6.2.1. UV – VISIBLE STUDIES:

Results are summarized in the Table: 6.A.

No change in the UV – Visible spectra are observed with amines except dilution effect. (Figure: 6.2.1.a).

6.2.2. CYCLIC VOLTAMMETRIC STUDIES:

Results are summarized in the Table: 6.B.

6.2.2.(i). Cu(II)[T(4-OMeP)P]:

The voltammogram consists of two redox couples with $E_{½}$ values 0.8645 V and 1.2665 V. The voltammogram exhibits two successive one – electron oxidation of the porphyrin ligand (Figure: 6.2.2.i)

6.2.2.(ii) Cu(II)[T(naphthyl)P]:

The voltammogram presents two redox couples for two successive one – electron oxidation of the porphyrin ligand (Figure: 6.2.2.ii). The $E_{½}$ values are 0.8485 V and 1.248 V.

6.3. DISCUSSION:

The first oxidation potentials of Cu(II)[T(4-OMeP)P] and Cu(II)[T(naphthyl)P] are slightly lower than the first oxidation of CuTPP [3,4]. This is most likely due to substituents which are electron donating in nature and also due to distorted conformations.

6.4. CONCLUSION:

From the UV – Visible and Cyclic Voltammetric studies following observations are made:

(i) Addition of amine does not affect the UV – Visible spectra indicating no axial ligation (as expected).

(ii) Oxidation potentials are lower than that of CuTPP which is due to electron donating substituents and due to distorted conformations.

TABLE 6.A : UV-Vis Absorption Spectral Data Of Copper Porphyrins At Room Temperature.
SOLVENT : Dichloromethane.
CONCENTRATION : 10^{-5} M.

COMPOUNDS	AMINE USED	VOL. OF AMINE ADDED (mL	ABSORPTION BANDS (nm)		
			B	Q	
Cu^{II}[T(4-OMeP)P]		0	419	541	541
	Diethylamine	0.1	419	541	541
	Triethylamine	0.1	419	541	541
Cu^{II}[T(naphthyl)P]		0	420	540	540
	Diethylamine	0.1	420	540	540
	Triethylamine	0.1	420	540	540

TABLE: 6.B. **Cyclic Voltammetric Data of Copper Porphyrins at Room Temperature.**

Solvent : Dichloromethane

Concentration : 10^{-3} M

Supporting Electrolyte : TBAP

Reference Electrode : Ag/AgCl

Scan Rate : 0.1 (V/S)

COMPOUND	$E_{pa}(1)$ (V)	$E_{pa}(2)$ (V)	$E_{pc}(1)$ (V)	$E_{pc}(2)$ (V)	$E_{1/2}(1)$ (V)	$E_{1/2}(2)$ (V)	ΔE_1 (V)	ΔE_2 (V)	REFERENCE
$Cu^{II}TPP$					0.90	1.16			4
Cu^{II} [T(4-OMeP)P]	1.076	1.476	0.653	1.057	0.8645	1.2665	0.423	0.419	
Cu^{II} [T(naphthyl)P]	0.988	1.418	0.709	1.078	0.8485	1.248	0.279	0.340	

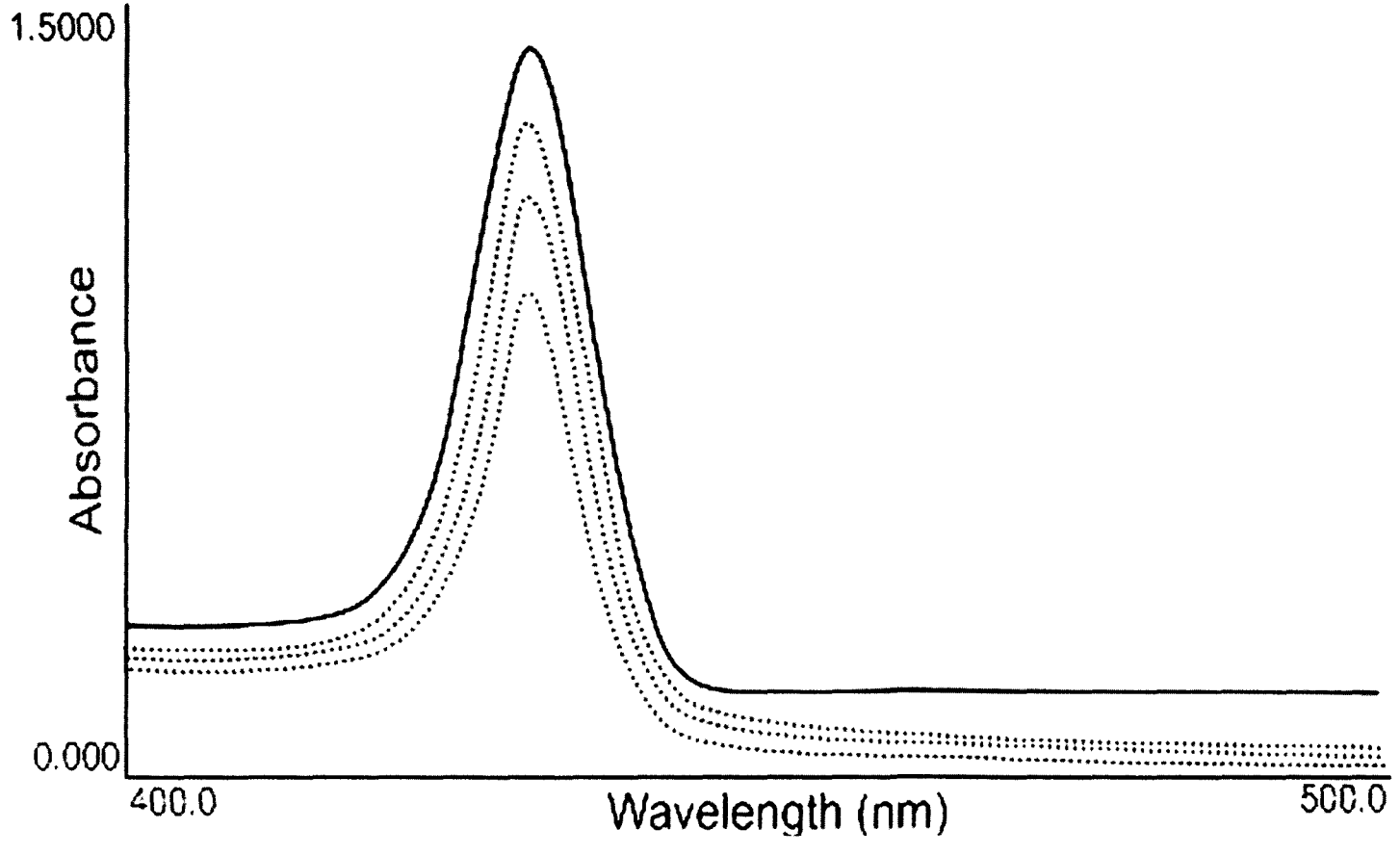

Figure: 6.2.1.a. UV-Visible overlay spectra of Cu(II)[T(naphthyl)P] in CH_2Cl_2 at Room Temperature (_____) on continuous addition of Diethylamine (- - - - - - -).

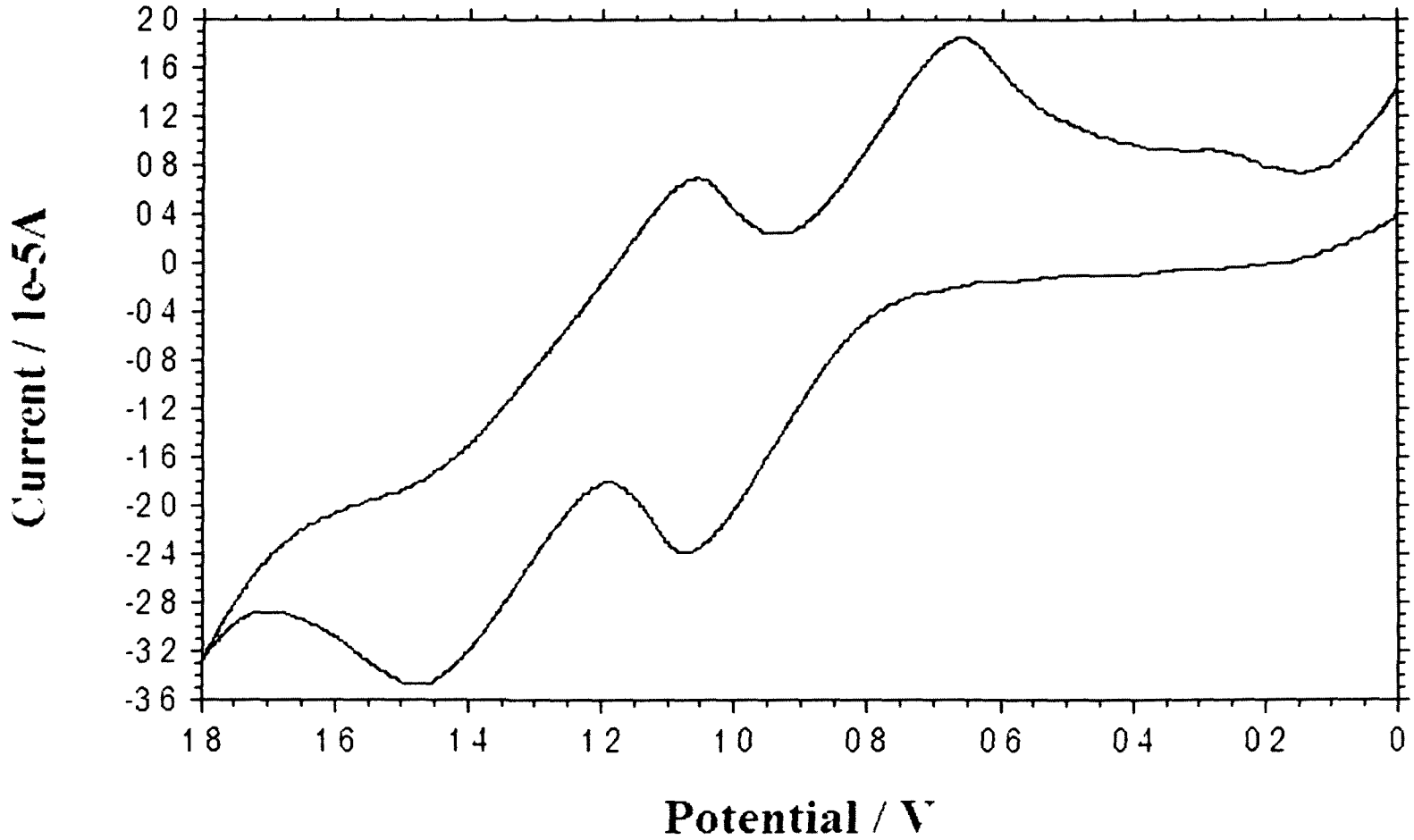

Figure: 6.2.2.i. Cyclic Voltammogram of Cu(II)[T(4-OMeP)P] in CH_2Cl_2 containing 0.1M TBAP at Room Temperature.

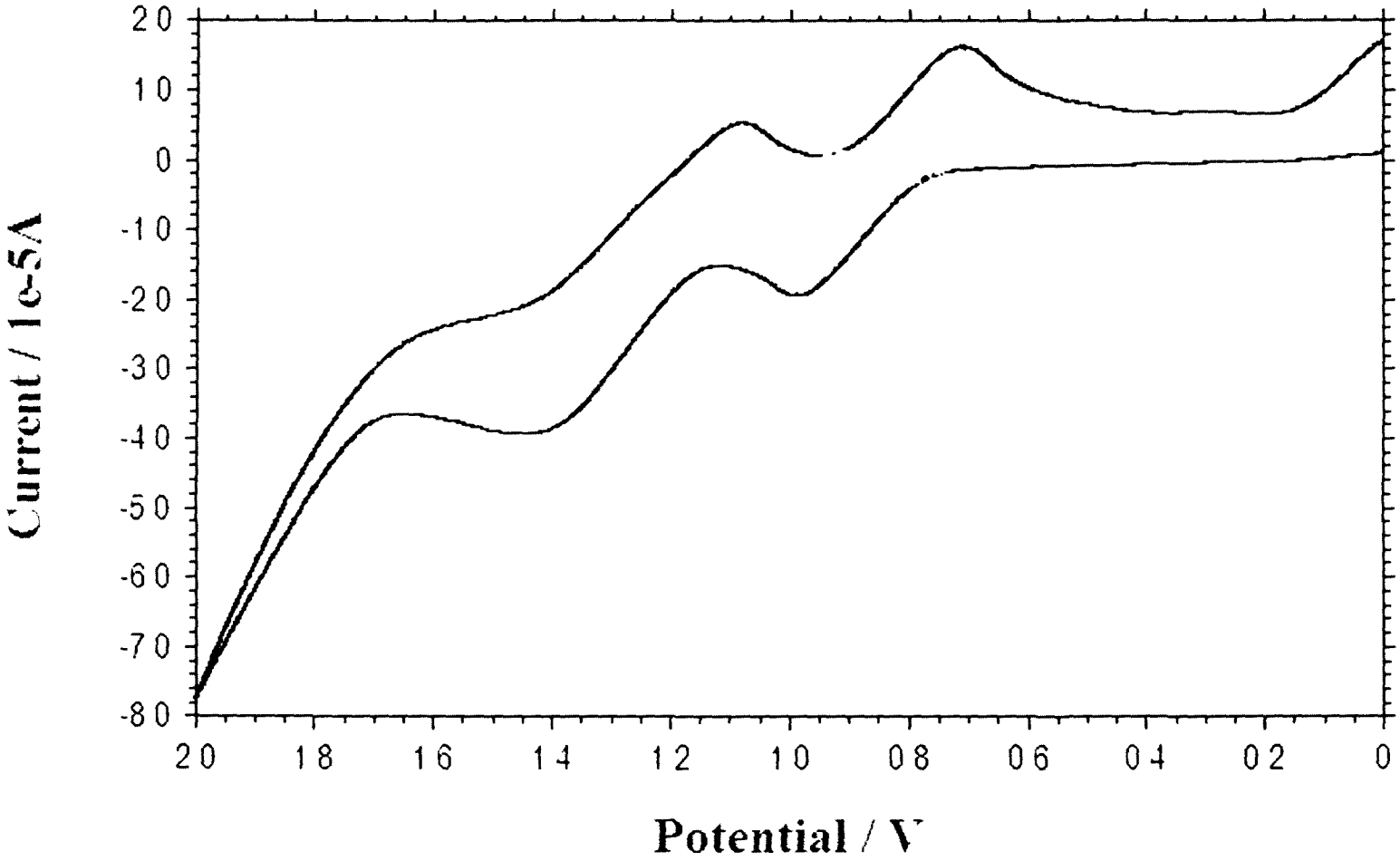

Figure: 6.2.2.ii. Cyclic Voltammogram of Cu(II)[T(naphthyl)P] in CH_2Cl_2 containing 0.1M TBAP at Room Temperature.

REFERENCES:

1. M. Gouterman in *The Porphyrins* **Vol.III**, part A, Edited by D. Dolphin, Academic Press, INC, Newyork, 1979.

2. W.R. Scheidt in *The Porphyrins* **Vol. III**, part A, Edited by D. Dolphin, Academic Press, INC, Newyork, 1979.

3. A. Wolberg and J. Manassen, *J. Am. Chem. Soc.*, **92,** 2982 (1970).

4. R.H. Felton in *The Porphyrins* **Vol. V**, part C, Edited by D. Dolphin, Academic Press, INC, Newyork, 1979.

5. P.J. Chmielewski, L.L. – Grazynski and I. Schmidt, *Inorg. Chem.*, **39**, 5475 – 5482 (2000).

S U M M A R Y

SUMMARY

This thesis entitled **"EFFECTS OF AXIAL LIGANDS ON THE REDOX PROPERTIES OF SOME METALLOPORPHYRINS"** discussed the information and results of investigations on the physico – chemical studies of some Metalloporphyrins. It consists of **six chapters**. We restrict our investigations mainly to UV – Visible absorption spectroscopy and Cyclic Voltammetric studies of some transition metal porphyrins like Manganese, Zinc and Copper porphyrins.

In the **Introduction**, natural occurrence of some metalloporphyrins and their biological functions are briefly mentioned. Also, the importance of UV – Visible spectroscopy and cyclic voltammetry in understanding the redox behaviour of metalloporphyrins is highlighted in the Introduction.

A Brief Review on the theory behind UV – Visible and Cyclic Voltammetric studies on the Effects of Axial Ligands in some Metalloporphyrins (emphasis is given to Manganese porphyrins) is presented in **Chapter 1**. This review provides us the background information to pursue our research investigation in the right direction and to give a proper perspective for the results of the investigations presented in subsequent chapters.

Chapter 2 describes the details of the experimental procedures adopted for purification of solvents and chemicals, synthesis, purification and characterization of samples used during the course of our investigation. Besides this, brief description of physical measurements is also presented.

The Effects of Axial ligands on the UV – Visible spectra of some manganese porphyins are discussed in **Chapter 3**. In general, all three Manganese porphyins chosen to study, viz., Mn(III)[T(2-OMeP)P]OAc,

Mn(III)[T(Naphthyl)P]OAc and Mn(III)[T(4-OMeP)P]OAc, exhibit similar spectral pattern. A UV – Visible absorption spectrum of a manganese porphyrin consists of one B – band or Soret band (Band V) in the range 440 – 480 nm and two Q – bands (Band III and Band IV) in the range 500 – 650 nm. Additional bands (Band Va and Band VI) are also observed in the range 350 – 420 nm. Nitrogenous bases like Diethylamine, Triethylamine and Imidazole are used as axial ligands. It is found out that on initial addition of amine to the three Manganese porphyrins the Soret band suffers a Blue shift. This is attributed to the replacement of the axial ligand OAc^- by amine molecule which comes as a fifth ligand. On continuous addition of amine to the reaction mixture the intensity of the original Soret band diminishes and a new Soret band appears at a shorter wavelength. This could be due to two possibilities:

(i) the coordination of another amine molecule as the sixth ligand, with the oxidation state of Mn remaining Mn(III).

(ii) The second possibility is the reduction of Mn(III) to Mn(II) with amine molecules coordinating as the fifth and sixth ligands.

In our studies, the first possibility is more probable. The details of this are presented in Scheme 3.1 and 3.2 in Chapter 3.

In our discussion, we also incorporate the conformations of metalloporphyrin which are affected by axial ligand – metalloporphyrin interactions. This effect brings about a change in the energy levels of the porphyrin when the axial ligand binds with the central metal atom which appears as shift in the position of absorption bands in the UV – Visible spectrum.

Chapter 4 describes the Cyclic Voltammetric studies of the three Manganese porphyrins i.e., Mn(III)[T(2-OMeP)P] OAc, Mn(III)[T(4-OMeP)P]OAc and Mn(III)[T(naphthyl)P]OAc. All these three exhibit voltammograms of similar pattern. The positive scan voltammogram consists of three redox couples. This is

attributed to the oxidation of Mn(III) to Mn(IV) and the first and second porphyrin ligand oxidations. Similarly, the negative scan gives a voltammogram which consists of three redox couples. This may be due to the reduction of Mn(III) to Mn(II) and the first and second porphyrin ligand reductions. It has been observed that out of the three Manganese porphyrins, redox potential of the first ligand oxidation is lowest in the case of Mn(III)[T(naphthyl)P]OAc. This is because non-planar porphyrins are easier to oxidize due to the interaction of d-orbitals of the metal atom with the porphyrin ligand orbitals (a_{1u}/a_{2u}) and Mn(III)[T(naphthyl)P]OAc, being more distorted due to steric hindrance, gets oxidized at a lower potential. Thus structural effect on the redox potentials is reflected in the voltammograms which also supplements the results observed in Chapter 3.

Chapter 5 discusses the Axial Ligand Effects On The UV-Visible Spectra and the Cyclic Voltammetric studies of Zinc(II)porphyrins viz., Zn(II)[T(4-OMeP)P] and

Zn(II)[T(naphthyl)P]. Zn(II) porphyrins belong to regular porphyrins which contain closed shell metal toms (d^0 or d^{10}). On axial ligation with amine the absorption bands in the UV – Visible spectrum of these Zinc porphyrins experience a Bathochromic shift (Red shift). This is due to the flow of charge from the axial ligand to the porphyin ring through the Zinc ion.

The results of the Cyclic Voltammetric studies of these Zn(II)porphyrins are also presented in this chapter. Two reversible redox couples are observed although their ΔE values are quite large. We also observed that the oxidation potentials of these Zinc porphyrins studied are lower than that of Zn(II)TPP. We attribute this to the presence of electron donating substituents which makes oxidation easier.

Chapter 6 deals with the Axial Ligand Effects On The UV-Visible Spectra and the Redox Tuning of Copper (II) porphyrins viz., Cu(II)[T(4-OMeP)P] and Cu(II)[T(naphthyl)P].

Copper porphyrins belong to d^9 complexes. Addition of amine does not affect the UV – Visible spectra of Copper porphyrins which indicate that they do not accept axial ligands readily. In the Cyclic Voltammetric studies, the Voltammogram consists of two redox couples whose potentials are lower than that of CuTPP. This is attributed to the presence of electron donating substituents.